# Measurement Methods for Calculating of the Direction to a Flicker Source

**PETER AXELBERG**

*Department of Electric Power Engineering*
CHALMERS UNIVERSITY OF TECHNOLOGY
Göteborg, Sweden 2003

THESIS FOR THE DEGREE OF LICENTIATE OF ENGINEERING

# Measurement Methods for Calculating of the Direction to a Flicker Source

**PETER AXELBERG**


Department of Electric Power Engineering
CHALMERS UNIVERSITY OF TECHNOLOGY
Göteborg, Sweden, 2003

# Measurement Methods for Calculating of the Direction to a Flicker Source

**PETER AXELBERG**



Technical report No. 463L
ISSN 1651-4998

Department of Electric Power Engineering
Chalmers University of Technology
SE-412 96 Göteborg
Sweden
Telephone +46 (0)31-772 1000

Chalmers Bibliotek, Reproservice
Göteborg, Sweden 2003

# Abstract

This thesis proposes a method to help finding the source of small fast variations (often referred to as “fluctuations”) of the voltage in a power system. Even very small variations in the rms voltage with a frequency between 0.001 Hz and 25 Hz can cause annoying flickering from light bulbs. This is a well-known power quality phenomenon called “light flicker”, or simply “flicker”. Also the somewhat incorrect term “voltage flicker” is in use. The main sources of flicker are large loads like arc furnaces, welding machines, motor drives but also certain types of wind turbines cause flicker. Since the mid 1980s, measurement methods characterising the power network regarding the level of flicker exist. However, very little of research activities have focused on developing measurement methods for identifying the flicker source. Information of the source of flicker is of great interest both for the utility and for their customers.

This Licentiate thesis focuses on variations in voltage and current in the power network leading to light flicker. The aim of this thesis is to define basic working conditions for the research area, like appropriate models and definitions. A new quantity: “flicker power” is introduced and used to determine the direction to a flicker source. By using the newly-introduced definitions, three measurement methods are proposed. All methods have been validated by simulations in Matlab and one of the measurement methods has also been validated in several field measurements. The results both from the simulations and from the field tests are encouraging. The simulations show high precision in the results for all three measurement methods. Even more interesting were the results from the field tests using measurement method 3. The field tests were performed on a small 2 kW electric heater, on an 850 kW wind turbine and in a 130 kV substation feeding a 70 MW arc furnace. All measurements gave the expected results. For example, when analysing the flicker power measured in the 130 kV substation, the source of flicker was easily identified. The results of the validation tests have been sufficiently promising for the measurement methods to be included in a patent application.

This work confirms that applying digital signal processing methods to power quality signals (voltages and currents) enables the extraction of valuable information: in this case the direction to a flicker source.

**Keywords:** power engineering, power systems, power quality, power quality measurements, flicker, sources of flicker, flickermeter, signal-processing applications.

# Acknowledgement

The work presented in this thesis has been carried out at Unipower AB, Sweden, in cooperation with the Department of Electric Power Engineering at Chalmers University of Technology.

This project has not been a one man show. Several people have been involved and have contributed to the results. First, I would like to give my special thanks to my supervisor and examiner Professor Math Bollen for support, valuable comments and for excellent fellowship. Thanks to my colleagues at Unipower for all support and encouraging discussions. Special thanks to Jonny Carlsson and Johan Adolfsson for valuable comments to the project from the very beginning.

Many thanks go to my personal friend Bengt Andersson for always supporting my further education and personal development.

I also would like to give special thanks to Daniel Wall, Vattenfall Sveanät AB, for valuable assistance during the field tests in Sandviken.

I am grateful for the Knowledge Foundation (Stiftelsen för Kunskaps- och Kompetensutveckling) giving me a scholarship. Without their financial support this project could never have been started.

Last but not least, I would like to thank my wife Hanna and our son John and daughter Lisa for their full support and patience, also during periods when the work took a lot of my spare time.

Alingsås, February 1st 2003

Peter Axelberg

# Contents

# Chapter 1

# Introduction

## 1.1 Background

The society of today is depending on having access to electrical energy with high reliability and quality to function satisfactory. That is one important reason why the concept of *power quality* has become in focus during the last decade. In a broad sense, the concept of power quality is a summary of different parameters estimating the compatibility between the electrical network and the customer equipment. To determine the degree of power quality, specific power quality related parameters are measured in the network and the results of a measurement are compared to existing standards or are being used as a basis for mitigating activities. The most common power quality parameters are discussed further in Chapter 2.
The interest in power quality can also be explained by a number of reasons like:

The *electric energy is to be considered a product* and shall therefore, like products in general, be quality assured.

*Equipment has become more sensitive to bad power quality*. Examples of such equipment are computers, automation devices and devices containing different kinds of power electronics.

*Equipment causes bad power quality*. An important reason is the increasing use of power electronics, which are often a source of disturbances and distortion.

*A sudden voltage drop can cause a costly interruption to a customer*. Power quality sensitive enterprises like paper and pulp industries, semiconductor industries, hospitals, airports etc, have become focused on the power quality because of the consequences of an interruption.

In some cases, *the ongoing deregulation of the electricity market* (worldwide) has decreased the maintenance activities in the network giving negative impact on the power quality [2]. Lower investments have increased the demand for quality assurance of the electrical energy. In some countries in South America, for example, the governments have established specific power quality laws in order to guarantee the customer a certain level of power quality. In Peru, the utilities have to pay the customer a fee for each kWh that doesn't meet the agreed power quality levels. In Sweden, Vattenfall compensates their customers for voltage interruptions longer than 24 h. Norway and Great Britain have similar guarantees to their customers.

*Utilities have an interest to measure the power quality regularly*. The power quality parameters give valuable information about the current status and performance of the network. The information is used in the dialogue between the utility and the customer. The information is also valuable when planning the network.

It is expected that the power quality issue will develop further. For example, a new standard, IEC 61000-4-30 will soon be published that describes measurement methods for different power quality parameters. This new standard will be an important document since it defines how to calculate specific power quality parameters from measured (sampled) voltage waveforms. Earlier standards have defined only how to calculate harmonics and flicker, but this new standard describes methods for calculating other important power quality parameters as well. The new standard has also defined the accuracy required. This will guarantee that measured data from two different power quality analysers measuring in the same point will produce fully comparable results. Another challenge is to develop new (smarter) evaluation methods that not only give "diagrams" but also present solutions how to improve the power quality.

# 1.2 The network model

A basic network model commonly used when studying power quality phenomena is shown in Figure 1.1. This model sometimes includes more elements but the main structure is always the same. This means the model always contains a voltage generator (in most cases an independent voltage source), a transmission line (cable, wire etc.) and a load. The power quality phenomena are normally generated by the load and propagate in the network influencing the supply system as well as other loads. In general, the level of power quality is determined by the loads connected to the network as well as by the design of the network.
Generally speaking, a strong network (low source impedance) will reduce power quality phenomena while a weak network (high source impedance) is more sensitive to bad power quality.

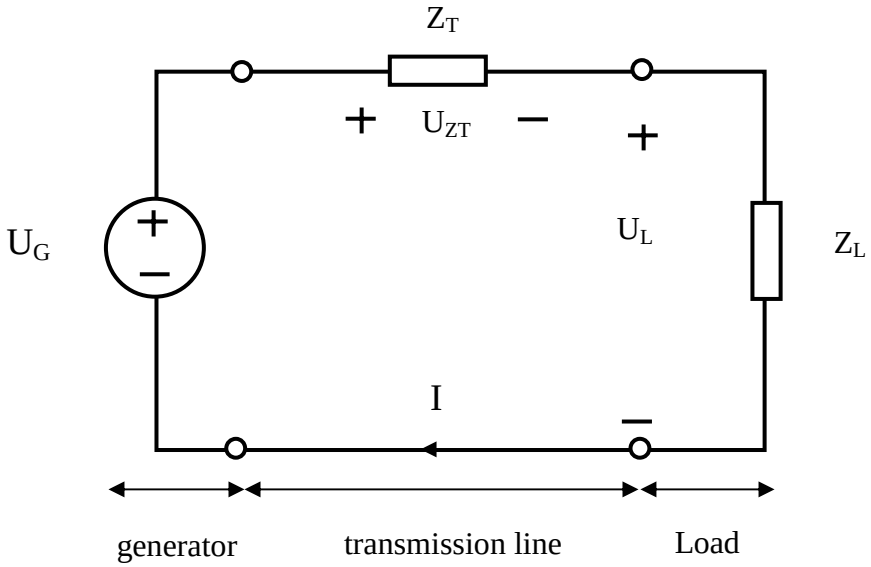


$$U_L = U_G - Z_T \cdot I$$

*Figure 1.1. Basic network model.*

Consider an independent voltage generator in Figure 1.1 maintaining the voltage $U_G$, regardless of the current taken by the load. Also consider the source impedance $Z_T$ to be linear and passive. When $Z_L$ is connected, a load current $I$ will flow in the circuit on the other hand if $Z_L$ is a nonlinear load the current $I$

will be distorted and the consequence will be a nonlinear voltage drop $U_{ZT}$ across $Z_T$. Depending on the characteristics of the load $Z_L$, the voltage $U_L$ will also be (more or less) distorted. If the voltage distortion is of a certain level, it will affect the functioning of the loads connected to the network. An alternative way to describe the influence between a load and the rest of the network is discussed in [3] and shown in Figure 1.2. As shown in Figure 1.2 loads are affecting the level of power quality but they are also affected by power quality.

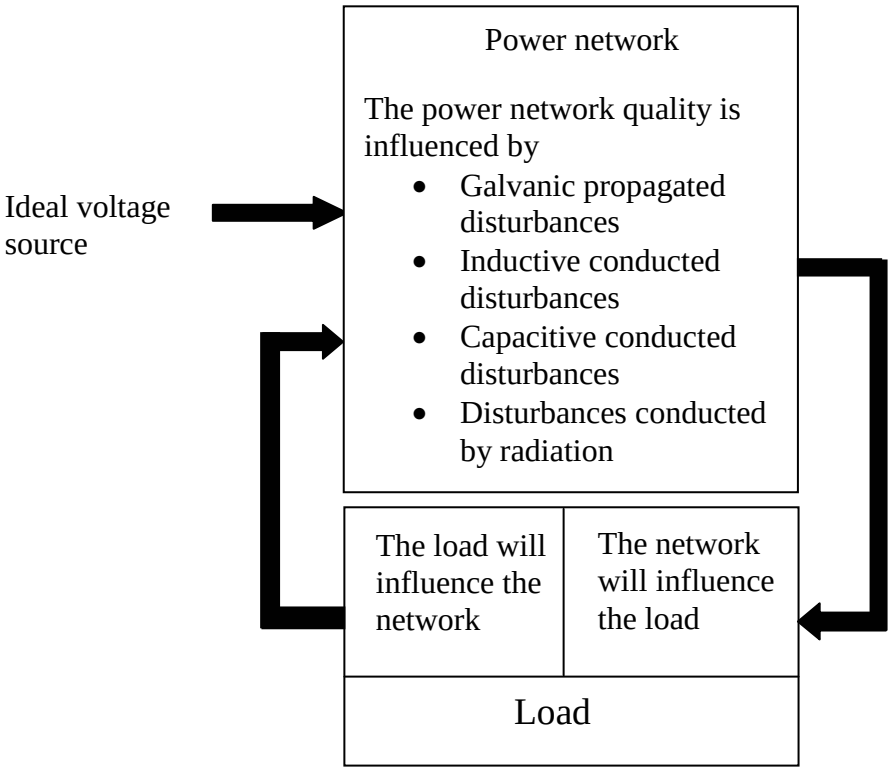


*Figure 1.2. The interaction between the power network and a load.*

# 1.3 Description of the research

Voltage fluctuations caused by loads which vary repeatedly with a frequency between 0.001 Hz and 25 Hz cause irritating flicker phenomena if the fluctuating voltage is supplied to a light bulb. This phenomena, named “light flicker” or short “flicker”, is one of the power quality parameters that should be measured during a power quality survey according to the voltage characteristics standard EN 50160 [1]. The so-called long-term flicker severity $P_{LT}$ that is defined in the standard gives only information about the flicker level (i.e. the level of voltage variations) but it gives no information about the propagation of flicker in the network or the direction to the flicker source. To identify the source of flicker is of great interest for a network operator especially in those cases when a ‘flicker producing’ customer has to share or pay the costs for reducing the level of flicker. The most common ‘flicker reducing’ solutions are either to strengthen the network or to install a flicker reducing equipment like an SVC (Static Var Compensator) or statcom. Both solutions are expensive.

The background to this research is the increasing interest in flicker worldwide. Not only the level of (voltage) flicker is of interest. As mentioned above, it is also of interest to identify the flicker source. The aim of the work presented is to develop measurement methods giving the direction to a flicker source in relation to a monitoring point. The first step in the project was to find what is already developed or known regarding such measurement methods. Searches in databases like IEEE and INSPEC gave very few results within the scope of this work. The closest article [13] found describes a method for identifying a flicker source. However that method is based on a different methodology. Encouraged by that, three different measurement methods have been developed and verified. The results of the verifying field tests have been so promising that the measurement methods have been described in a patent application [11].

The research described in this thesis also includes two more general power-quality issues. First a study was made of general power quality concepts and the most commonly used parameters. Further the whole chain from digital samples of voltage and current up to the final interpretation was studied. A general model was described for a modern power quality monitor; the use of modern signal processing techniques was discussed; and some of the standards related to measurements were interpreted.

## 1.4 Outline of the thesis

*Chapter 2*
This chapter contains descriptions of the terminology used within the field of power quality. Also the most common power quality parameters are discussed. In the last part of the chapter the most common power quality standards are introduced.

*Chapter 3*
Chapter 3 describes how different power quality parameters are calculated. The chapter has also one section exploring fundamental signal processing methods and another section is discussing the design of a modern power quality analyser.

*Chapter 4*
In this chapter a basic model for determining the direction to a flicker source is introduced. Furthermore, the quantity "flicker power" is defined and three measurement methods based on the flicker power concept are presented.

*Chapter 5*
Chapter 5 presents the results of simulations in Matlab as well as results of four field tests. The simulations and the field tests are all based on the measurement methods presented in Chapter 4.

*Chapter 6*
This chapter contains a summary and some discussions regarding further research activities.

# References

[1] CENELEC EN 50160, *Voltage characteristics of electricity supplied by public distribution systems*, CENELEC publication 1999.

[2] P. Axelberg, G. Pool, *Experiences from the Deregulated Electricity Markets in South America,* Nordic Distribution Automation Conference, 2000

[3] D. Blume, J. Schlabbach, T. Stephanblome, *Spannungsqualität in elektrischen Netzen*, VDE-Verlag GmbH, 1999

[4] M. F. McGranaghan, *Electrical Power Systems Quality*, Mc Graw Hill, 1996.

[5] M. H.J. Bollen, *Understanding Power Quality Problems-Voltage Sags and Interruptions*, IEEE Press, 2000

[6] IEC, *Flickermeter – Functional and design specifications*, IEC 61000-4-15 standard, 1999

[7] J. Arrilaga, *Power System Quality Assessment*, John Wiley & Sons, 2000.

[8] IEC, *Testing and Measurement Techniques - Power Quality Measurement Methods*, IEC 61000-4-30 standard, 2001

[9] IEC, *Testing and Measurement Techniques - General guide on harmonics and interharmonics measurements and instrumentation, for supply systems and equipment connected thereto*, IEC 61000-4-7 standard, 1999

[10] S. Svensson, *Power Measurement Techniques for Nonsinusoidals Conditions*, PhD work at Chalmers University of Technology, Sweden, 1999

[11] P. Axelberg, J. Carlsson, *Measurement methods for calculating of the direction to a flicker source*. Patent application, 2002.

[12] UIE, *Guide to Quality of Electrical Supply for Industrial Installations – part V Flicker*. Union for Electricity Applications (UIE), 1999.

[13] A.M. Dán, *Identification of Flicker Sources*, 8th International conference on harmonics and quality of power, volume 2, pp. 1179-1181, Athens Greece, Oct 1998.

# List of publications

- P. Axelberg, G. Pool, *Experiences from the Deregulated Electricity Markets in South America*, Nordic Distribution Automation Conference, Trondheim, Norway, 2000.
- P. Axelberg and D. Peck, *Current and Emerging Trends in IEC Standards and their Implications for Power Quality Measurement Systems*, Distribution 2001 Conference, Brisbane, Australia, 2001.
- P. Axelberg, M. H. J. Bollen, *International standards for power quality measurement systems*, CIRED 2002, Kuala Lumpur, Malaysia, 2002.
- P. Axelberg, M.H.J. Bollen, *Power Quality – Standards and trends*, Nordic Workshop on Power Systems, Tampere, Finland, February 2002.

# Chapter 2

# Power Quality Parameters and Standards

## 2.1 Introduction

To fully understand the concept of power quality it is necessary to have a good knowledge of the terminology. It is also necessary to have some knowledge of the most common power quality standards. A general description of different power quality parameters is therefore introduced and discussed in this chapter as well as an introduction to the most common power quality standards.

## 2.2 Terminology

So far, there is no world wide accepted definition of power quality. Different people interpret the term power quality slightly different. People working with system protection often identify power quality with reliability. People developing and designing electrical equipment identify power quality with certain characteristics of the voltage in the network when the equipment works properly. Thus, it is quite obvious that several opinions exist regarding the meaning of power quality.

One possibility is to place power quality under the definition of electromagnetic compatibility (EMC) as in the standard IEC 61000-1-1:
*Electromagnetic compatibility is the ability for an equipment or system to function satisfactory in its electromagnetical environment without introducing intolerable electromagnetic disturbances to anything in that environment.*
The interpretation of the definition should be something like: Any equipment connected to the network should not disturb or cause malfunctions to other equipment and vice versa. A disadvantage with such a "broad" definition is that it also includes radiated disturbances which normally are not included in the concept of power quality. Another disadvantage is that the definition does not state how to measure the power quality.
Another maybe more accurate definition of power quality exists. This definition notices that most of the power quality phenomena are propagated galvanically and can therefore be quantified if voltage and current are measured. According to this definition [4] power quality includes: *"Any power problem manifested in voltage, current or frequency deviations that results in failure or misoperation of customer equipment"*. This definition is quite good, just because it is formed from the quantities voltage, current and frequency. From these quantities most of the power quality parameters can be calculated. Since the concept of power quality has been in use for such a long time without any precise definition, it will be difficult to find a definition that will be accepted generally. Probably, for a long time, we have to accept that the meaning of power quality will differ from person to person.

There are some other terms used in publications [5], closely related to power quality, worth mentioning here:

*Voltage quality* is concerned with the deviations of the voltage from a sinusoidal waveform. The utility is responsible to maintain the voltage in the network and thus responsible for the voltage quality.

*Current quality*. Current quality is concerned with the deviations of the current from a sinusoidal waveform and is determined by the load. Thus, it is the customer who can affect the level of current quality. Normally, the utility has no legal rights to prevent a customer to connect any load to the network. If a certain load adversely affects the power quality, the utility can at least advise the customer to install mitigation equipment like a filter etc. to increase the quality.

*Quality of supply*. This term covers technical aspects as well as non-technical aspects like the interaction between the customer and the utility, e.g. the speed with which the utility reacts to complaints etc. What level of customer service does the utility offer? How quick will a fault in the network be repaired? Questions like those are part of Quality of supply**.**

## 2.3 Power quality parameters

Since years back several measurable parameters have been accepted as power quality parameters. These parameters quantify the level of power quality in a monitoring point in the network. Some of the parameters like the magnitude of the supply voltage and the frequency are well known and basic while others, for example flicker, are not. Various national and international standards give limits for several of these parameters. A power quality parameter is categorised as a *variation* or as an *event* [5]. A variation is a slow change of a parameter over time. An event, on the other hand, is a short duration change (less than second) in the voltage or current waveform. The most common variations and events are given below:

Variations:

- Power frequency
- Magnitude of the supply voltage
- Voltage supply unbalance
- Voltage harmonics and voltage distortion
- Flicker

Events:

- Transients
- Voltage sags and swells
- Voltage interruptions

Above parameters will be discussed further in this chapter and in Chapter 3.

*About the voltage*
Voltage is the most important parameter when determining power quality.
Fluctuations in the voltage are either slow variations or events. A slow variation is categorised as quasi-stationary and for such phenomena the same calculations as for stationary signals can be used: for example calculation of the rms voltage or transformation from the time domain to the frequency domain. An event, on the other hand must be “captured” using a triggering mechanism. Depending on the characteristics of the event, different kinds of calculations are performed. For example calculation of the unbalance during an event gives valuable information about fault type etc.

*Short undervoltage, in the rms voltage (voltage dip)*
A voltage dip is a short reduction in the voltage rms. According to EN 50160, the rms voltage during the dip is 90% or less of the nominal voltage with a duration between 10 ms and 60 s. A voltage dip is often caused by starting of large loads such as motors etc. but also by faults in the power system such as single phase to ground faults.

*Short overvoltage in the rms voltage (voltage swell)*
A voltage swell is a short increase in the rms voltage. According to EN 50160, the rms voltage is 110% or more of the nominal voltage. The duration is between 20 ms and 120 s (for 50 Hz). If the duration is shorter than 20 ms it is called a transient overvoltage.

*Interruptions*
A voltage interruption is defined as a reduction in the rms voltage to zero (or close to zero). The interruption is defined as short if the duration is between 10 ms and 3 minutes and long if it continues more than 3 minutes (definition taken from EN 50160). The reasons for short interruptions can be switching actions in the power network as well as temporary faults on the power network or in a load. A longer interruption is often caused by a (sudden) faulted system component or caused by planned maintenance.

*Transient overvoltages between phase and ground*
The word transient is used (or misused) by many as a common term for all kinds of short duration voltage disturbances. In power quality, a transient is usually defined as a short-duration non-oscillating voltage spike or a short duration voltage oscillation superimposed on the power frequency voltage waveform. The voltage spikes can be either positive or negative. The rise time varies from less than one microsecond to a few milliseconds. The decay time varies and can in some cases be very short. The duration of positive and negative transients are, per definition, less than 10 milliseconds. The duration of damped oscillating transients can be a little longer. Transients are caused when loads or capacitor banks are connected to the network or during switching activities in the network.

*Unbalance*
The phase voltages in a three-phase network are expressed as

$$u_{L1}(t) = U_{L1}\sin(\omega t + \beta_{L1}) \qquad [2.1]$$

$$u_{L2}(t) = U_{L2}\sin(\omega t - 120° + \beta_{L2}) \qquad [2.2]$$

$$u_{L3}(t) = U_{L3}\sin(\omega t + 120° + \beta_{L3}) \qquad [2.3]$$

If the amplitudes on the three phases are equal, the voltage is said to be symmetric otherwise unsymmetric. An unsymmetric voltage can always be split into three symmetric voltages called positive, negative and zero sequence voltages or components. The three voltage phasors in the positive sequence are all 120° out of phase and are rotating counter-clockwise. The same phase shift occurs for the negative sequence, but the rotation is clockwise. The voltages in the zero sequence are all in-phase and do not rotate. The voltages in the three sequences are called symmetrical components and are expressed as $U_1$ (positive sequence), $U_2$ (negative sequence) and $U_0$ (zero sequence).
Equation [2.4] shows how to calculate the symmetrical components from the three unbalanced voltages $U_{L1}$, $U_{L2}$ and $U_{L3}$.

$$\begin{bmatrix} U_1 \\ U_2 \\ U_0 \end{bmatrix} = \frac{1}{3}\begin{bmatrix} 1 & a & a^2 \\ 1 & a^2 & a \\ 1 & 1 & 1 \end{bmatrix}\begin{bmatrix} U_{L1} \\ U_{L2} \\ U_{L3} \end{bmatrix} \qquad \text{a} = \text{e}^{\text{j}120^\circ} \qquad [2.4]$$

The unbalance (factor) $u_u$ is defined as the ratio of negative to positive sequence voltage and is calculated by using the relation in [2.5]

$$u_u = \frac{|U_2|}{|U_1|} \cdot 100\% \qquad [2.5]$$

An alternative way of calculating the unbalance factor is expressed in [2.6]. The voltages $U_{12fund}$, $U_{23fund}$ and $U_{31fund}$ are fundamentals of the line-to-line voltages.

$$u_u = \sqrt{\frac{1-\sqrt{3-6\beta}}{1+\sqrt{3-6\beta}}} \cdot 100\% \quad \text{where} \quad \beta = \frac{U_{12\,fund}^4 + U_{23\,fund}^4 + U_{31\,fund}^4}{(U_{12\,fund}^2 + U_{23\,fund}^2 + U_{31\,fund}^2)^2} \qquad [2.6]$$

*Harmonics and interharmonics*
Harmonic distortion is caused by nonlinear devices in the power system. A nonlinear device is one in which the current is not proportional to the applied voltage. That means, if the applied voltage is sinusoidal, the resulting current will contain harmonics. The power system itself can usually be considered as (remarkably) linear. Harmonic currents are therefore mainly related to the loads. Devices like switched power supplies, adjustable speed drives, office equipment etc. are all examples of nonlinear loads. A nonlinear load is also affecting the

voltage quality since voltage distortion is a result of distorted currents flowing through the source impedance. The harmonic current causes a voltage drop (in the source impedance) for each harmonic resulting in a voltage distortion at the load bus (see Section 1.2). The amount of voltage distortion depends on the source impedance (strong or weak network) and on the current.

Harmonics phenomena sometimes result in serious consequences on the power network. An example of such a phenomenon is the triplen harmonics. Triplen harmonics are the (odd) multiples of the third harmonic (i.e. 150Hz, 450Hz etc.). Triple harmonics are of great concern for grounded wye-systems since they are in phase and therefore will be added in the neutral with possible overheating as a consequence. For example, consider equal nonlinear loads connected to each phase in a low voltage three phase system. Also consider that each load produces a fundamental current of 150A and a third harmonic current of 100A. The rms current in each phase will be $I_e = \sqrt{150^2 + 100^2} \approx 180A$. In the neutral, the fundamental current will be cancelled but the third harmonic will be added. This means 300A flowing in the neutral (!). The example shows that even if the loads are the same in the three phases, high currents can appear in the neutral due to triplen harmonics.

Also transformer winding connections have a significant impact on the flow of triplen harmonic currents from single-phase nonlinear loads. In a wye-delta transformer, the triplen harmonic currents will be “trapped” and circulate in the delta winding. A consequence can be an overheated transformer and a significantly shorter life span of the transformer. This example also shows the importance of measuring harmonic currents on the wye-side of a wye-delta transformer since the triplens cannot be measured on the delta side. When making a harmonic survey, it is preferable to use a logging three phase power quality analyser during at least one load cycle. A non-recording instrument will not give enough information about the harmonic situation since the harmonic currents in the network typically vary over time.

Capacitor banks are sensitive to harmonic currents. Even if the harmonic current is quite low, amplification due to parallel resonance between the source impedance and the capacitor bank can occur. If the frequency of the harmonic current and the resonance frequency are the same, an amplification of the harmonic current occurs and will sometimes damage the capacitor bank. The best way to prevent damages is to install a shunt filter consisting of a capacitor and a reactor in series (a so-called serial resonance circuit). The shunt filter works by short-circuiting the harmonic currents as close to the source of distortion as possible. This keeps the harmonics out of the supply system. At the fundamental frequency, the shunt filter acts as a phase compensator.

Stray currents can also be a consequence of high levels of harmonic currents. Normally the currents flow in the phase-neutral connectors but with an increase in harmonic content, the conductor impedance increases and the harmonics tend

to flow alternative ways like in water pipes, reinforcing irons etc. The stray currents can become quite high and cause unacceptable high levels of magnetic fields in the surroundings. This again holds especially for the triplen harmonics.

An interharmonic is a current (or voltage) with a frequency not an (integer) multiple of the fundamental (e.g. 16⅔Hz). Example of devices generating interharmonics are adjustable speed drives, frequency converters etc. Interharmonics can also cause a flicker phenomenon if two (relatively strong) signals are separated in frequency corresponding to a frequency which is within the spectrum of flicker.

*Distorsion (THD)*
The Total Harmonic Distorsion, $THD_F$, is the ratio of the root-mean-square value of the harmonics to the root-mean-square of the fundamental of a waveform [2.7]. An alternative definition is the ratio of the root-mean-square value of the harmonics to the root- mean-square of the signal itself [2.8].

$$THD_F = \frac{\sqrt{\sum_{n=2}^{\infty} X_{ne}^2}}{X_{1e}} \qquad [2.7]$$

$$THD_R = \frac{\sqrt{\sum_{n=2}^{\infty} X_{ne}^2}}{X_{eff}} \qquad [2.8]$$

The most common used definition is [2.7] which also is natural since the rms-value of the harmonics is in relation to a non-distorted waveform.
In [2.8] the distortion is both in the numerator and in the denominator which leads to difficulties in the interpretation. According to expression [2.9], with low levels of distortion, the $THD_F$ and $THD_R$ values will become quite equal.

$$THD_R = \frac{\sqrt{\sum_{n=2}^{\infty} X_{ne}^2}}{X_{eff}} = \frac{\sqrt{X_{2e}^2 + X_{3e}^2 + \ldots + X_{ne}^2 \ldots}}{\sqrt{X_{1e}^2 + X_{2e}^2 + \ldots + X_{ne}^2 \ldots}} = \frac{\sqrt{X_{2e}^2 + X_{3e}^2 + \ldots + X_{ne}^2 \ldots}}{X_{1e}\sqrt{1 + \frac{X_{2e}^2 + \ldots + X_{ne}^2 \ldots}{X_{1e}^2}}} = \qquad [2.9]$$

$$= \frac{THD_F}{\sqrt{1 + THD_F^2}} \approx \frac{THD_F}{1 + \frac{THD_F^2}{2}}$$

Suppose a $THD_F$ of 8% (which is the upper limit of voltage distortion stated in EN 50160). The corresponding $THD_R$ will be 7.9% which is quite close to the

$THD_F$. Thus, when measuring the voltage distortion in a power network during normal operating conditions, in a practical sense, both [2.7] and [2.8] can be used. The situation is different when measuring current distortions. It is not unusual to measure a $THD_F$ of 80% or more (it depends on the load). Corresponding $THD_R$ will be 62%, which is quite different from the $THD_F$. In some standards the distortion is referred to the $THD_R$ and in others to the $THD_F$. Another definition occurs in the EN 50160 which states the voltage rms value of the harmonics shall be related *to the declared voltage rms* (i.e. 230V). Such a definition is called TDD (Total Demand Distortion). There exist more definitions related to distortion. Some examples are:

- $THD_{odd}$ (only odd harmonics are included in [2.7])
- $THD_{even}$ (only even harmonics are included in [2.7])
- $THD_{triple}$ (only triplen harmonics are included in [2.7])
- $THD_{xy}$ (only harmonics between harmonic number x and y are included in [2.7])
- $THD_{HF}$ (only harmonics of high-frequency are included in [2.7])

*Flicker*

Heavy loads like arc furnaces, pumps, motors etc. will increase the level of voltage fluctuations in the network. In many cases these fluctuations are (more or less) repeated with a low frequency. The phenomenon is called flicker. Depending on the load, the frequency of the fluctuations and the supply system an irritating flicker from lamp bulbs can occur. Studies have shown that a human being has a peak-sensitivity to a flickering light if the frequency of the fluctuations is close to 9 Hz. At this frequency, a modulation of only 0.25% is enough to create annoying flicker. The phenomenon of flicker occurs mainly in areas with heavy industries or sometimes in areas close to wind turbines. The standard IEC-61000-4-15 [6] states how to measure flicker. This standard will be discussed in more detail in Section 2.5.1.

# 2.4 Standard-Setting Organisations

On international basis, the main standard-setting organisations regarding power quality are IEC, CENELEC and IEEE. In addition to these, some regional and national organisations are preparing and are responsible for domestic standards. In this section, some information about the most important organisations will be given.

## 2.4.1 International organisations

- *IEC (International Electrotechnical Commission)* is a global organisation that prepares and publishes international standards for all electrical, electronics and related technologies. Detailed information is available on www.iec.ch.

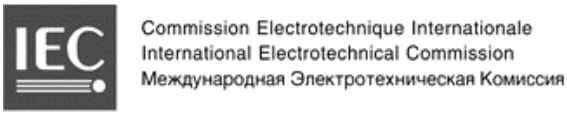


*ISO* (International Organisation for Standardisation) is a network of national standard institutes from 145 countries working in partnership with international organisations, governments and industry business and consumer representatives. Detailed information is available on www.iso.org.


*ITU* (International Telecommunication Union) was established last century as an impartial, international organisation within which governments and the private sector could work together to coordinate the operation of telecommunication networks and services and advances the development of communications technology. The ITU's standardisation activities are being used in defining the building blocks of the emerging global information infrastructure.

## 2.4.2 European standardisation organisations.

Standardisation issues on European level are handled by the following organisations

*CEN, European Committee for Standardisation*


CEN's mission is to promote voluntary technical harmonisation in Europe (both EU and EFTA countries are members) in conjunction with worldwide bodies and its partners in Europe. In Europe, CEN works in partnership with CENELEC - the European Committee for Electrotechnical Standardisation and ETSI - the European Telecommunications Standards Institute. More detailed information is available on www.cenorm.be.

*CENELEC, European Committee for Electrotechnical Standardisation*


CENELEC is the European Committee for Electrotechnical Standardisation. It was set up in 1973 as a non-profit-making organisation under Belgian law. It has been officially recognised as the European Standards Organisation in its field by the European Commission in Directive 83/189/EEC. Its members have been working together in the interests of European harmonisation since the late fifties, developing alongside the European Economic Community. CENELEC works with 35000 technical experts. More detailed information is available on www.cenelec.org.

### 2.4.3 Other organisations

***IEEE*** *- the Institute of Electrical and Electronics Engineers.*

IEEE - "EYE triple E" – is an association of more than 377 000 individual members in 150 countries. IEEE is active within technical areas ranging from computer engineering, biomedical technology and telecommunications, to electric power, aerospace and consumer electronics, among others. The institute produces 30 percent of the world's published literature in electrical engineering, computers and control technology and has nearly 900 active standards with 700 under development. More detailed information is available on www.ieee.org.

## 2.5 Power Quality standards

The standards developed within power quality are centred on the following objectives [7]:

- description and characterisation of different phenomena (e.g. EN 50 160)
- measurement techniques and methods (e.g. IEC 61000-4-30)
- emission and immunity levels for different classes of equipment (e.g. IEC 61000-3-2 etc.).
- mitigation guidelines.

Two different kinds of standards are needed when measuring and verifying power quality: Measurement method standards and voltage characteristics standards. These standards are related to each other with following explanation (see also Figure 2.2): In a modern power quality analyser, the waveforms of voltage and current are sampled. The sampled waveforms contain the information necessary for calculating the power quality parameters. Unfortunately, power quality parameters can be calculated in different ways, giving slightly different results. This is quite confusing, especially if measured results are to be compared between different instruments. A lot of instruments are not calculating the power quality parameters according to recognised standards. Therefore it is important to the users of instruments to know *how* the power quality parameters are calculated in order to fully understand the results. Manufacturers of instruments must therefore specify how parameters are calculated. In the near future, the forthcoming IEC 61000-4-30 will be a

valuable document making the power quality measurement data more standardised.

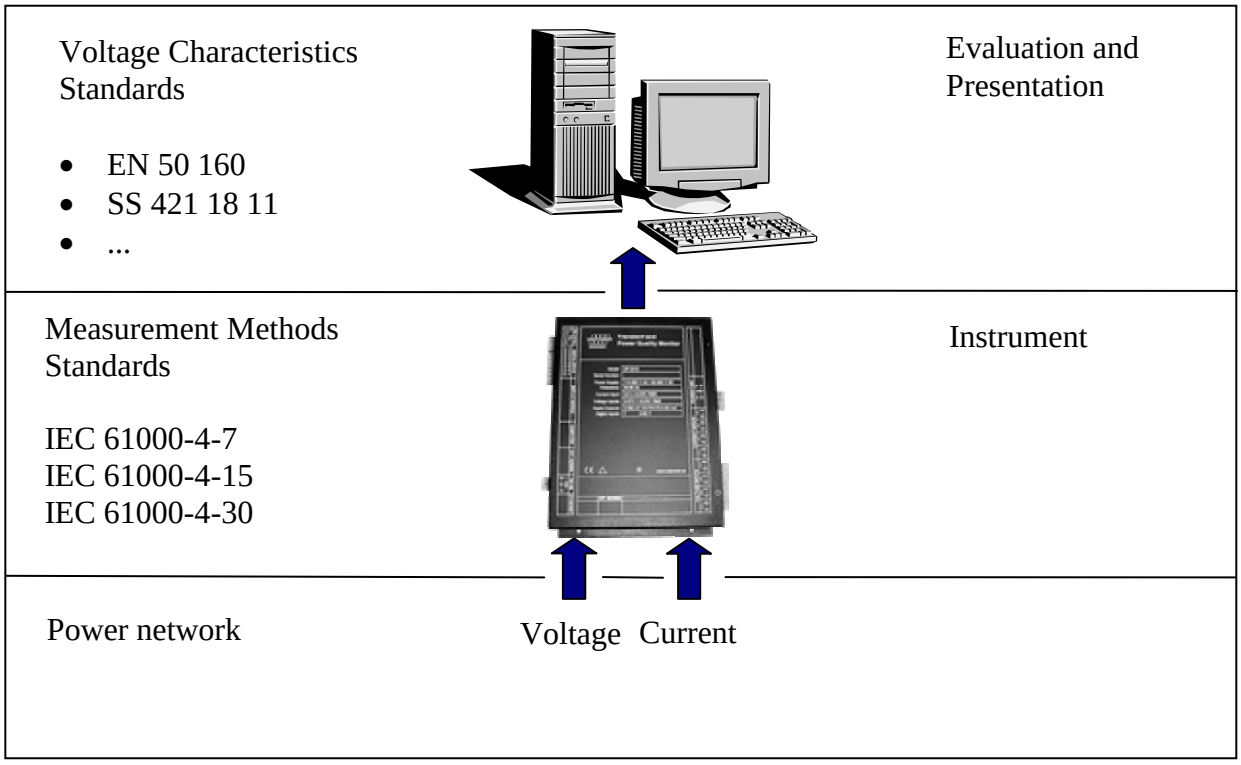


*Figure 2.1. Categories of Power Quality Standards*

The measurement data produced by the instrument is normally analysed in specially designed evaluation software. The most common way is to present the data in diagrams and tables. Another efficient way of evaluating the data is to use report generators, automatically evaluating the data. The reliability in the results is directly related to the overall performance (hardware as well as software) of the power quality measurement system. A challenge for the manufacturers of power quality analysers is to develop instruments and systems where the extensive data is presented in a comprehensive way. Too many measurement systems give a lot of information where the results are difficult to interpret for the user. The value to the user of a power quality measurement system is very much dependent of the design of the concept. The trend is towards measurement systems useful also for non-experts in power quality. The trend is also towards a state where the measurement systems are integrated in the mitigation process.

## 2.5.1 Measurement methods standards

The increasing need for power quality measurements has driven the requirement for standards describing measurement methods and how the different power quality parameters are calculated and interpreted. IEC has defined a series of standards, called Electromagnetic Compatibility Standards, to deal with power quality issues. The most important IEC standards concerning calculation of power quality are described in this section.

**IEC 61000-4-30/FDIS (Testing and measurement techniques – Power quality measurement methods) [8]:**

The standard IEC 61000-4-30 is the first overall standard available covering the measurement techniques and calculations for all major power quality parameters and events. This document describes how a number of power quality parameters shall be calculated. Furthermore, it also classifies these parameters into two different classes (class A and B) depending on how the calculations are made. The aim of the standard is to make it possible to obtain reliable, repeatable and comparable results regardless of the instrument being used. The standard deals with the following parameters:

- Power frequency
- Magnitude of the supply voltage
- Flicker
- Voltage dips, swells, transients and interruptions
- Unbalance
- Harmonics and interharmonics in voltage and current
- Mains signalling

Below is an overview of the standards for class A and 50Hz instrumentation. These discussions are also valid for 60Hz.

*Class A and class B instruments*
There are different applications of power quality measurements like load analysis, trouble shooting and contractual measurements. Different types of applications require different instruments. An instrument being used for load analysis does not need the same accuracy as an instrument used for resolving contractual disputes. IEC 61000-4-30 therefore has defined two different classes of accuracy (class A and B). Class A is the higher accuracy class used for measurements like verifying compliance with standards, contractual

measurements etc. Another intention with a class A instrument is that any measurements of a parameter carried out with two different class A instruments measuring in the same point should give fully comparable results. Class B performance may be used for statistical surveys etc. where low uncertainty is not required. In class B, no calculation methods are defined like in class A, but the manufacturer of the instrument shall specify the measurement method being used.

*Integration times*

For a class A instrument, the time integration window (see Section 3.4.2) shall be 10 cycles in a 50Hz system. With this time integration window as a base, three measuring intervals are defined. These are: 150 cycles, 10 minutes and 2 hours. The 150 cycles rms value is calculated as the root mean square of fifteen 10 cycles rms values. The windows shall be continuous and non-overlapping so it is easy to proof that the calculated 150 cycle value is the correct rms value obtained.

The aggregation from 150 cycles to 10-minutes is more complicated since the actual frequency will vary. When the system frequency is exactly 50Hz, there are exactly 200 intervals. For a frequency of 49.5 Hz the 150 cycles become 3.03 seconds long and there will be only 198 of them in a 10-minute interval. In most cases the number of intervals is not an integer number and the last interval is discarded in the calculation. Despite the discarded data, it remains safe to calculate the $U_{rms/(10\text{-}min)}$ as the rms voltage. Each 10-minute interval must begin on an absolute 10 minutes clock time, +/- 20 ms. These intervals are used when calculating the voltage magnitude, harmonics and interharmonics and the voltage unbalance.

*Flagging*

A sudden event like a voltage dip, swell or an interruption will influence other power quality parameters like flicker, unbalance etc. In order not to count an event twice, IEC 61000-4-30 defines a flagging concept. When an event such as a voltage dip, swell or a short interruption occurs the instrument shall record that specific event and indicate that the other parameters may be affected by this event. Therefore the interval is flagged and during the interpretation phase of the measurements it should be decided if the value obtained during this interval is to be included in the final result. The other power quality parameters shall not be recorded. Instead, the interval shall be flagged, meaning that it is marked to show the specific event and that other measured data during the interval should be ignored.

*Frequency*
The frequency shall be calculated every 10 seconds for class A instruments. To calculate the frequency, zero-crossings during 10 seconds are counted. The accuracy for class A shall be better or equal to ± 10 mHz and less than ±100 mHz for a class B instrument. An accuracy of 10 mHz requires a measurement window of 10 second ± 2 ms(!)

*Voltage rms value*
The voltage rms value is calculated every 10 cycles for class A instruments. Based on this rms value, the 150 cycles and 10 minute rms values are calculated. The accuracy for class A shall be better than or equal to ± 0.10 % of nominal voltage and for class B ± 1.0 %.

*Flicker*
The flicker calculations for class A instruments shall follow the restrictions in the standard IEC 61000-4-15 (Flickermeter – functional and design specifications) [6].

*Sags, swells and interruptions*
The registration of sag/swell events shall be based on 1 cycle rms values updated every ½ cycle for a class A instruments. When a rms value exceeds or falls below a stated trigger level (in one of the phases), the instrument shall start recording and continue until the rms value has returned to normal (on all phases). The first instant is referred to as the start of the event, the second as the end of the event. The time between the start and the end of the event is called the duration of the event. The lowest rms value for a voltage dip is called the retained voltage. The accuracy for class A instruments shall be within ± 0.2 % of the stated nominal voltage and ± 2.0 % for class B.

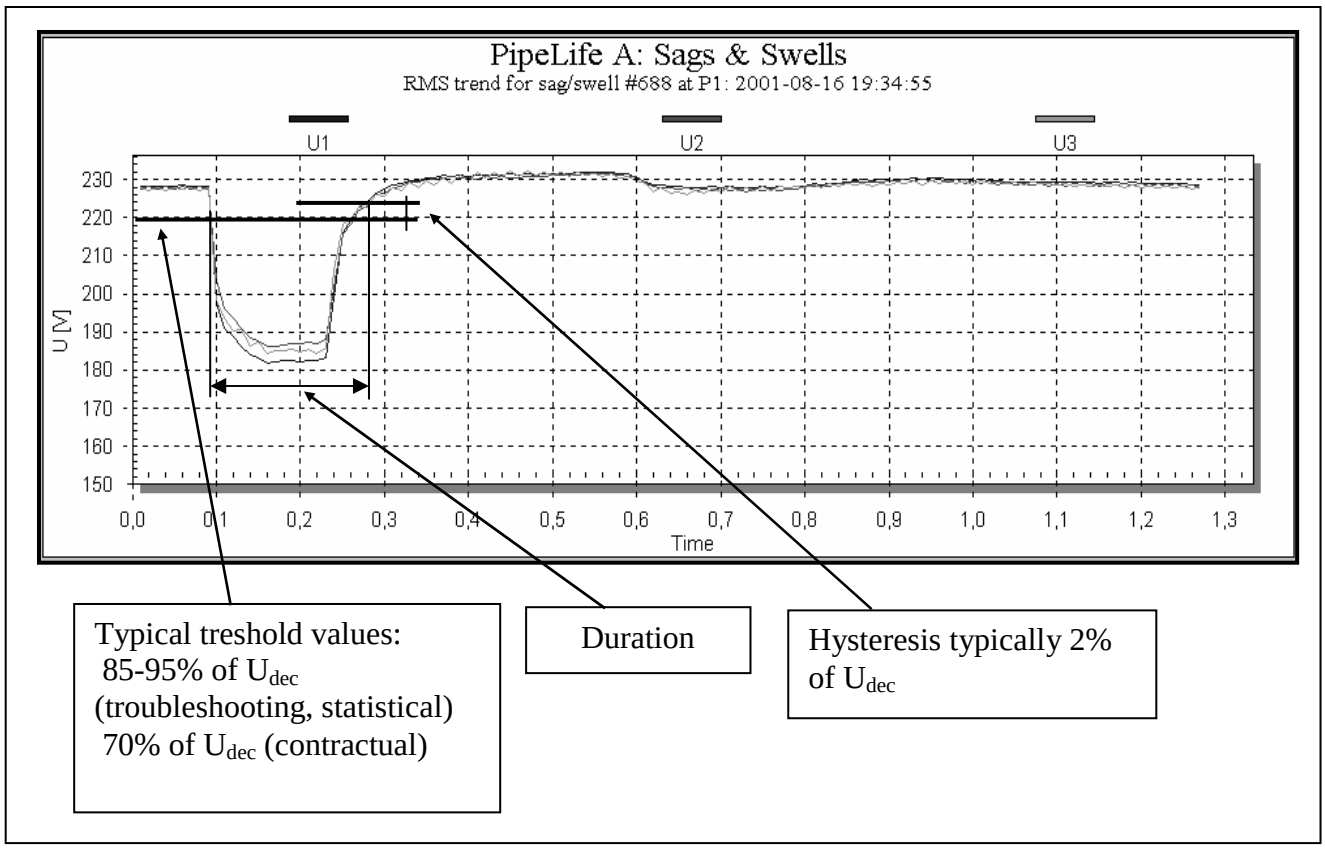


*Figure 2.2. Definition of a voltage sag according to IEC 6100-4-30. Voltage swell and interruption have similar definition.*

*Unbalance*

To fulfil the restrictions of class A, unbalance shall be calculated using the method of symmetrical components. From the measured phases, the three symmetrical components are calculated (positive, negative and the zero sequence component). The unbalance factor is calculated as the ratio between the negative and the positive sequence component expressed as a percentage. Unbalance shall be calculated over 10-cycle, 150-cycle and 10-minutes intervals.

*Harmonics and interharmonics*

To fulfil the requirements for class A, the calculations shall be made according to IEC 61000-4-7 (see further on in this section).

*Miscellaneous*

IEC 61000-4-30 also contains testing methods to verify an instrument according to the standard. The standard also contains a section describing installation, measurement techniques, transducers etc. See [8] for more information.

**IEC 61000-4-7 Ed 2.0 (Testing and measurement techniques – General guide on harmonics and interharmonics measurements and instrumentation for power supply systems and equipment connected thereto) [9]:**

IEC 61000-4-7 edition 2.0 replaces the earlier edition IEC 61000-4-7 edition 1.0 from 1991 and describes measurement methods for harmonics and interharmonics up to 9 kHz. The standard gives guidelines how to design an instrument fulfilling the requirements in IEC 61000-4-7. Moreover, the standard also defines the instrumentation being used for verifying tests according to IEC 61000-3-2 (emission). Also, the standard deals only with instrument based on sampled data and digital signal processing methods. The basic interval for harmonic measurements is again the 10-cycle interval. A DFT (Discrete Fourier Transform) over a 10-cycle window gives a spectrum with a frequency resolution of 5 Hz. This implies that in between the harmonic frequencies (integer multiples of 50 Hz), nine additional values are available. The lowest and the highest of these are "added" to the (integer) harmonic. The remaining seven together form the "interharmonic". Thus for the interval from 245 Hz to 305 Hz: 255 Hz is added to 250 Hz and 245 Hz to form the 5:th harmonic; 295 Hz, 300 Hz and 305 Hz form the 6:th harmonic. The remaining values from 260 Hz to 290 Hz will form the "interharmonic 6.5". Figure 2.3 shows a functional block diagram for an instrument fulfilling the requirements in IEC 61000-4-7. OUT 1 gives the frequency spectrum of the signal. OUT 2 gives the grouped data (i.e. harmonics and interharmonics components). OUT 3 and OUT 4 are used for emission tests.

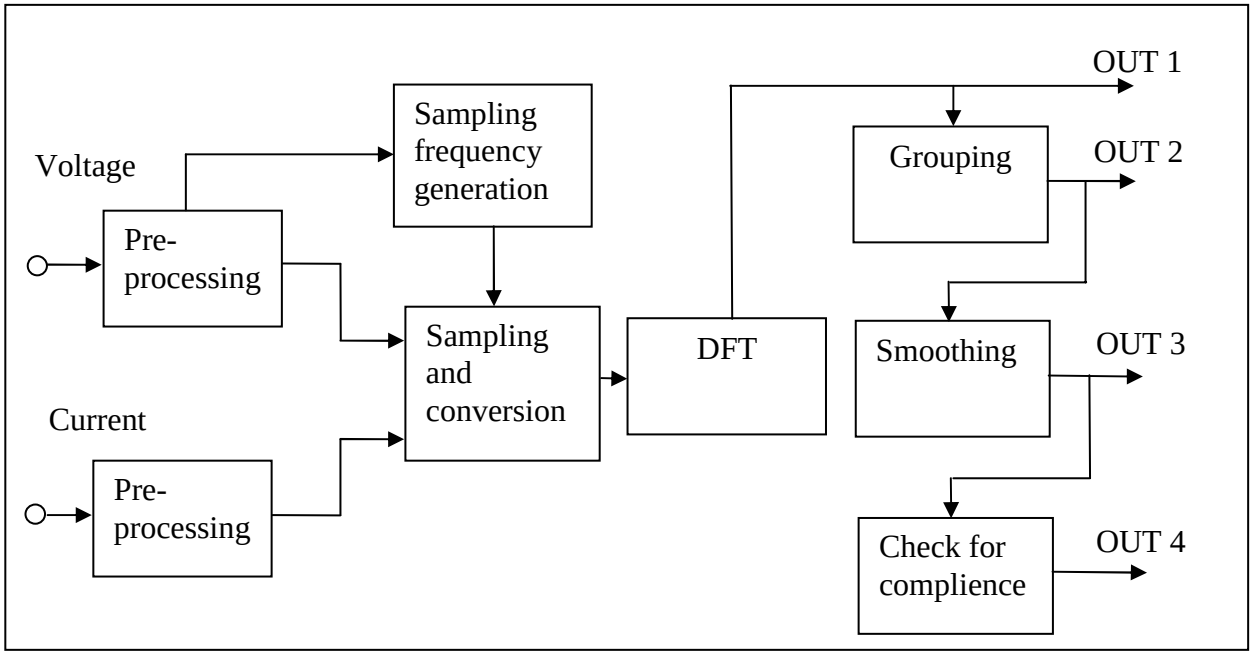


*Figure 2.3. Functional diagram to calculate harmonics according to IEC 61000-4-7.*

**IEC 61000-4-15 (Testing and measurement techniques – Flickermeter – Functional and design specifications):**

In the beginning of the 1980th UIE (Union Internationale D'Electrothermie) defined a model to estimate the level of flicker in a power network. The input signal to the model is voltage waveform data. The model describes how the chain lamp-eye-brain reacts on voltage fluctuations. The outputs of the model are the flicker parameters $I_{FL}$, $P_{ST}$ och $P_{LT}$. Based on the model from UIE, the flicker standard IEC 61000-4-15 has been developed. Figure 2.4 shows a functional diagram of a flickermeter designed according to the IEC 61000-4-15.

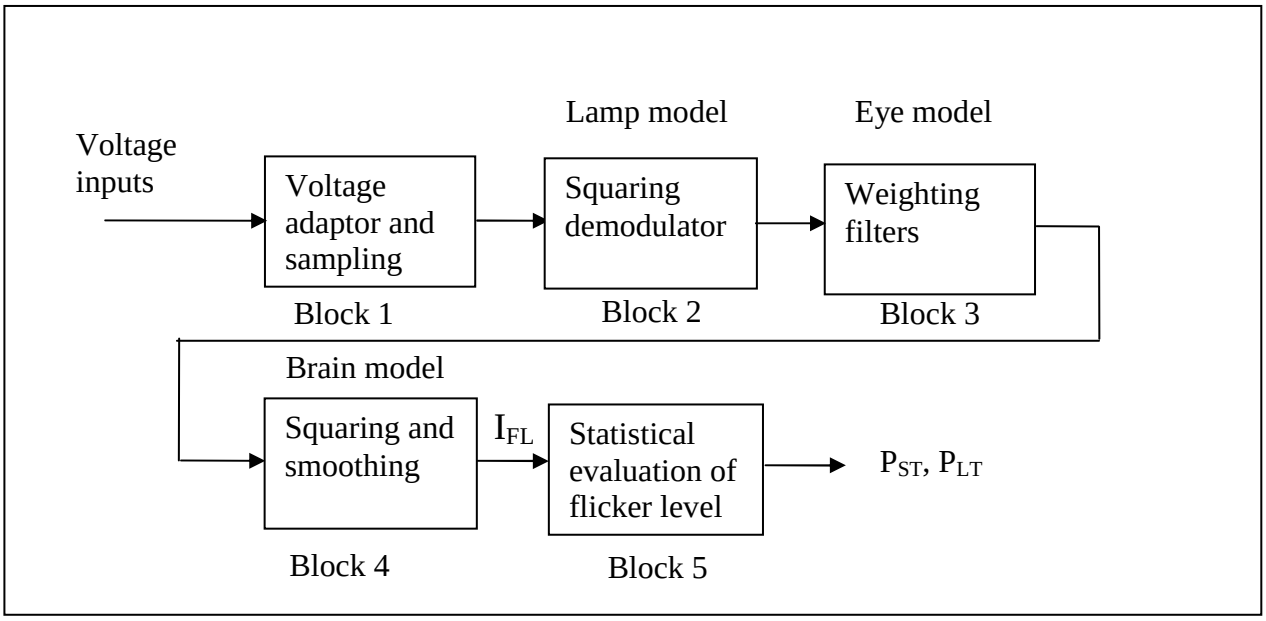


*Figure 2.4. Functional diagram of a flickermeter according to IEC 61000-4-15.*

In block 1, the input signal is scaled, anti-alias filtered and sampled. Block 2 is a squaring demodulator separating the modulating signals from the carrier and the low frequency variations are moved to the baseband of 0-30 Hz. Block 3 consists of two bandpass filters in cascade. The first one eliminates the DC and double mains frequency ripple component. The second one has a centre frequency of 8.8 Hz and simulates the frequency response to sinusoidal voltage fluctuations of a coiled filament lamp (60W-230V) combined with the human visual system. Block 4 is composed of a squaring multiplier and a first order low-pass filter. The human flicker sensation is simulated by block 2, 3 and 4. The output of block 4 is the instantaneous flicker value $I_{FL}$. If the 60W/230V lamp is connected to a voltage with $I_{FL}$=1.0, statistically 50 percent of the people in a reference group will apprehend annoying flicker from the lamp [12]. In block 5, a statistical analysis is performed of the data giving the flicker

parameters $P_{ST}$ and $P_{LT}$. According to EN 50160 the 95% value of the $P_{LT}$ shall not exceed 1.

$I_{FL}$-values are recorded continuosly during 10 minutes and the values are sorted in a duration diagram. The $P_{ST}$-value is calculated from the formula:

$$P_{ST} = \sqrt{\begin{aligned} &0.0314IFL_{0.1} + 0.0175IFL_{0.7} + 0.0175IFL_{1} + 0.0175IFL_{1.5} + 0.0219IFL_{2.2} + 0.0219IFL_{3} + \\ &+ 0.0219IFL_{4} + 0.056IFL_{6} + 0.056IFL_{8} + 0.056IFL_{10} + 0.056IFL_{13} + 0.056IFL_{17} + \\ &+ 0.0267IFL_{30} + 0.0267IFL_{50} + 0.0267IFL_{80} \end{aligned}}$$

where $I_{FLn}$ are the IFL-value exceeded for n% of the 10 min period.

The $P_{LT}$ value is normally based on an observation time of 2 hours and takes into account the effect of several disturbing loads operating randomly. The formula for $P_{LT}$ is given by

$$P_{LT} = \sqrt[3]{\frac{\sum_{i=1}^{N} P_{STi}^{3}}{N}}$$

where $P_{STi}$ are consecutive 10-minutes $P_{ST}$ values and N=12 for an observation time of 2 hours.

## 2.5.2 Voltage Characteristics Standards

**Voltage characteristics of electricity supplied by public distribution systems – EN 50160:**

EN 50160 gives the main characteristics of the voltage at the customer's supply terminals in public low voltage and medium voltage under normal operating conditions. The standard is valid within the EU and in some other countries like Switzerland and Norway. A measurement period of one week is divided into 10-minute intervals. EN 50160 defines limits of different power quality parameters within which any customer can expect the voltage characteristics to remain. The power quality parameters characterised in the standard are power frequency, supply voltage, unbalance, harmonics and interharmonics, signalling and flicker. Also some events like voltage dips, swells and interruptions are mentioned.

*Power frequency*
The nominal frequency is 50Hz. During normal operating conditions, the mean value of the fundamental measured over 10 seconds shall be within a range of:

- for systems with synchronous connection to an interconnected system:
  50 Hz ± 1% (i.e. 49.5 – 50.5 Hz) during 99.5 % of a year.
  50 Hz + 4% / -6% (i.e. 47 – 52 Hz) during 100 % of the time.

- for systems with no synchronous connection to an interconnected system :
  50 Hz ± 2% (i.e. 49 – 51 Hz) during 95 % of a week.
  50 Hz ± 15% (i.e. 42.5 – 57.5 Hz) during 100 % of the time.

Above intervals are valid for both low- and medium distribution. Sometimes regional variations occur. For example, the Nordel system strives to keep the frequency within 50Hz ± 0.1Hz which is a narrower frequency span compared to the interval defined in EN 50160.

*Supply voltage*
Under normal operating conditions, during each period of one week 95% of the 10 min mean rms values of the supply voltage shall be within the range of $U_n$ ±10% and all 10 minutes mean rms values shall be within the range of $U_n$ +10% - 15%. The intervals are valid for both low- and medium voltage distribution.

*Supply voltage dips (voltage sags)*
EN 50160 gives only indicative values for supply voltage dips. Under normal operating conditions the expected number of voltage dips per year may be from up to a few tens to up to one thousand. The majority of the dips have duration of less than 1 s and a depth of less than 60%. However voltage dips with greater depth and duration can occur infrequently.

*Temporary overvoltages between live conductor and earth (voltage swell)*
Only indicative values are given. For example a fault occurring upstream of a transformer will produce temporary overvoltages on the low voltage side. Such overvoltages will generally not exceed 1.5 kV.

*Short interruption:*
EN 50160 gives only indicative values. Under normal operating conditions the annual occurrence of short interruptions ranges from a few to up to several hundreds. The duration of approximately 70% of the short interruptions may be less than one second.

*Long interruption*
EN 50160 gives only indicative values. Under normal operating conditions the frequency of voltage interruptions longer than 3 minutes may be less than 10 or up to 50 per year depending on the area.

*Transient overvoltages between live conductor and earth*
According to EN 50160, transient overvoltages will normally not exceed 6 kV peak, but will higher values occur occasionally. No indicative values are given in EN 50 160 regarding the annual occurrence of transient overvoltages.

*Flicker*
Under normal operating conditions, in any period of a week the 95% value of the long term flicker severity, $P_{LT}$, shall not exceed 1.0.

*Unbalance*
Under normal operating conditions, in any period of a week the 95% value of the 10 minute mean rms values of the negative phase sequence component of the supply voltage shall not exceed 2% of the positive phase sequence component.

*Harmonics and $THD_F$*

Under normal operating conditions, in any period of a week the 95% value of the 10 minute mean rms values shall be less than or equal to the values in table 2.1. The values are given in percent of the voltage nominal value $U_n$. The voltage distortion $THD_F$ shall be based on harmonics up to the 40:th. The 95% value of the $THD_F$ shall not exceed 8%.

| Odd harmonics | | | | Even harmonics | |
|---|---|---|---|---|---|
| Not multiples of 3 | | Multiples of 3 | | | |
| Harmonics Order, n | $U_n/U_1$ [%] | Harmonics Order, n | $U_n/U_1$ [%] | Harmonics Order, n | $U_n/U_1$ [%] |
| 5 | 6 | 3 | 5 | 2 | 2 |
| 7 | 5 | 9 | 1,5 | 4 | 1 |
| 11 | 3,5 | 15 | 0,5 | 6..24 | 0,5 |
| 13 | 3 | 21 | 0,5 | | |
| 17 | 2 | | | | |
| 19 | 1,5 | | | | |
| 23 | 1,5 | | | | |
| 25 | 1,5 | | | | |

*Table 2.1 Values of individual harmonics at the supply terminals for order up to 25.*

*Mains signalling*

Mains signalling voltages are (low level) signals superimposed on the supply voltage for transmission of information. These include ripple control signals within the frequency range of 110-3000 Hz and power line carrier signals 3 kHz to 148.5 kHz. Their voltage levels (based on 3-second mean rms values) between 0.1 and 100 kHz are regulated by the standard EN 50160.

# Chapter 3

# Power Quality Monitoring

## 3.1 Need for power quality measurements

Power quality measurements are needed for several different purposes. Some important purposes are

- verifying of disturbance levels.
- reducing equipment mal-operation caused by power quality phenomena
- troubleshooting
- preventive maintenance
- load analysis
- planning and design of network investments.
- long time surveys
- network modelling.

Some of the above measurements are mainly of interest to the utilities, others are of concern to the customers and some of the measurements are of concern both to the utility and the customer. Power quality *disturbance levels* specified in a contract must be possible to verify by measurement. Therefore, verifying measurements are performed by the customer or by the utility at the interface between the network and the customer.

Another purpose for a power quality measurement is *troubleshooting*. It is initiated when operational problems are detected. Normally, the recording starts when an event (like a fault etc.) is detected, e.g. when a certain parameter (e.g. the rms voltage) crosses a threshold (e.g. 90% of the nominal voltage). The recorded data give useful information about the condition of the network during and around the time of the event. The instrument must be efficient to handle the data in order to save memory space and to reduce the time it takes to transfer the data to a host for evaluation. Therefore, development of smarter methods for evaluation is progressing continuously. Among many other features, the system may automatically detect the direction (downstream or upstream) to a fault.

For customers whose connection fee is based on the peak load, it is of importance to monitor the load profile in order to reduce the peak demand. Also for the utilities a *load analysis* is of interest, since the peak demand determines the rating of system components like transformers and cables. The power system will be better utilised if the load peaks are reduced.

When *planning* a new power system or extending an existing one it is important to have as accurate information about the characteristics of the network as possible in order to make cost effective solutions. Sometimes, enough information is available from the SCADA system, but sometimes additional information like the level of harmonics etc. is required. More detailed information regarding the power quality is not handled by SCADA but is fully supported by the power quality measurement system.

*A long term survey* of different power quality parameters is valuable for the owner of the network since it will give better and more detailed characteristics of the network compared to the information received from a traditional metering system.

# 3.2 The signal concept

There are many ways that signals can be classified. The most straightforward classification (which is of importance in many applications) is between periodic and non-periodic signals. A periodic signal (see Figure 3.1) repeats itself after a fixed length of time known as the period *T*. More formally, a signal *x(t)* is periodic if:

$x(t) = x(t+T)$, for all $t$

The smallest positive value of T which satisfies this condition is the period. The peak value *X* of *x(t)* during a period is called the amplitude. If a signal does not repeat itself after a fixed length of time it is non-periodic.

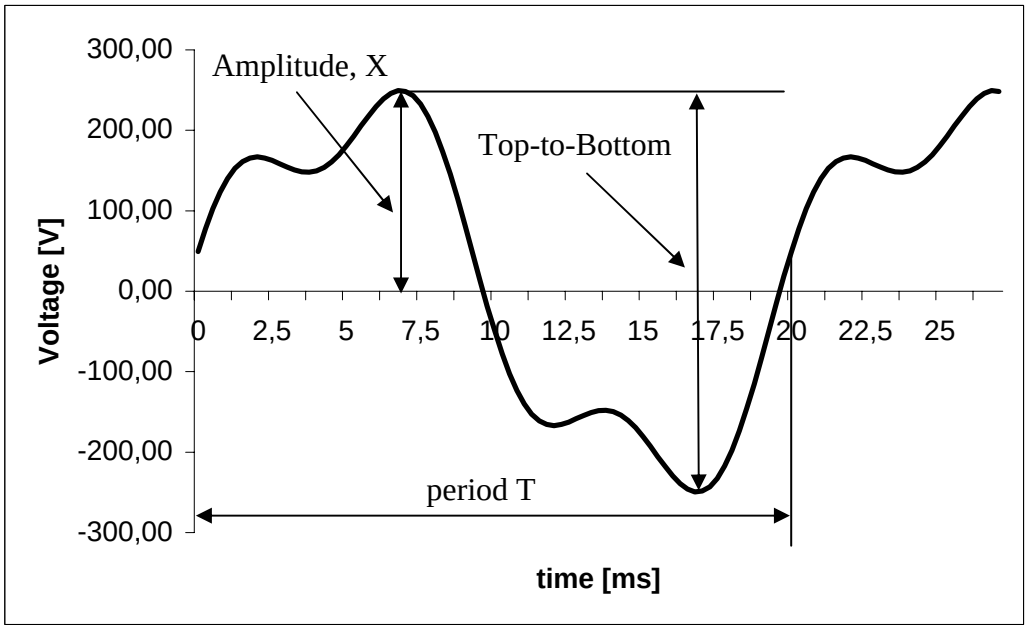


*Figure 3.1.Signal definitions.*

The relation between the period T [s], the frequency f [Hz] and the angular frequency ω [rad/s] is given in [3.1] and [3.2]:

$$\omega T = 2\pi \qquad [3.1]$$

$$\omega = 2\pi \frac{1}{T} = 2\pi f \qquad [3.2]$$

Very important and often used in applications is the frequency domain representation of a signal. This representation (for periodic signals) is known as the trigonometric Fourier series and states that: Any periodic signal x(t) with a period of T seconds can be represented as a summation of sinusoidal components:

$$x(t) = X_0 + \sum_{n=1}^{\infty} X_n \sin(n\omega_1 t + \varphi_n) = A_0 + \sum_{n=1}^{\infty} \left( A_n \cos(n\omega_1 t) + B_n \sin(n\omega_1 t) \right) \qquad [3.3]$$

where

$$A_0 = X_0 = \frac{1}{T} \int_0^T x(t)dt \qquad [3.4]$$

$$A_n = \frac{2}{T} \int_0^T x(t) \cos(n\omega t)dt \qquad [3.5]$$

$$B_n = \frac{2}{T} \int_0^T x(t) \sin(n\omega t)dt \qquad [3.6]$$

$$X_n = \sqrt{A_n^2 + B_n^2} \qquad [3.7]$$

$$\varphi_n = \arctan \frac{A_n}{B_n} \ (+ \pi \text{ if } B_n < 0) \qquad [3.8]$$

Expression [3.3] is the time domain representation of the periodic signal *x(t)*. The signal *x(t)* is a summation of an infinite number of sinusoidal components with increasing frequency and (typically) decreasing amplitude. The sinusoidal component with the lowest frequency (*n=1*) in [3.3] is called the fundamental and has the same period *T* as the signal *x(t)*. The remaining components (*n>1*) are called harmonics. $X_0$ is the average value of *x(t)* (also referred to as the DC component) whilst $X_n$ corresponds to the amplitude of the *n*th harmonic. The harmonics are causing the deviation (i.e. distortion) of the signal from the (ideal) sinusoidal waveform. When specifying a certain harmonic, $X_n \sin(n\omega_1 t + \varphi_n)$, it is common to refer to the order *n* of the harmonic. For example *n=1* refers to the fundamental with the angular frequency $1 \cdot \omega_1$, *n=2* refers to the second harmonic with the angular frequency $2 \cdot \omega_1$ and *n=m* refers to the harmonic of order m and the angular frequency $m \cdot \omega_1$ etc. In a power network, voltages and currents are normally of halfwave symmetry (x(t) = *-x(t+T))* which means only odd multiples (n=1, 3, 5 ,..) of the fundamental will exist.

Equation [3.3] shows that a signal *x(t)* can be represented both in the time domain as well as in the frequency domain. In practical applications, both ways of representation are valuable when describing different phenomena.

## 3.2.1 Calculation of the root mean square (rms) value

The root mean square value $X_e$ (also called the rms value) of a periodic signal *x(t)* with a period of T is defined as:

$$X_e = \sqrt{\frac{1}{T}\int_0^T x^2(t)dt} \qquad [3.9]$$

For a sinusoidal signal, $x(t) = X\sin(\omega t)$, with a amplitude of *X*, the rms value $X_e$ is calculated from the well known formula [3.10]:

$$X_e = \frac{X}{\sqrt{2}} \qquad [3.10]$$

An alternative way to compute the rms value of any periodic signal *x(t)* is to use the amplitudes in the Fourier series:

$$X_e = \sqrt{X_0^2 + \sum_{n=1}^{N}\left(\frac{X_n}{\sqrt{2}}\right)^2} = \sqrt{X_0^2 + \sum_{n=1}^{N} X_{ne}^2} \qquad [3.11]$$

where $X_0$ is the mean value (or DC component), $X_{1e}$ is the rms value of the fundamental and $X_{ne}$ is the rms value of the *n*th harmonic etc. As shown in [3.11], the presence of harmonics increases the rms value of a signal *x(t)*.

# 3.3 Power

## 3.3.1 Power quantities for sinusoidal voltages and currents.

Calculating the power quantities (active-, reactive-, apparent-, and power factor) is quite straightforward as long as the voltages and the currents are sinusodial. Contrary, defining power quantities for signals containing harmonics is not so easy. One way to do it is to start from the instantaneous power *p(t)* given by

$$p(t) = u(t) \cdot i(t) \quad [W] \qquad [3.12]$$

Except when studying rotating machines, the instantaneous power is of limited practical interest. Instead, the time average of the instantaneous power, called the active power *P*, is of more interest and is defined as:

$$P = \frac{1}{T}\int_0^T u(t) \cdot i(t)dt = \frac{1}{T}\int_0^T p(t)dt \quad [W] \qquad [3.13]$$

For a sinusoidal current, $i(t) = I\sin(\omega t + \alpha)$ or voltage, $u(t) = U\sin(\omega t + \beta)$, with a phase shift of $\varphi = \beta - \alpha$, the active power is given by

$$P = \frac{U}{\sqrt{2}} \cdot \frac{I}{\sqrt{2}} \cdot \cos(\beta - \alpha) = U_e \cdot I_e \cos(\beta - \alpha) = U_e \cdot I_e \cos(\varphi) \qquad [3.14]$$

The apparent power *S* is defined as the product of the rms value of voltage and current. For a sinusoidal voltage and current the apparent power is calculated from the equation [3.15]:

$$S = \frac{U}{\sqrt{2}}\frac{I}{\sqrt{2}} = U_e \cdot I_e \qquad [3.15]$$

where $U$ and $I$ are the amplitudes in voltage and current.

The power factor *PF* (or $\lambda$), is defined as the ratio of the active power to the apparent power describing the utilisation of the power system where a low value of PF corresponds to low utilisation. The power factor for a voltage and a current which is sinusoidal with an angular frequency $\omega$ and a phase shift $\varphi$ is given by:

$$PF = \frac{P}{S} = \frac{U_e \cdot I_e \cdot \cos(\varphi)}{U_e \cdot I_e} = \cos(\varphi) \qquad [3.16]$$

From [3.16] it is obvious that if the voltage and current are sinusoidal the power factor can be associated with an angle, $\varphi$, corresponding to a time shift of $\tau = \frac{\varphi}{\omega}$ seconds.

## 3.3.2 Power quantities under harmonic conditions

If voltage and current signals are distorted (i.e. contain harmonics), the active power will be given by the equation:

$$P = U_o \cdot I_o + U_{1e} \cdot I_{1e} \cos(\varphi_1) + U_{2e} \cdot I_{2e} \cos(\varphi_2) + .. + U_{ne} \cdot I_{ne} \cos(\varphi_n) + \ldots =$$
$$= P_0 + P_1 + \ldots + P_n + ... \qquad [3.17]$$

where $P_0 = U_o \cdot I_o$ is the DC (direct current) power and $P_n = U_{ne} \cdot I_{ne} \cos(\varphi_n)$ is the harmonic power corresponding to the *n*th harmonic of voltage and current. From [3.17] it is obvious that both a voltage and a current component (with the same frequency) are needed to produce active power (and of course $\varphi_n \neq 90°$). In strong networks, the power harmonics will be quite small because of low levels of voltage harmonics. Also from [3.17] it is obvious that a power harmonic has either positive or negative sign. That means, the harmonic power flows either towards the load (positive sign) or towards the network (negative sign). A nonlinear load produces (most often) harmonics where the power propagates in both directions for different harmonic orders.

For a distorted voltage and current, the apparent power *S* is defined in the same way as in [3.15], but the equation [3.11] must be used to calculate the rms value of the voltage and current:

$$S = U_e \cdot I_e = \sqrt{U_0^2 + U_{1e}^2 + \ldots + U_{ne}^2 + \ldots +} \cdot \sqrt{I_0^2 + I_{1e}^2 + \ldots + I_{ne}^2 + \ldots +} \qquad [3.18]$$

$$PF = \lambda = \frac{P}{S} = \frac{P_0 + P_1 + P_2 + \ldots + P_n + \ldots}{U_e \cdot I_e} \qquad [3.19]$$

Finally some words about the reactive power *Q*. The definition of reactive power is, like for active power, quite straightforward when voltage and current are sinusoidal. If they are distorted several different definitions of reactive power exist. However, in practical applications, it is mainly the reactive

component $Q_1=U_{1e}\cdot I_{1e}sin(\varphi_1)$, corresponding to the fundamental of voltage and current, that is of interest. This one is the one which is compensated by a capacitor. The reactive power $Q$ does not produce any active work but increases the losses in the network and thus, decreases the efficiency. A more rigorous discussion regarding the power quantities for non-sinusoidal conditions is presented in [10].

## 3.4 Power quality analysers

Advanced surveys in the power network are performed by portable power quality instruments or by permanently installed ones. These instruments are specially designed to measure power quality quantities as well as voltage, current and power. A lot of different kinds of instruments exists on the market. From simple single-phase, non-logging instruments to advanced three-phase instruments measuring simultaneously all power quality parameters of interest. The difference in performance between the instruments is one important reason why the forthcoming standard IEC 61000-4-30 is longed for.

The more advanced power quality instruments are designed to measure all power quality parameters of interest simultaneously. It also communicates with a host computer via modem, Ethernet, RS-485 etc. preferably without interrupting the ongoing measurement. This makes a modern power quality analyser a quite complicated device. Further, the instruments are processing sampled data using digital signal processing methods in order to guarantee highest possible accuracy and reliability. Some design aspects of power quality instruments will be discussed further in this chapter.

## 3.4.1 Analogue to digital conversion

As mentioned earlier, a modern power quality instrument processes sampled data, which means the signals are stored and represented in a digital format. The conversion from an analogue signal to digital representation is done by an ADC (Analogue to Digital Converter). The analogue signal is sampled (read) by the ADC at discrete times (sampling points). The time between two samples is called the sampling period ($T_s$). At the sampling points, the instantaneous value of the analogue signal is converted into a corresponding digital (binary) value and stored in the memory.
In Figure 3.2 the principle of sampling is shown. The output signal of the ADC is quantified into $2^M$ levels, where $M$ is the number of bits of the ADC. Most of the ADCs used in modern power quality instruments are using 12 to 14 bits. The number of conversions per second is referred as the sampling frequency $f_s$ and is related to the sampling period $T_s$ as:

$$f_s = \frac{1}{T_s} \qquad [3.20]$$

According to the well-known sampling theorem, the analogue signal shall be sampled at the rate of at least twice the frequency of the highest frequency component existing in the analogue signal. If not, a certain frequency component can be mistaken as a lower frequency component and this is what aliasing is about. In practise, frequency components higher than half the sampling frequency are attenuated by an (analogue) anti-alias filter placed before the ADC. This anti-alias filter will reduce the problems of aliasing effectively.
Since the ADC continuously produces a stream of sampled data, it is common to gather a number of samples together. The gathered samples are often referred to as a time window. The samples within the time window are normally subjected to mathematical processes. In some instruments there are no time gaps between the time windows. In some instruments the hardware is not powerful enough to process the data without time gap. Such instruments will not fulfil the requirements in the standard IEC 61000-4-30.

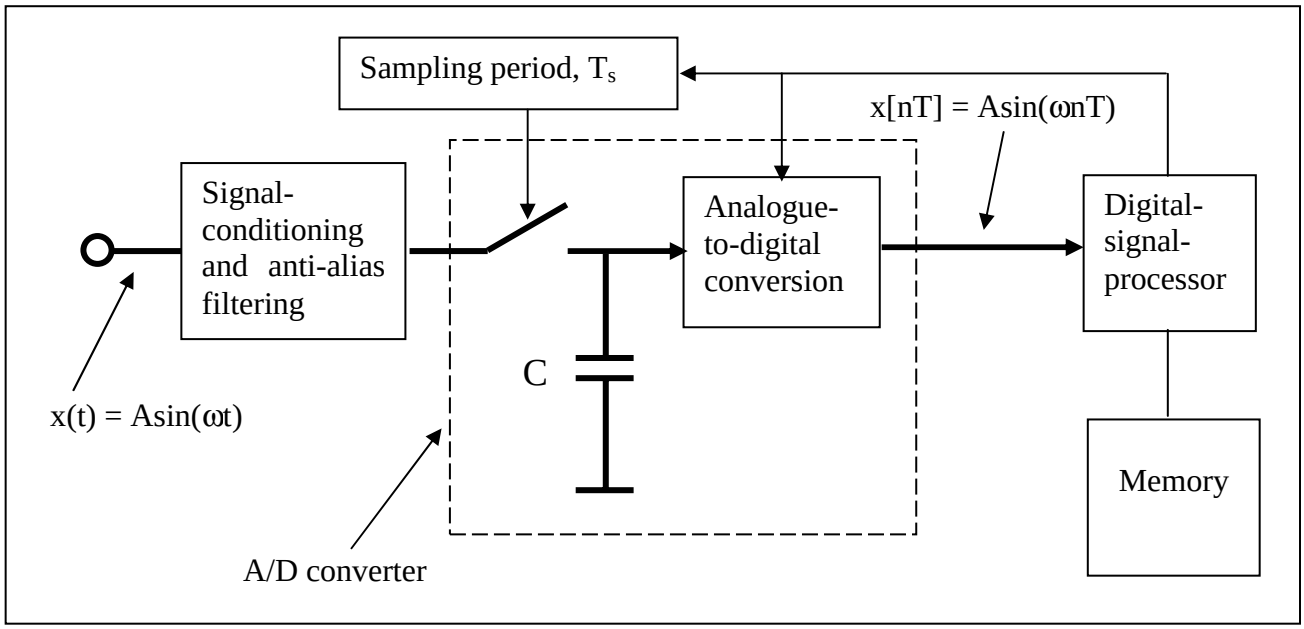


*Figure 3.2. The principle of sampling.*

The sampling process is mathematically described as a substitution of the independent variable *t*:

$$t \rightarrow n \cdot T_s \qquad \text{where } n = 0, 1, 2, ... \qquad [3.21]$$

As mentioned earlier, the analogue signal *x(t)* is, after the ADC, represented as a time- and amplitude discrete signal $x[nT_s]$. The quantisation in amplitude has a resolution of $2^M$*-1* quantisation steps, where *M* is the number of bits of the ADC. The quantisation step size *q* is determined by full-scale level of the ADC, referred as $U_{REF}$, and the number of bits *M*:

$$q = \frac{U_{REF}}{(2^M - 1)} \approx \frac{U_{REF}}{2^M} \quad V \qquad [3.22]$$

The quantisation step size *q* for a 12-bit ADC with a full range of ±10V is $20/2^{12}$, which is 4.9 mV.

As an example, [3.23] shows the sampling process of a sinusoidal with amplitude of 230V and a frequency of 50 Hz:

$$x(t) = X \sin(2\pi 50t) \quad \rightarrow \quad \text{int}\left\{\frac{X}{U_{FS}} \cdot q^M \cdot \sin(2\pi 50 n T_s)\right\} \qquad n = 0, 1, 2, 3, ... \qquad [3.23]$$

where $U_{FS}$ is the full scale value of the signal corresponding to the full scale value of the ADC reference signal. The conversion process in [3.23] is shown in Figure 3.3.

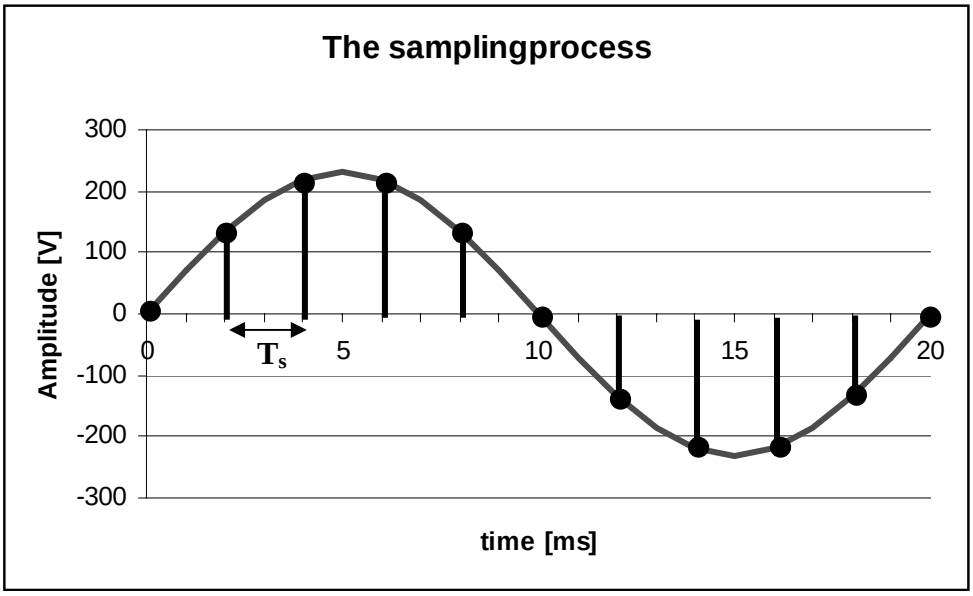


*Figure 3.3. The sampling process of a sinusoidal.*

It is quite easy to perform calculations of the sampled data. For example the rms value $X_e$ of a sampled sequence of $N$ samples is calculated from the equation:

$$X_e = \sqrt{\frac{1}{N}\sum_{n=0}^{N-1} x^2(n)} \qquad [3.24]$$

where x(0), x(1), x(2) ,..., x(N-1) are the sampled values.

The frequency spectrum of a time discrete signal *x(n)* is obtained by using the *Time Discrete Fourier Transform* (TDFT or DFT). The DFT says that a N-point sampled signal $x(nT_s)$ is represented in the frequency domain by $N$ complex frequency components *X(k)* according to the formula

$$X(k) = F_D[x(nT_s)] = \sum_{k=1}^{N-1} x(nT_s) e^{-jk\omega_1 nT_s} = \left\{ \omega_1 = \frac{2\pi}{NT_s} \right\} = \sum_{k=1}^{N-1} x(nT_s) e^{-jkn\frac{2\pi}{N}} \qquad k = 0, 1, ..., N-1 \qquad [3.25]$$

In [3.25], index *k* is representing the harmonic with the corresponding order (i.e. *k=1* corresponds to the fundamental, *k=3* to the 3rd harmonic etc.). Thus, the time discrete input signal will give a discrete frequency spectrum as output from

the DFT. The frequency resolution between two harmonics *k=n* and *k=n+1* is given by the equation:

$$\omega_1 = \frac{2\pi}{N \cdot T_s} \quad \rightarrow \quad f_1 = \frac{1}{N \cdot T_s} = \frac{f_s}{N} \quad [Hz] \qquad [3.26]$$

In practise when calculating the frequency spectrum of the signal, a fast algorithm referred to as the *Fast Fourier Transform (FFT)* is used. The FFT is based on the DFT but is using the symmetry properties of the trigonometric functions to (significantly) reduce the number of calculations needed in [3.25].

*Quantisation noise*

Before conversion to digital representation the analogue signal is assigned to one of $2^M$ levels. This process, called quantisation, introduces an error which cannot be removed. The amount of quantisation error is a function of the number of bits *M* of the ADC. This means an *average error* of one half of an LSB (least significant bit) which is

$$\frac{1}{2} \cdot 2^{-M} = 2^{-(M+1)} \qquad [3.27]$$

The *quantization error e* is defined as the difference between the correct value and the value produced by the ADC. This error is normally assumed to be random and uniformly distributed (i.e. P(e) = 1/q) in the interval ± q/2 with zero mean. In this case the *quantisation noise power*, $\sigma^2$, is given by

$$\sigma^2 = \int_{-q/2}^{q/2} e^2 \frac{1}{q} de = \frac{q^2}{12} \qquad [3.28]$$

If relating the (average) power of the signal to the quantisation noise power, the signal-to-noise power (SQNR) can be calculated. For a sinusoidal with an average power of $A^2/2$ (converted to a digital representation by an M bits ADC), the *SQNR* is given by

$$SQNR = 10\log\left(\frac{A^2/2}{q^2/12}\right) = 10\log\left(1.5 \cdot 2^{2M}\right) = (6.02M + 1.76)\ dB \qquad [3.29]$$

In practise, the achievable *SQNR* will be less than the theoretical maximum value given in [3.29] due to the signal-to-noise (SNR) ratio of the analogue signal. The *SQNR* increases with the number of bits *M* but it is not necessary to use an ADC giving better resolution than the *SNR* of the analogue signal. It will only result in a better representation of the analogue noise.

Finally, some advantages using digital signal processing techniques are given here:

*High accuracy*. The results of (mathematical) manipulations of a time discrete signal are normally very accurate. The accuracy is very much obtained by the number of bits of the ADC and the overall performance of the device containing the ADC.

*Flexibility*. In a digital system, all calculations are performed by the software. New algorithms and measurement functions can (easily) be implemented by updating the software.

*Limited ageing*. After the ADC, the signal processing is digital. This means, the algorithms being used are all in software and results will not change due to ageing, which always will happen in analogue systems.

*Easy to transfer the data*. To transfer data represented in digital format from one point to another is easy with today's communication techniques.

## 3.4.2 Block diagram of a modern power quality analyser

Figure 3.4 shows an example of the building blocks of a power quality instrument. A modern power quality instrument is always designed for three phase measurements. The instrument allows for at least four voltage channels and four current channels. Three of the voltage channels are dedicated to measure the phase-to-neutral voltages or the phase-to-phase voltages. The fourth channel can be used to measure any voltage like the neutral-to-protective ground voltage etc. Three of the current channels are dedicated to measure the phase currents. The fourth channel is often used to measure the current flowing in the neutral.

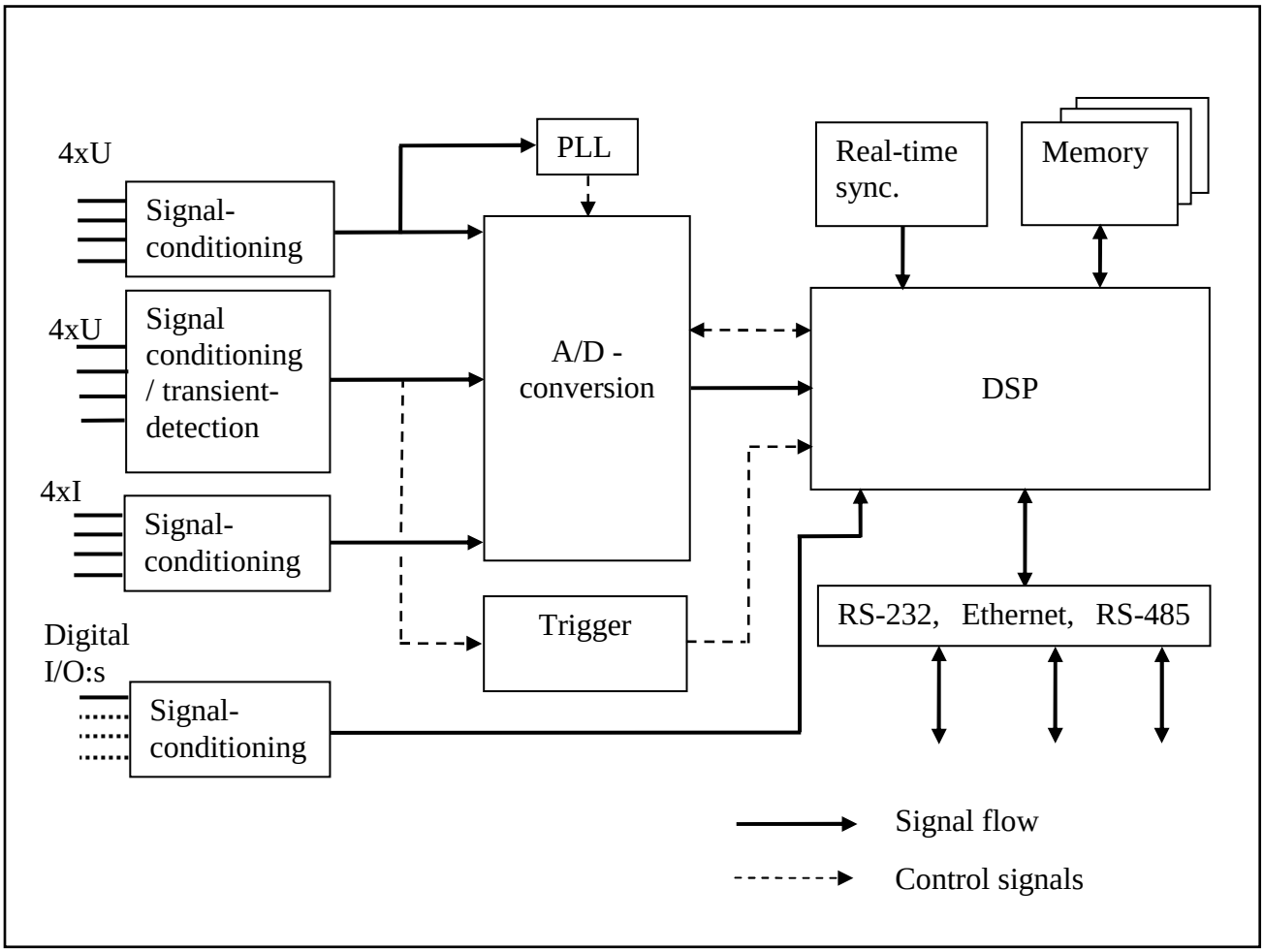


*Figure 3.4. Building blocks of a modern power quality instrument.*

*Analogue inputs and A/D conversion*

The input signal conditioning and the A/D conversion forms the basis of a modern monitoring system. The digitalisation simplifies the design of analogue circuitry and provides greater flexibility for altering the algorithms to be used for manipulating (processing) the (sampled) data. The overall accuracy of the system depends on the input dynamic range, the sampling rate, and the number of bits in the ADC.

Two different signal paths exist on the input channels. The signal from the first path is used for calculation of power quality parameters referred as variations (see Section 2.3) while the signal from the second path is used to detect events like transients etc. The signal from the first path is passing an anti-alias filter in order to minimise aliasing. All analogue signals are connected to a multiplexer which is a channel selector for the ADC. The multiplexer must switch between the input channels at a high speed rate; otherwise the time delay between the conversions will introduce an error when certain parameters like the power quantities are calculated. Instead of using a multiplexer and a single-ADC, one

ADC can be used per input channel. The most important advantage with such a multi-ADC system is that the A/D conversion will start exactly at the same time on all channels. No time delay is introduced. See Figure 3.5. Although the multi-ADC system is a more accurate solution; most of the existing systems are based on the concept of one multiplexer and a single-ADC because the implementation of a multi-ADC system is too expensive compared to the benefits it gives.

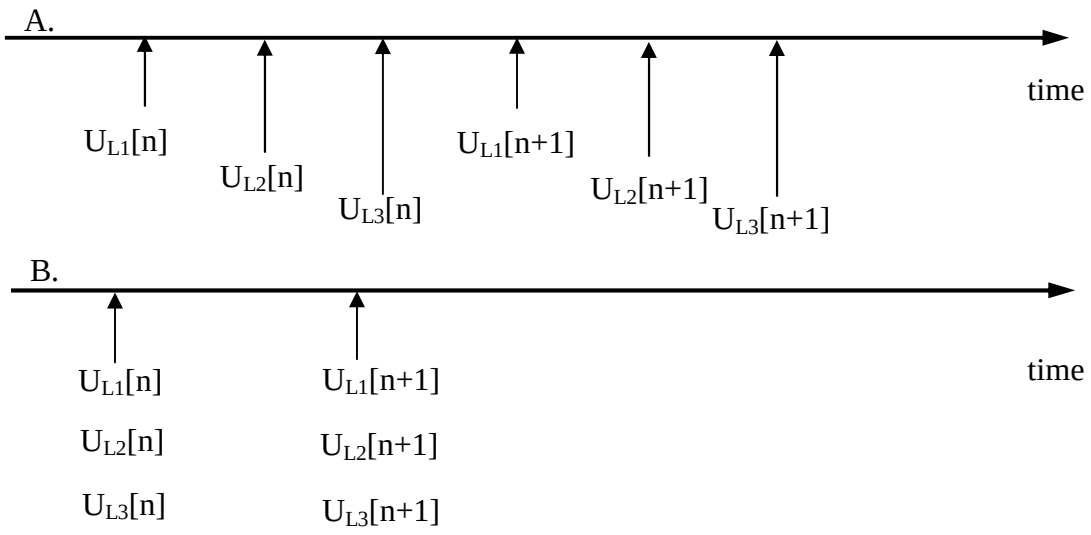


*Figure 3.5. Two different methods of sampling a multi-channel system. A is using a multiplexer and single-ADC while B is a multi-ADC solution.*

*Digital input and output channels*

The new generation of power quality systems will be able to monitor other types of phenomena than pure power quality related ones. Therefore, in some power quality measurement systems also digital input and output channels are implemented. One reason for implementation is the increasing demand of equipment which is a combination of a traditional power quality analyser and a fault recorder. The digital inputs are monitoring the (actual) status of relays, circuit breakers etc. When such a device is tripping, the information from the digital channels are stored along with the traditional power quality parameters. A fault can thereby be evaluated more accurately.

*Generation of the sampling frequency*

The sampling frequency is locked to a multiple of the actual power frequency by using a Phase Locked Loop (PLL). Figure 3.6 shows a block diagram of a PLL. The PLL consists of a comparator, a phase detector, a low-pass filter (LP-filter), a Voltage Controlled Oscillator (VCO) and a divider (counter). The purpose of the PLL is to take a signal from the VCO, divide the frequency by an integer N and compare (in the phase detector) that result with the frequency of the reference signal $U_{L1}$ (i.e. power network signal). The phase detector output is fed back to the VCO through a lowpass filter. The loop works to adjust the output of the phase detector to zero automatically. That means the output of the divider is precisely on the same frequency as the reference signal. If the frequency of the reference signal is changing, the output of the phase detector will give a non-zero output. The frequency of the VCO will thereby change until the PLL is locked to this new frequency. The output from the VCO is used to trigger A/D conversion at a sampling rate which is exactly *N* times higher than the actual power frequency.

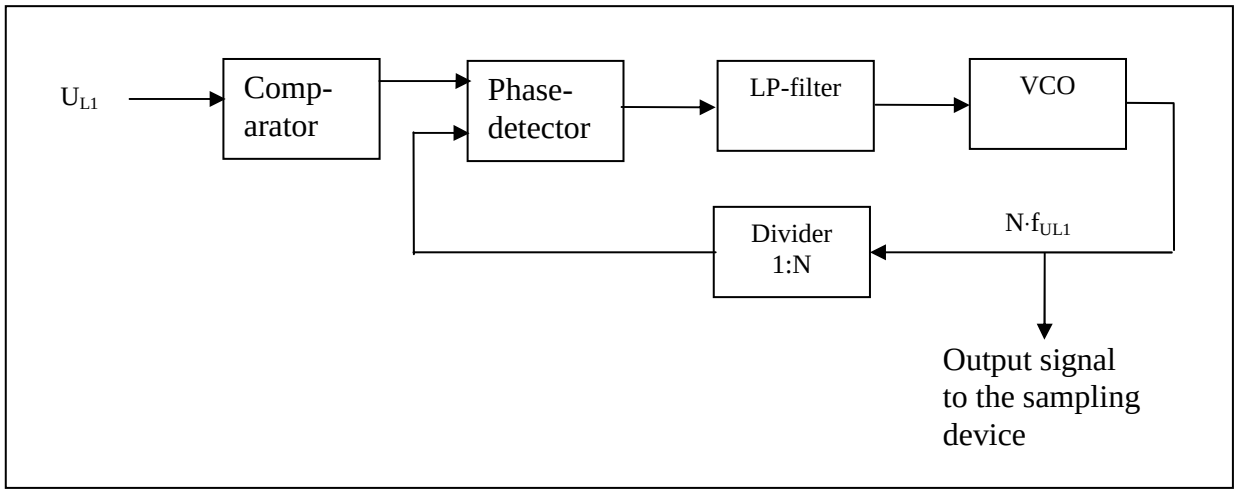


*Figure 3.6. Functional blocks of a simple Phase-Locked-Loop (PLL).*

*Time synchronisation*

In a power quality survey (especially troubleshooting) is it important to know *when* certain phenomenon occurs. Therefore, all power quality instruments have a built-in real-time clock. Moreover, if it is necessary to carry out simultaneous measurements at different geographical locations, time synchronisation is a must. Depending on the requirements in such a measurement, the accuracy of the internal real-time clock is often enough. But in some application a more accurate time synchronisation is needed. In those cases, a GPS receiver connected to the instrument will manage the time synchronisation. The cost for

such a device has decreased significantly over the past years and therefore making it to an attractive solution in many applications where extreme accuracy in real time is needed. One possible disadvantage of a GPS is that the signals from the satellites are sometimes too weak. This happens especially at indoor locations.

*Memory*

The memory size and structure of the memory used in a modern power quality instrument depend on the amount of data to be processed and transferred. The design is critical if continuous data acquisition with no interruption in the measurement is to be achieved. Circular memory buffers are used for quick access to the data when calculations are performed. Normally an instrument has memories of two different types. One type is a fast memory (i.e. SRAM) in which the software is stored and running. The other one is a non-volatile memory (i.e. flash memory) in which the measurement data is stored. In some instruments, a hard drive is used to store measurement data. The advantage of using a hard-drive is the memory capacity. On the other hand, it is a disadvantage to use a hard-drive in portable instruments since it is sensitive to mechanical damages.

*Communication*

Configuration of a measurement instrument and transfer of measurement data to a host are two examples where a communication link is needed. Therefore, a power quality instrument is always equipped with at least one communication link. A serial interface like RS-232 is always implemented, but also Ethernet have been more common in newer instruments.

*Error*

The total error in a measurement is a sum of errors that can (mainly) be divided into three different categories:

- instrument errors (quantisation, offset- and linearity errors etc.)
- transducer errors
- errors due to the measure signal (low signal level etc.)

The (theoretical) maximum error that can occur is the sum of the absolute values of each individual maximum error. This error is probably greater than the actual one since a summation of the absolute values will give the “worst case” error. A more realistic estimation of the total possible error is achieved by the concept of uncertainty where each error contribution can be considered statistically

distributed. If the uncertainties can be considered independent and if they follow the normal (Gaussian) distribution, the total uncertainty is calculated as the root square sum of the individual errors.
An example: Consider an instrument contributing with a maximum error of 0.2%, the transducer is contributing with a maximum error of 0.5% and the signal itself is contributing with a maximum error of 0.5%. The maximum error according to the summation of the absolute values of each individual error gives a total maximum error of 1.2%. Using the concept of uncertainty, the root square sum gives a total uncertainty of only 0.73%.

*Time window*
As mentioned earlier (see Section 3.4.1) a time window is defined as a number of sampling values used as a base for different kinds of calculations. From this base window (e.g. 10 periods for 50 Hz according to IEC 61000-4-30) other time windows can be defined (150 periods, 10 seconds, 10 minutes and 2 hours according to IEC 61000-4-30). The principle of aggregation of a base window to another time window is shown in Figure 3.7.

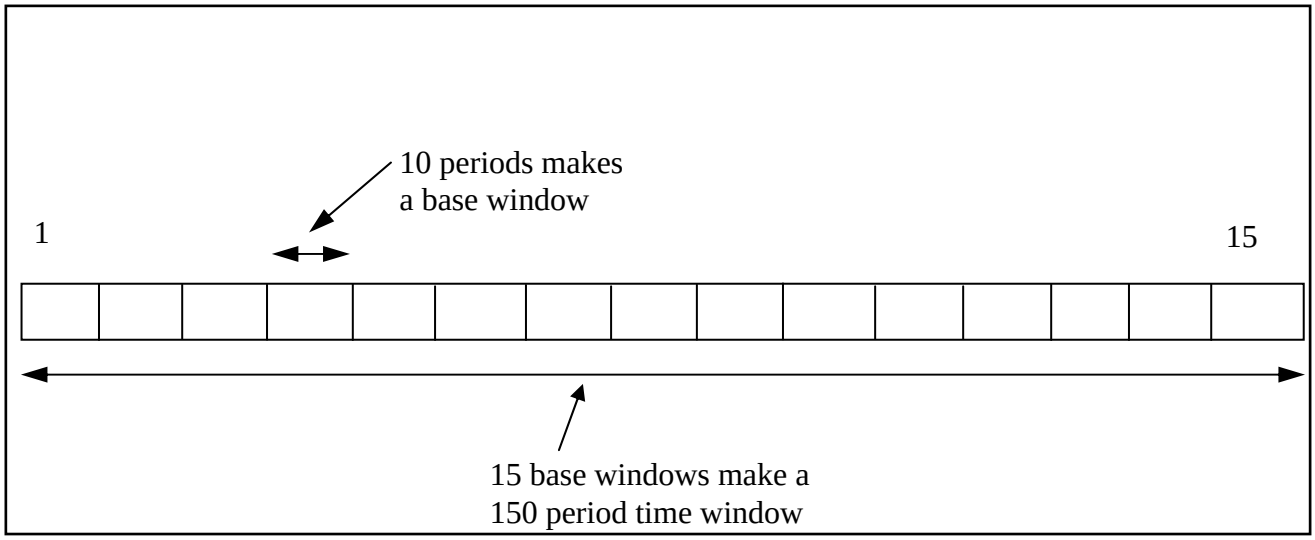


*Figure 3.7. Example of time aggregation from a number of base windows.*

As an example, the calculation (and aggregation) of a rms value is shown in equation [3.30] to [3.32]. The calculation of the rms value of the base window is shown in [3.30] and the aggregation process is shown in [3.31] and [3.32]. As shown in the equations, the time resolution of the rms value depends only on the number of samples included in the calculation. The rms value of the base window is given by

$$U_{10-cycles} = \sqrt{\frac{1}{N}\sum_{k=0}^{N-1} u_k^2} \qquad [3.30]$$

where $u_k$ is the $k$th sample value. The 150 cycle rms value, $U_{150\text{-}cycles}$, is calculated from 15 $U_{10\text{-}cycles}$ values (no time gap between two base windows) and is given by:

$$U_{150-cycles} = \sqrt{\frac{1}{15}\sum_{k=0}^{14} U_{10-cycles}^2(k)} \qquad [3.31]$$

The aggregation to a 10 minute rms value, $U_{10min}$, includes 3000 $U_{10\text{-}cycles}$ values as shown in [3.32]:

$$U_{10\,\min} = \sqrt{\frac{1}{3000}\sum_{k=0}^{2999} U_{10-cycles}^2(k)} \qquad [3.32]$$

With the above definitions, and if there is no time gap between the base windows, an alternative way to calculate the 10 minutes rms value is to use 200 $U_{150\text{-cycles}}$ values. The time aggregation described in [3.30]-[3.32] can of course be used to calculate other quantities as well.

Traditionally, a sampling frequency of 6400 Hz has been used as a de facto standard among manufacturers of power quality instruments. A sampling frequency of 6400 Hz means 128 sampling points per period at 50 Hz. The FFT algorithm can be used since 128 is a power of 2. To follow the forthcoming IEC 61000-4-30 the situation will be slightly different. The requirement in IEC 61000-4-30 is a frequency resolution of 5 Hz. With the required base window of 10 periods, and a wish to use the FFT algorithm, 1024-point FFT calculation must be performed on each base window. The "new" sampling frequency will be 5120 Hz. Harmonics up to the 51st can be evaluated with a resolution of 5 Hz.
Some more words about the (Fast Fourier Transform) FFT algorithm. In practise, the frequency spectrum of a signal is almost always obtained by the FFT algorithm because of the savings in complex multiplications and additions compared to the DFT. The number of complex multiplications and additions performed in a N-point DFT calculation is proportional to

$$N^2 \qquad [3.33]$$

The FFT calculation is much more efficient and thus, less time consuming. The number of complex multiplications and additions performed in a N-point FFT calculation is proportional to

$$\frac{N}{2}\log_2 N \qquad [3.34]$$

The difference between [3.33] and [3.34] is significant, especially with high values of *N*.

Calculation of the frequency spectrum is the most time consuming task in a power quality analyser. Therefore it is of great interest to see the consequence when calculations are changed from 128-point FFT to 1024-point. The 1024-point FFT calculation corresponds to ten 128-points FFT calculations since the 128-point FFT is based on one cycle. The comparison is given in [3.35]:

$$\frac{\frac{1024}{2}\log_2 1024}{10\frac{128}{2}\log_2 128} = 1.142 \qquad [3.35]$$

If only the time of calculation is taken in account, it will take about 14% longer time to calculate a 1024-point FFT compared to ten 128-point FFT. In practise, the difference in time will be shorter since it takes some time to process ten 128-point FFT further. Taken this into account, the difference in time will not be significant at all. One advantage of making many 128-point FFT calculations is the possibility to use the time between two FFT calculations for other tasks (i.e. time sharing). A possible disadvantage of using a 1024-point FFT is the demand of more buffer memory.

# Chapter 4

# Measurement methods for calculation of the direction to a flicker source

## 4.1. Introduction

It is important to keep the level of flicker in the network as low as possible, especially since a single flicker source often affects a large number of customers. The flicker sources are devices like arc furnaces, welding machines etc. which are connected to the high voltage grid. The connection of the devices to the high voltage grid is one reason why flicker propagates widely in the network. Solutions available to reduce the level of flicker are either strengthen the network, isolate the flicker source or installing a special device like a Static Var Compansator (SVC). It is of mutual interest for both the utility and the customers to find the flicker source. The network operator wants to be perfectly sure that they are discussing with the actual producer of the flicker. The customer wants to be perfectly sure that the flicker originates within its premises. Any disagreements regarding the flicker source will cause a slow-down in the mitigation process. Therefore, a measuring instrument helping to locate the source of flicker is highly demanded. Existing instruments measure only *the level of flicker* and do not give any information regarding the direction to the flicker source. Therefore, in this work three new measurement methods

are proposed with the purpose to give information of the direction to the flicker source. These new measurement methods can easily be implemented in existing measuring instruments.
In Chapter 4 the measurement methods are developed theoretically and in Chapter 5 verifying tests are presented. The overall results are so promising that a patent application for the three developed measurement methods has been submitted.

# 4.2 Measurement method model

The measurement methods developed are based on the model show in Figure 4.1. On the left in Figure 4.1 is a Thevenin source, consisting of the independent voltage source, $U_g$, and the source impedance $Z_{ig}$. The source is feeding the linear impedances $Z_1$, $Z_2$ and $Z_3$. Furthermore, the impedances $Z_2$ and $Z_3$ are the flicker sources since the switches $B_{Z2}$ and $B_{Z3}$ are manoeuvred at a frequency $f_m$ within the frequency spectrum of visible flicker. Impedance $Z_T$ is the connection between the impedances $Z_1$ and $Z_2$ and the Thevenin source.
The developed model is based on the following assumptions: The voltage source $U_g$ is kept constant independent of the current flowing through the source. Furthermore, the characteristics of the impedances $Z_1$ and $Z_2$ are approximately the same ($R_1/X_1 \approx R_2/X_2$) and the voltage $U_{L1}$ will drop very little when the impedance $Z_2$ is connected.

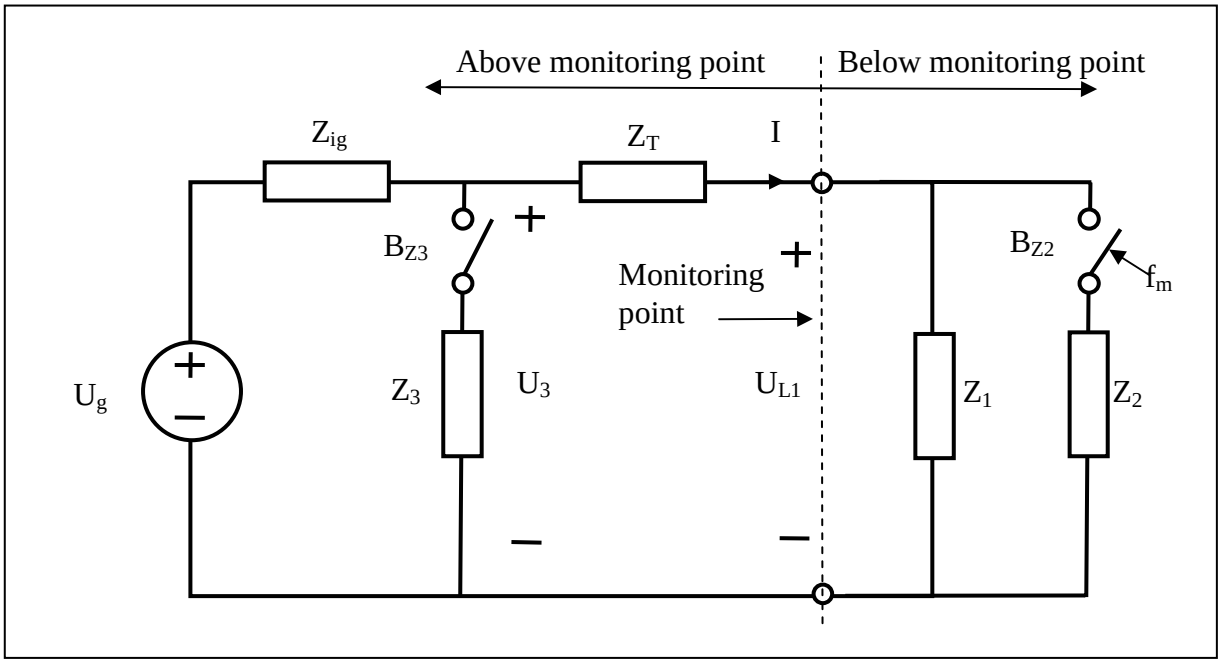


*Figure 4.1. Model used for case 1. Switch $B_{Z3}$ is open and switch $B_{Z2}$ opened and closed at a rate which is within the flicker spectrum.*

The question at issue is:

*Is it possible to determine if a flicker source is placed above- or below the monitoring point by examining how the envelopes of the voltage $U_{L1}$ and current I are changing with respect to each other?*

Two different cases will occur depending on where the flicker source is located with respect to the monitoring point:

*Case 1*: Determine how the envelopes of $U_{L1}$ and *I* are changing with respect to each other if the *flicker source is placed <u>below</u> the monitoring point*. In the model, switch $B_{Z3}$ is open and switch $B_{Z2}$ is manoeuvred at a rate which is within the flicker spectrum. See Figure 4.1.

*Case 2*: Determine how the envelopes of $U_{L1}$ and *I* are changing with respect to each other if the *flicker source is placed <u>above</u> the monitoring point*. In the model, switch $B_{Z2}$ is open and switch $B_{Z3}$ is manoeuvred at a rate which is within the flicker spectrum. See Figure 4.3.

*Case 1:*

When $B_{Z2}$ is open, Kirchoff's voltage law and Ohm's law (considering steady-state condition) give:

$$U_g = (Z_{ig} + Z_T) \cdot I + U_{L1} \qquad [4.1]$$

When $B_{Z2}$ is closed, the current $\Delta I$ will flow through $Z_2$ giving:

$$U_g = (Z_{ig} + Z_T)(I + \Delta I) + U_{L1}^{'} = (Z_{ig} + Z_T)I + (Z_{ig} + Z_T)\Delta I + U_{L1}^{'} = (Z_{ig} + Z_T)I + \Delta U + U_{L1}^{'} \qquad [4.2]$$

Changes in the voltage $U_{L1}$ due to closing and opening of $B_{Z2}$, (i.e. [4.2] – [4.1]) are given by

$$U_{L1}^{'} - U_{L1} = -\Delta U$$

The corresponding change in current is given by:

$$I \rightarrow I + \Delta I$$

The interpretation of the above calculations is: When the impedance $Z_2$ is connected, the voltage across $Z_2$ <u>*decreases*</u> with $\Delta U$. At the same time the current will increase with $\Delta I$. These changes are shown in Figure 4.2.

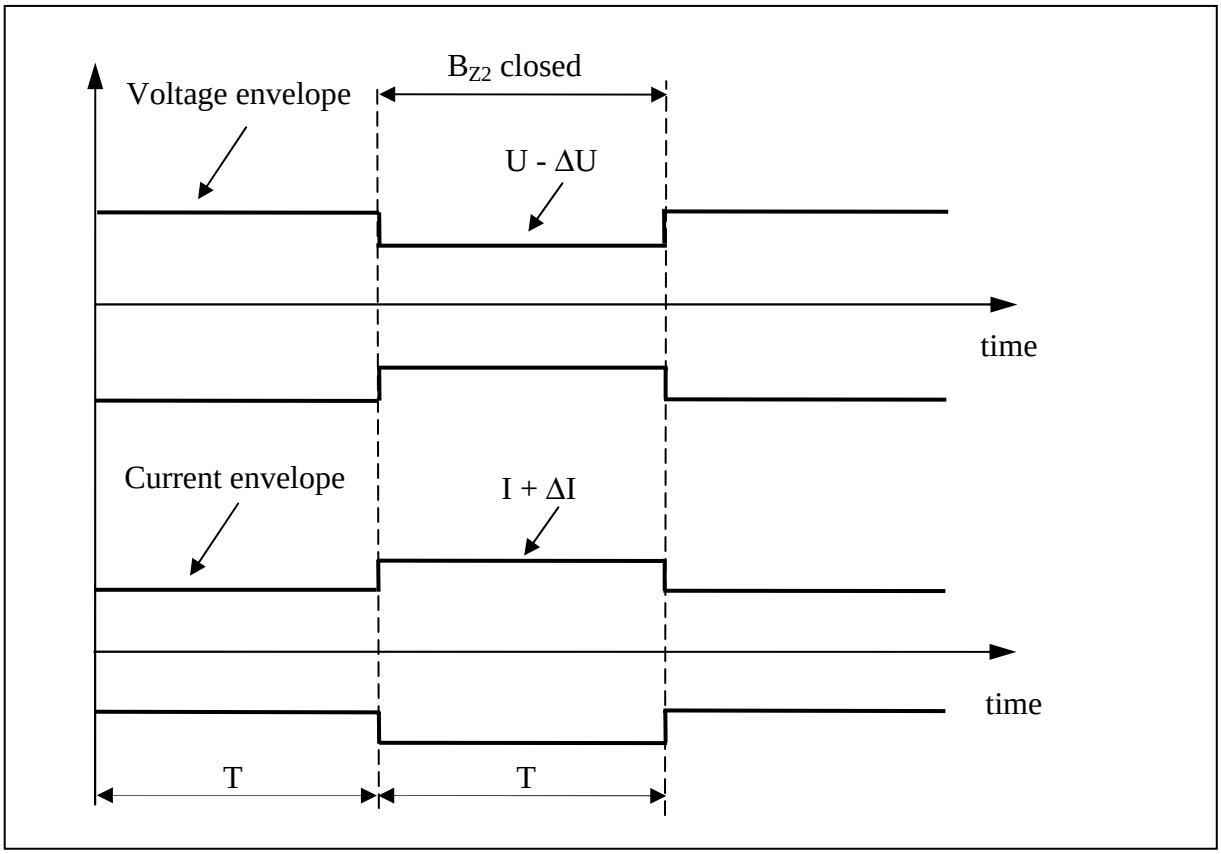


*Figure 4.2. The envelopes of $U_{L1}$ and I before and after the switch $B_{Z2}$ is closed. The changes in voltage- and current envelopes with respect to each other show that the flicker source is placed below the monitoring point.*

*Case 2:*

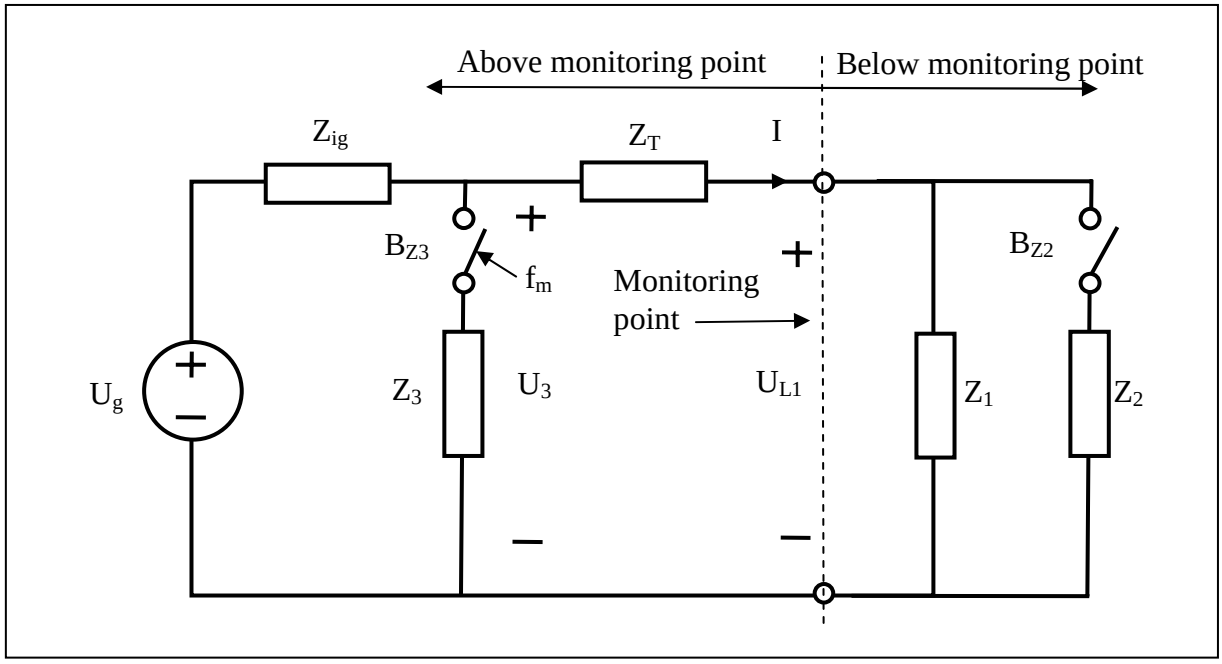


*Figure 4.3. Model used for case 2. Switch $B_{Z2}$ is open and switch $B_{Z3}$ is manoeuvred at a rate within the frequency spectrum of flicker.*

In case 2 $B_{Z2}$ is open and $B_{Z3}$ is manoeuvred at a rate $f_m$ within the frequency spectrum of flicker. When looking at Figure 4.3, it is obvious when $B_{Z3}$ is closing, the voltage $U_3$ will decrease. Since the current $I$ and thereby the voltage $U_{L1}$ is determined by $U_3$, both $I$ and $U_{L1}$ will follow the changes of $U_3$ (all impedances are considered linear).

The voltage $U_3$ across $Z_3$ (when switch $B_{Z3}$ is closed) is given by (see Figure 4.3):

$$U_3 = \frac{U_g}{Z_{ig} + Z_3 //(Z_T + Z_1)} \cdot Z_3 //(Z_T + Z_1) =$$

$$\frac{U_g (Z_T + Z_1) \cdot Z_3}{Z_{ig} \cdot (Z_T + Z_1 + Z_3) + (Z_T + Z_1) \cdot Z_3} = \frac{U_g \cdot (Z_T + Z_1)}{Z_{ig} \cdot (1 + \frac{Z_T + Z_1}{Z_3}) + (Z_T + Z_1)}$$

The current $I$ flowing through $Z_1$ is determined by using $U_3$:

$$I = \frac{U_3}{(Z_T + Z_1)} = \frac{U_g}{Z_{ig} \cdot (\frac{Z_T + Z_1}{Z_3} + 1) + (Z_T + Z_1)}$$

The voltage $U_{L1}$ across $Z_1$ is given by

$$U_{L1} = I \cdot Z_1 = \frac{U_g}{Z_{ig} \cdot (\frac{Z_T + Z_1}{Z_3} + 1) + (Z_T + Z_1)} \cdot Z_1 \qquad [4.3]$$

Studying equation [4.3] it is obvious that a decrease in the current $I$ (because $B_{Z3}$ is closing) is associated with a decrease in the voltage $U_{L1}$, and vice versa (if all impedances are considered linear). The changes of voltage and current envelopes in case 2 will therefore be in phase (see Figure 4.4), which is a different pattern compared to case 1.

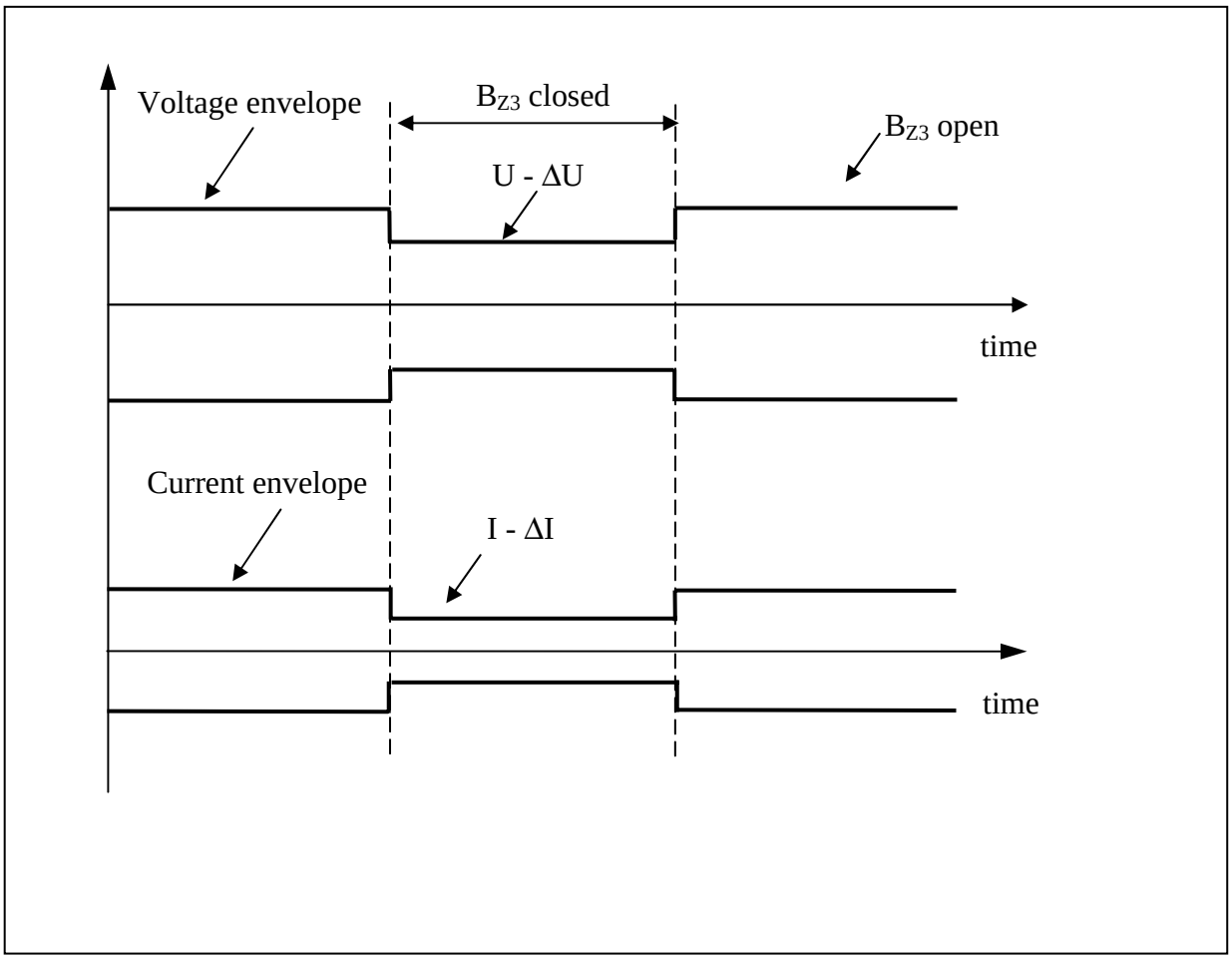


*Figure 4.4. The envelopes of $U_{L1}$ and I before and after the switch $B_{Z3}$ is closed. The flicker source is placed above the monitoring point.*

The conclusions from case 1 and case 2 are:

1. A flicker source will cause changes in the envelopes in *both* voltage and current at the monitoring point. Another way to say it: A flicker source will cause an *amplitude modulation (AM)* of the voltage and current signals in the monitoring point.

2. Changes in the voltage- and current envelopes are *180° out of phase* if the flicker source is located *below* the monitoring point (Figure 4.2).

3. Changes in the voltage- and current envelopes are *in phase* if the flicker source is located *above* the monitoring point (Figure 4.4).

Points 2 and 3 above state: Since changes in the envelopes differ between case 1 and case 2, it must be possible to develop measurement methods which can determine the direction to a flicker source with respect to the monitoring point.

## 4.2.1 Amplitude modulation

According to point 1 above, the voltage and current signals are considered amplitude modulated. A general expression of an amplitude modulated signal $u_{AM}(t)$ is given by

$$u_{AM}(t) = E(t)\cos(2\pi f_c t) \qquad [4.4]$$

where $f_c$ is the carrier frequency (50Hz or 60Hz in this application). Furthermore, equation [4.4] shows that the amplitude $E(t)$ in $u_{AM}(t)$ is varying in time and can be expressed as

$$E(t) = E_c + m(t)$$

$E_c$ is the amplitude of the carrier and $m(t)$ is the modulating signal. Furthermore, the modulating signal $m(t)$ defines the envelope of $u_{AM}(t)$.
In Figure 4.2 and Figure 4.4 the modulating signal $m(t)$ is a square wave with an amplitude of $\Delta U/2$ and $\Delta I/2$ and a modulation frequency $f_m$ of $1/(2T)$ (in Hz).

Let the amplitude modulated signals in voltage and current be expressed as:

$$u_{AM}(t) = (U_c + m_u(t)) \cdot \cos(2\pi f_c t) \qquad [4.5]$$

$$i_{AM}(t) = (I_c + m_i(t)) \cdot \cos(2\pi f_c t) \qquad [4.6]$$

The frequency spectrum of the amplitude modulated signal consists of three signal components (if the modulating signal is a single tone with amplitude $U_m$ at frequency $f_m$): The carrier wave with amplitude $U_c$ at carrier frequency $f_c$, the upper sideband signal with amplitude $U_m/2$ at frequency $(f_c + f_m)$ and the lower sideband signal with amplitude $U_m/2$ at frequency $(f_c - f_m)$ (see Figure 4.5).

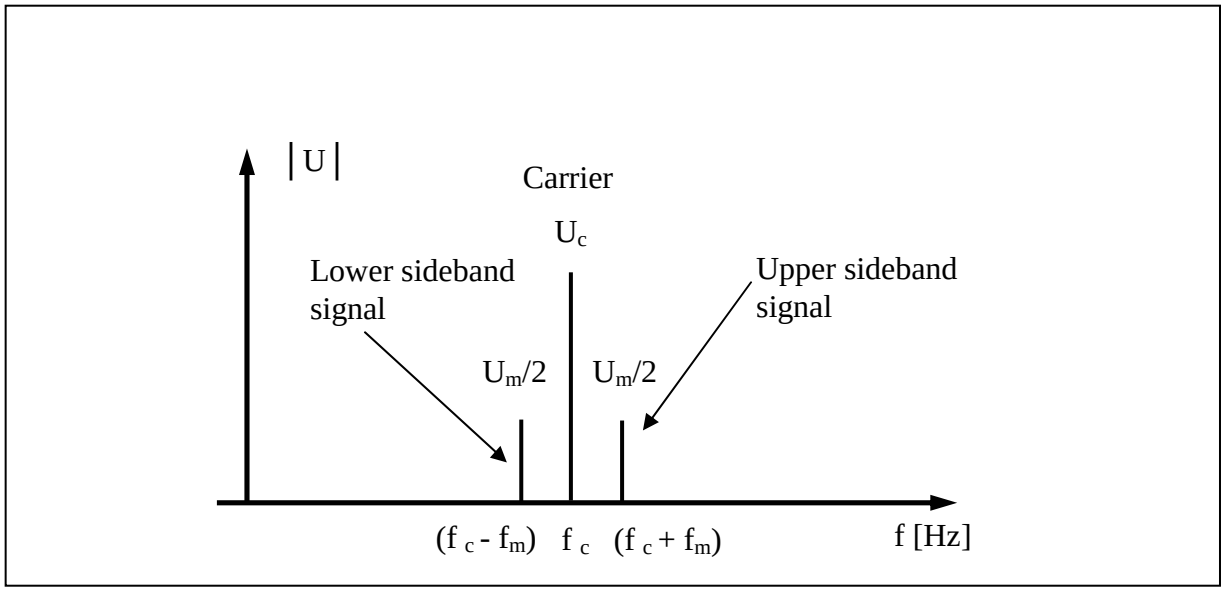


*Figure 4.5. Amplitude spectrum of an amplitude modulated signal (single tone modulation).*

Demodulating the amplitude modulated signal means to recover the modulating signal *m(t)*. Several types of demodulation exist but in the measurement methods developed here, the demodulation process is performed by a square demodulator described in [4.19].

## 4.2.2 Flicker power

The modulating signals $m_u(t)$ and $m_i(t)$ are representing the envelopes of the amplitude modulated signals, and are used for calculation of the *flicker power Π or FP* according the following definitions:

The *instantaneous flicker power*, $p_\Pi(t)$, is defined as

$$p_\Pi(t) = m_u(t) \cdot m_i(t) \quad [\mathrm{W}] \qquad [4.7]$$

The mean of $p_\Pi(t)$ is called the *flicker power, Π or FP*, and is defined as

$$\Pi = FP = \frac{1}{T}\int_o^T p_\Pi(t)dt \quad [\mathrm{W}] \qquad [4.8]$$

There is no real physical interpretation of above definitions. However the sign in [4.8] gives information about direction of propagation of the flicker power with respect to a monitoring point:

If the direction of propagation of flicker power is *from load toward generator* (*case 1*), $m_u(t)$ and $m_i(t)$ will be *out of phase* and the flicker power $\Pi$ will have a negative sign ($\Pi<0$).

If the direction of propagation of flicker power is *from generator toward load* (*case 2*), $m_u(t)$ and $m_i(t)$ will be *in phase* and the calculated flicker power $\Pi$ will have a positive sign ($\Pi>0$).

If the modulating signals $m_u(t)$ and $m_i(t)$ can be considered periodic and containing other frequency components than the fundamental of the modulating signal, $m_u(t)$ and $m_i(t)$ can be written as a Fourier series:

$$m_u(t) = \sum_{k=1}^{\infty} U_{mk} \cos(k\omega_c t + \beta_k) \qquad [4.9]$$

$$m_i(t) = \sum_{k=1}^{\infty} I_{mk} \cos(k\omega_c t + \alpha_k) \qquad [4.10]$$

Using [4.9] and [4.10] in [4.8] gives:

$$\Pi = \frac{1}{T}\int_{o}^{T} p_{\Pi}(t)dt = \frac{1}{T}\int_{o}^{T}\left(\sum_{k=1}^{\infty} U_{mk}\cos(k\omega_c t + \beta_k)\right)\left(\sum_{k=1}^{\infty} I_{mk}\cos(k\omega_c t + \alpha_k)\right)dt = \{orthogonality\} =$$
$$= \sum_{k=1}^{\infty}\frac{U_{mk}\cdot I_{mk}}{2}\cos(\beta_k - \alpha_k) = \sum_{k=1}^{\infty}\frac{U_{mk}\cdot I_{mk}}{2}\cos(\varphi_k)$$

[4.11]

From expression [4.11] it is obvious that the flicker power consists of both a modulating signal in both voltage and current. Expression [4.11] also shows that the term $cos(\varphi_k)$ determines the sign of flicker power.

As mentioned earlier, a sudden change in the current amplitude will immediately result in a change in the voltage amplitude. Therefore, in practice, only the two phase shifts 0° and 180° exist. Sometimes a short duration transient will occur when the amplitude is changing. Such a transient does not affect the accuracy as the transient is attenuated by the filtering process.

# 4.3 Measurement methods for calculating the flicker power

In the previous section, a definition of the flicker power $\Pi$ was given. With this definition as a base, three measurement methods have been developed to calculate the flicker power:

*Measurement method 1:*
The flicker power is determined by calculating the (complex) frequency spectrum of the sideband signals for both voltage and current. Thereafter, the power in the sideband signals is calculated, which is equal to the flicker power.

*Measurement method 2:*
The voltage and current signals are square demodulated. Thereafter, in the frequency domain, the flicker power is calculated from the demodulated base-band signals.

*Measurement method 3*:
The voltage and current signals are square demodulated. Thereafter, the demodulated signals are filtered through a band-pass filter with a transfer function defined in the standard IEC 61000-4-15. The output signals from each filter chain are multiplied giving the instantaneous flicker power, $p_{\Pi}(t)$. The flicker power $\Pi$ is determined as the time average of $p_{\Pi}(t)$.

Measurement method 1 and 2 are based on calculations in the frequency domain while method 3 is based on time domain calculations.

*Complex voltage, current and power*
Measurement method 1 and 2 are using N-point discrete Fourier transform (DFT) for calculation of the frequency spectrum. Input signals to the DFT are the time discrete signals *u[n]* (sampled waveform of voltage) and *i[n]* (sampled waveform of current). The result of the DFT calculation is the complex vector **U:**

$$\mathbf{U} = [U_1, U_2, U_3, ...U_N,] = [|U_1|\angle\beta_1, |U_2|\angle\beta_2, |U_3|\angle\beta_3, ..., |U_N|\angle\beta_N,] \qquad [4.12]$$

and the complex vector **I**:

$$\mathbf{I} = [I_1, I_2, I_3, ..., I_N,] = [|I_1|\angle\alpha_1, |I_2|\angle\alpha_2, |I_3|\angle\alpha_3, ..., |I_N|\angle\alpha_N,] \qquad [4.13]$$

Expressions [4.12] and [4.13] contain the frequency spectrum of *u[n]* and *i[n]* in terms of *N* complex voltages and currents with a resolution in frequency of $\Delta f = f_s / N$ where $f_s$ is the sampling frequency (see [3.26]).

The complex flicker power, $\boldsymbol{S_k=P_k+jQ_k}$ **(**per unit of frequency), is defined from $\boldsymbol{U}$ and $\boldsymbol{I}$**:**

$$\mathbf{S_k} = \frac{1}{2} U_k \cdot I_k^{\,*} = P_k + jQ_k$$

$$\mathbf{P_k} = \frac{1}{2} |U_k| \cdot |I_k| \cdot \cos\varphi_k \quad \text{(active flicker power component)}$$

$$\mathbf{Q_k} = \frac{1}{2} |U_k| \cdot |I_k| \cdot \sin\varphi_k \quad \text{(reactive flicker power component)}$$

and

$$\mathbf{S} = [S_1, S_2, S_3, ...S_N,] \qquad [4.14]$$

For example, the active flicker component $\mathbf{P_1}$ is calculated from the complex flicker power component $\mathbf{S_1}$ by

$$\mathbf{P_1} = \mathrm{Re}\{\mathbf{S}_1\} = \mathrm{Re}\{\mathbf{P_1} + j\mathbf{Q_1}\} \qquad [4.15]$$

*Scaling*

It is sometimes necessary to *scale* a complex vector in order to attenuate (or amplify) one or more of the frequency components. A convenient way to scale is to multiply the element $\boldsymbol{U}_k$ with a *scaling constant* $\boldsymbol{w_k}$ like:

$$\mathbf{U_{mod}} = \{ w_1 \cdot U_1, w_2 \cdot U_2, ..., w_k \cdot U_k, ..., w_N \cdot U_N \} \quad \text{where k=1,2,...,N} \qquad [4.16]$$

where $\boldsymbol{U_{mod}}$ is the modified vector and

$$\mathbf{W} = [w_1, w_2, w_3, ..., w_N] \qquad [4.17]$$

is the scaling vector.

The use of a scaling vector is given in the following example: The elements in the vector ***U*** and ***I*** shall be zero for all frequencies higher than $f_s/2$. The elements in the scaling vector ***W*** shall be chosen as follows:

$$\mathbf{w_{uk}} = \mathbf{w_{ik}} = \begin{cases} 1 & for\ 1 \le k \le \dfrac{N}{2} \\ 0 & for\ \dfrac{N}{2} < k \le N \end{cases}$$

The elements $\boldsymbol{w_k}$ in the scaling vector ***W*** can also be chosen to achieve a certain amplitude spectrum of the complex vector, by multiplying the signal component with the corresponding amplitude spectrum component. The use of a scaling vector is both powerful and flexible.

*Scaling vector and the flicker power*

In measurement method 1 and 2, the flicker power $\Pi$ is calculated as a sum of contributions from scaled flicker power components $\boldsymbol{\Pi_k}$ :

$$\Pi = \sum_{k=1}^{N} \Pi_k = \sum_{k=1}^{N} \mathrm{Re}\left\{ \frac{1}{2} w_k \cdot U_k . \cdot I_k^{\,*} \right\} \qquad [4.18]$$

The values of the elements $\boldsymbol{w_k}$ in the scaling depends on the measurement method being used.

*Square demodulation*

Measurement method 2 and 3 are using square demodulation to recover the modulating signals $m_u(t)$ and $m_i(t)$. A square demodulation of an amplitude modulated signal $u(t)$ will give the following expression:

$$\begin{aligned} u^2(t) &= \left( U_c + \sum_{k=1}^{\infty} U_{mk} \cos(k\omega_1 t + \beta_k) \right)^2 \cos^2(\omega_c t + \beta_c) = \\ &= \left( {U_c}^2 + 2 \cdot U_c \cdot \sum_{k=1}^{\infty} U_{mk} \cos(k\omega_1 t + \beta_k) + \left( \sum_{k=1}^{\infty} U_{mk} \cos(k\omega_1 t + \beta_k) \right)^2 \right) \cdot \frac{1}{2} \left(1 + \cos(2\omega_c t + 2\beta_c)\right) = \\ &= \left\{ \frac{{U_c}^2}{2} + \underline{\underline{\frac{1}{2} \cdot 2 \cdot U_c \cdot \sum_{k=1}^{\infty} U_{mk} \cos(k\omega_1 t + \beta_k) + \frac{1}{2} \cdot \left( \sum_{k=1}^{\infty} U_{mk} \cos(k\omega_1 t + \beta_k) \right)^2}} \right\} + \\ &+ \left\{ \frac{{U_c}^2}{2} + \frac{1}{2} \cdot 2 \cdot U_c \cdot \sum_{k=1}^{\infty} U_{mk} \cos(k\omega_1 t + \beta_k) + \frac{1}{2} \cdot \left( \sum_{k=1}^{\infty} U_{mk} \cos(k\omega_1 t + \beta_k) \right)^2 \right\} \cdot \cos(2\omega_c t + 2\beta_c) \end{aligned} \qquad [4.19]$$

Expression [4.19] shows that square demodulation creates two signal packages separated in frequency. The first package consists of a zero frequency component (DC component), the modulating signal (multiplied by $U_c$) and the square of the modulated signal (scaled by a factor ½). The second package is centred on twice the carrier frequency and contains the same components as the first package.

## 4.3.1 Measurement method 1

If the sampled voltage *u[n]* and current *i[n]* are considered amplitude modulated, the modulating signals will create upper- and lower sideband signals. In the frequency domain, the modulating signal is split into two signals (each with half the amplitude of the original signal) and placed on both sides of the carrier frequency at a frequency of $f_c \pm f_m$ (see Figure 4.5). Using the theory introduced in the previous section, the flicker power Π is calculated from the sidebands signals:

$$\Pi = \frac{1}{2} \cdot \sum_{k=0}^{j-1} \mathrm{Re}\left\{ w_{u(M-j+k)} \cdot (U_{(M-j+k)} + U_{(M+j-k)}) \cdot w_{i(M-j+k)} \cdot (I_{(M-j+k)} + I_{(M+j-k)})^* \right\}$$

Consider an amplitude modulated and sampled voltage signal *u[n]* and corresponding current *i[n]* containing *j* sideband signals on both side of the carrier frequency. Also consider that the frequency spectra of *u[n]* and *i[n]* are calculated by a N-point DFT.
The output of the DFTs are the complex voltage and current vectors **U** and **I.** The complex voltage and current of the carrier is placed in index (element) *k=M* of **U** and **I**. The flicker power *ΠΠ* is given by the equation:

$$\Pi = \frac{1}{2} \cdot \sum_{k=0}^{j-1} \mathrm{Re}\left\{ w_{u(M-j+k)} \cdot (U_{(M-j+k)} + U_{(M+j-k)}) \cdot w_{i(M-j+k)} \cdot (I_{(M-j+k)} + I_{(M+j-k)})^* \right\}$$

The scaling elements $\boldsymbol{w_{u(M-j+k)}}$ and $\boldsymbol{w_{i(M-j+k)}}$ are chosen to obtain a specific amplitude spectrum of the modulating signals (i.e. the bandpass filter used in IEC 61000-4-15). If all scaling elements are chosen to one (1), a rectangular window with no filtering is achieved.
Figure 4.6 shows the signal flow diagram of measurement method 1.

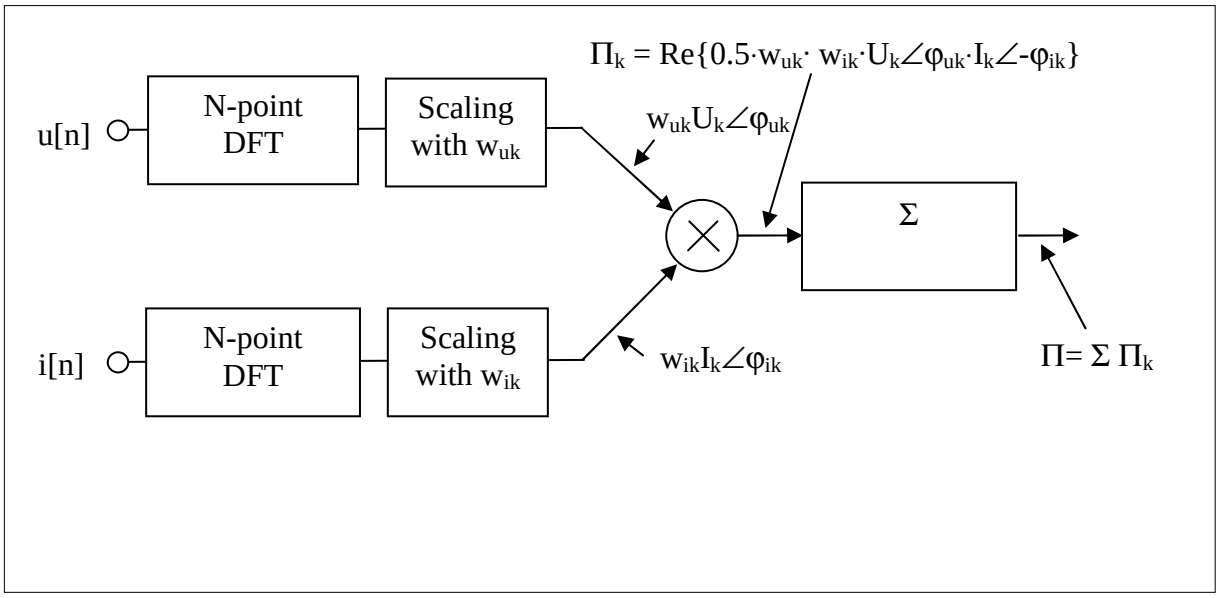


*Figure 4.6. Signal flow diagram of measurement method 1.*

An alternative way of calculating the flicker power is (if the amplitudes of upper- and lower sideband signals are equal) to use the signals *from one of the sidebands* only.
Calculating the flicker power from the *lower sideband* signals is given by:

$$\Pi = \frac{1}{2} \cdot \sum_{k=0}^{j-1} \mathrm{Re}\left\{ 2w_{u(M-j+k)} \cdot U_{(M-j+k)} \cdot 2w_{i(M-j+k)} \cdot I^{*}_{(M-j+k)} \right\}$$

and calculating the flicker power from the signals in the upper sideband is given by:

$$\Pi = \frac{1}{2} \cdot \sum_{k=0}^{j-1} \mathrm{Re}\left\{ 2w_{u(M+j-k)} \cdot U_{(M+j-k)} \cdot 2w_{i(M+j-k)} \cdot I^{*}_{(M+j-k)} \right\}$$

The advantage of measurement method 1 is that no demodulation is required. On the other hand, there are two major disadvantages. Number one: A DFT calculation is always a time consuming task which puts serious demands on the hardware calculating the flicker power. Number two: Since the input data to the DFT is truncated to N points, a loss in information will occur. The loss of information will cause a distortion in the output of the DFT. The signal components in the frequency domain will become “diffuse” and the frequency components close in frequency can be hard to distinguish because of *leakage*. Since the sideband signals are close to the fundamental frequency the leakage phenomenon can cause severe errors in the results when using measurement

method 1. One way to reduce leakage is to increase the number of sampling points *N* used in the DFT calculation.

## 4.3.2 Measurement method 2

This method is, like measurement method 1, based on frequency domain analysis. The main difference is that the analysis of the modulating signals is performed in the baseband. In measurement method 2, the *underlined* information in equation [4.19] is used for calculation of the flicker power. The first underlined term contains (after scaling) the modulating signals. The second term is a result of the nonlinear process of square demodulation introducing new signal components. This signal component is much smaller than the first one and will not affect the accuracy significantly. The advantage of measurement method 2 compared to measurement method 1 is the separation (in frequency) of the modulating signals and the carrier frequency. It eliminates the error introduced because of leakage. The block diagram of measurement method 2 is given in Figure 4.7 with the following explanation:

The N-point sampled data of voltage *u[n]* and current *i[n]* are the input signals to the measurement method 2. In block (1A) and (1B) the square demodulation of the input signals is performed by squaring each element in the vector. The demodulated signal is input signal to the N-point DFT (block (2A) and (2B)). The output signals of block (2A) and (2B) are the complex vectors (**U** and **I**) containing the frequency spectrum of u[n] and i[n] with a frequency resolution of $\Delta f = f_s/N$. Scaling is obtained in block (3A) and (3B) by multiplying each element in $\boldsymbol{U}$ and $\boldsymbol{I}$ with $\boldsymbol{w_{uk}}$ and $\boldsymbol{w_{ik}}$.

The flicker power is calculated from the formula:

$$\Pi = \frac{1}{2} \cdot \sum_{k=0}^{j-1} \mathrm{Re}\left\{ \frac{2}{U_c} w_{u(M-j+k)} \cdot U_{(M-j+k)} \cdot \frac{2}{I_c} w_{i(M-j+k)} \cdot I^{*}_{(M-j+k)} \right\} \qquad [4.20]$$

where $j$ is the number of modulating signals contributing to flicker, $M$ is the index in $\boldsymbol{U}$ and $\boldsymbol{I}$ containing the carrier signal, $U_c$ and $I_c$ is the amplitude of voltage and current of the carrier signals.
The scaling elements $\boldsymbol{w_{u(M-j+k)}}$ and $\boldsymbol{w_{i(M-j+k)}}$ are chosen, like in measurement method 1, to obtain a specific amplitude spectrum of the modulating signals.

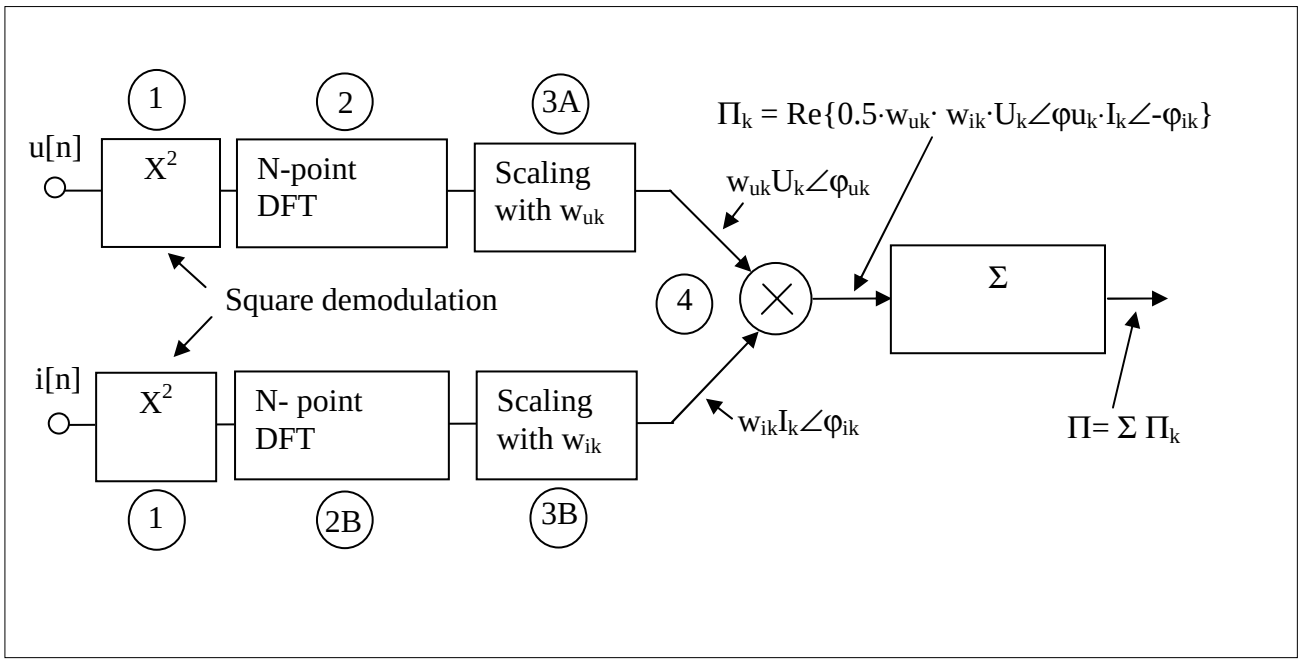


*Figure 4.7. Signal flow diagram of measurement method 2.*

## 4.3.3 Measurement method 3

Contrary to the other two measurement methods, measurement method 3 is solely based on calculations in the time domain. The signal flow diagram for measurement method 3 is shown in Figure 4.8. This method is partly based on the IEC 61000-4-15 since block 1 and 2 are identical to the filters as defined in IEC 61000-4-15. This means, the flicker power calculated from this method very much corresponds to the actual flicker situation in the network.

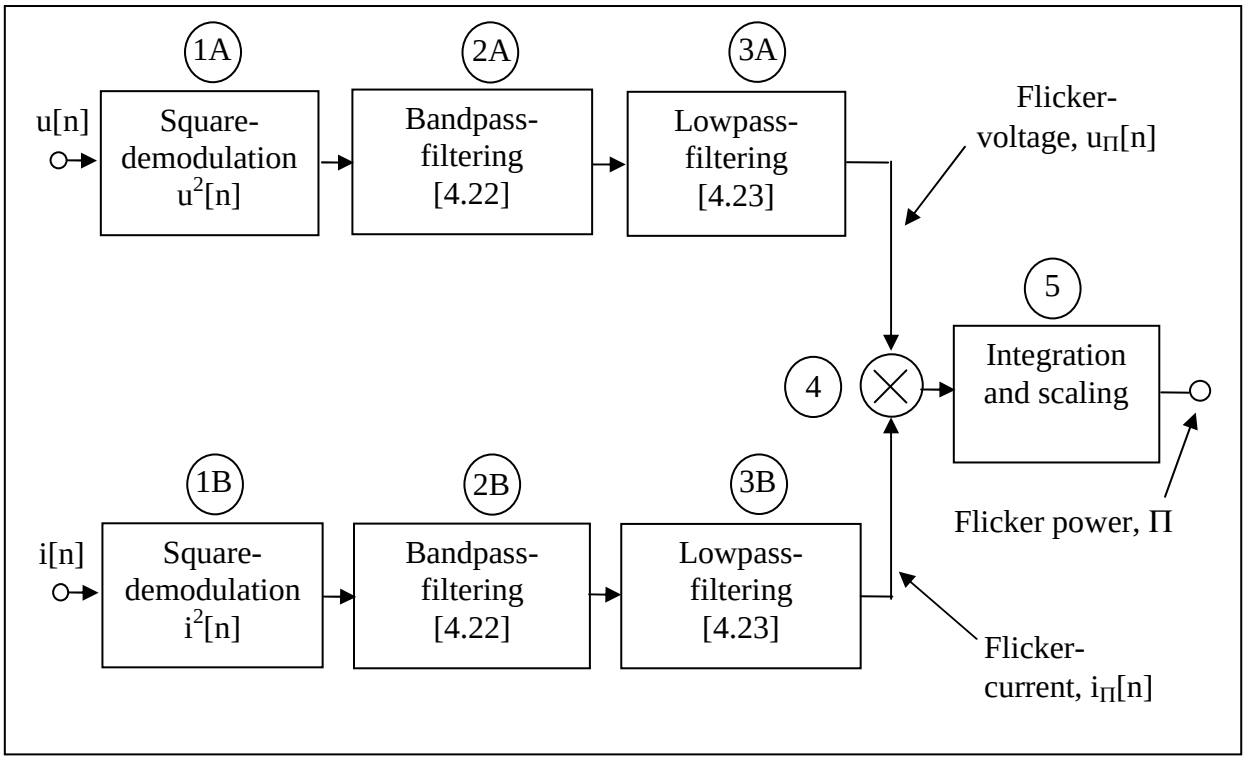


*Figure 4.8. Signal flow diagram for measurement method 3.*

Block (1) to (3) are identical for both voltage and current signals. The modulating signals are recovered by square demodulation performed in block (1A) and (1B) (see also [4.19]). The analogue transfer function of the band-pass filter used in block (2A) and (2B) are given in [4.21] and its coefficients are given in Table 4.1.

$$H(s) = \frac{k\omega_1 s}{s^2 + 2\lambda s + \omega^2} \cdot \frac{1 + s/\omega_2}{(s + 1/\omega_3)(s + 1/\omega_4)} \qquad [4.21]$$

| | |
|---|---|
| k=1,748 02 | $\lambda = 2\pi \cdot\cdot 4{,}059\ 81$ |
| $\omega_1 = 2\pi \cdot 9{,}154\ 94$ | $\omega_3 = 2\pi \cdot 1{,}225\ 35$ |
| $\omega_2 = 2\pi \cdot 2{,}279\ 79$ | $\omega_4 = 2\pi \cdot 21{,}9$ |

*Table 4.1. Filter coefficients for the transfer function given in [4.21].*

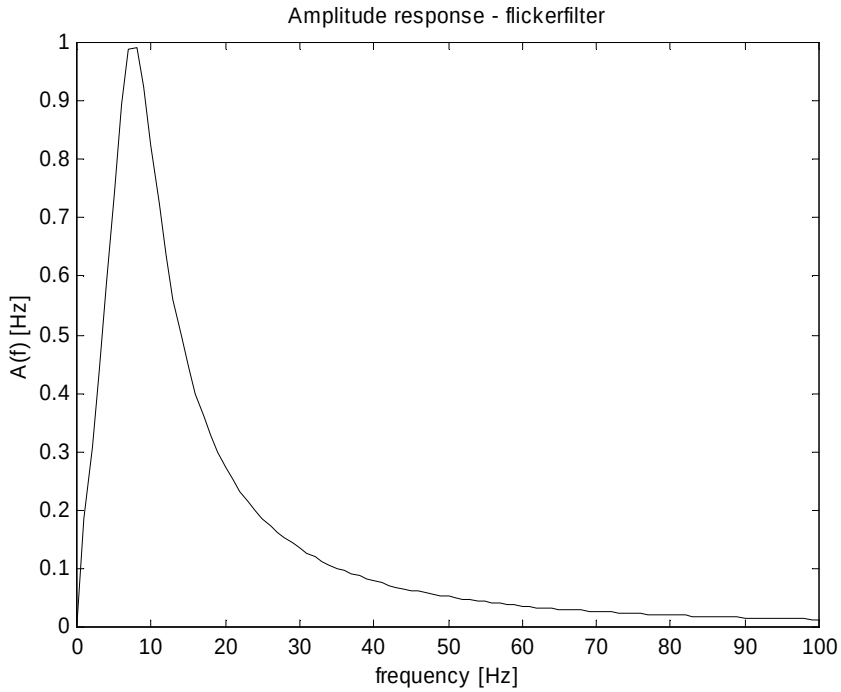


*Figure 4.9. Frequency response of band-pass filter given in [4.21] and Table 4.1.*

The band-pass filter in [4.21] is implemented as a digital equivalent by bilinear transformation. Its transfer function is given in [4.22]:

$$H(z) = \frac{0.0410 - 0.0410z^{-2}}{1 - 1.9561z^{-1} + 0.9584z^{-2}} \cdot \frac{0.0292 + 0.003z^{-1} - 0.0289z^{-2}}{1 - 1.8852z^{-1} + 0.8858z^{-2}} \qquad [4.22]$$

A block diagram of the transfer function in [4.22] is shown in Figure 4.10.

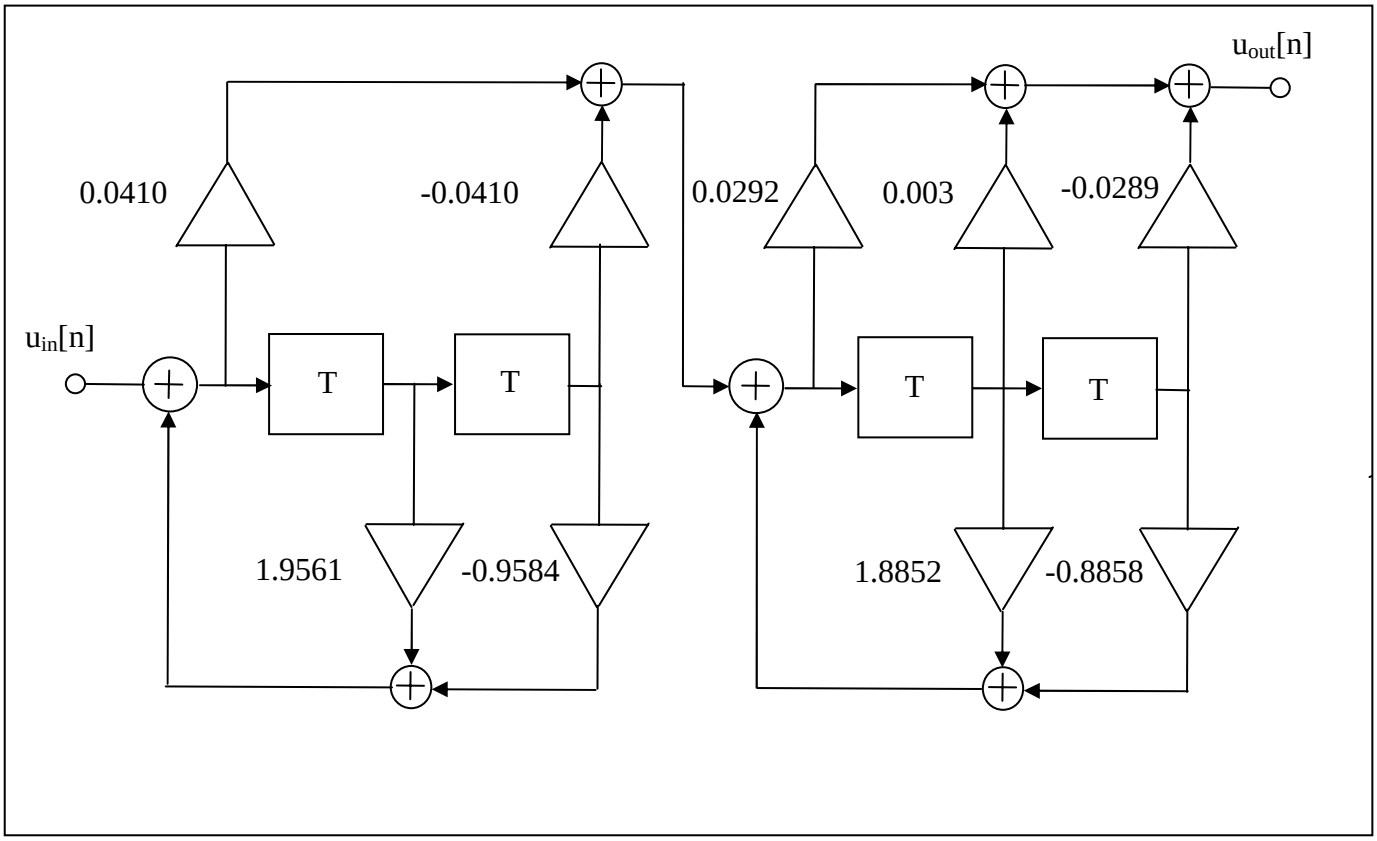


*Figure 4.10. Block diagram of the transfer function given in [4.22].*

The outputs of the band-pass filter are modulating signals weighted with the amplitude spectrum of the band-pass filter.
The low-pass filter in block (3A) and (3B) is needed for additional attenuation of the signal components corresponding to twice the carrier frequency (see [4.19]). Simulations in Matlab indicate that a 4th order Butterworth low-pass filter with a cut-off frequency of 30 Hz gives sufficient attenuation. The digital transfer function of the low-pass filter is given in [4.23]:

$$H(z) = 10^{-4} \cdot \frac{0.0215 + 0.0860z^{-1} + 0.1290z^{-2} + 0.0860z^{-3} + 0.0215z^{-4}}{1 - 3.7948z^{-1} + 5.4052z^{-2} - 3.4247z^{-3} + 0.8144z^{-4}} \qquad [4.23]$$

A block diagram of [4.23] is shown in Figure 4.11 (1200 Hz sampling frequency).

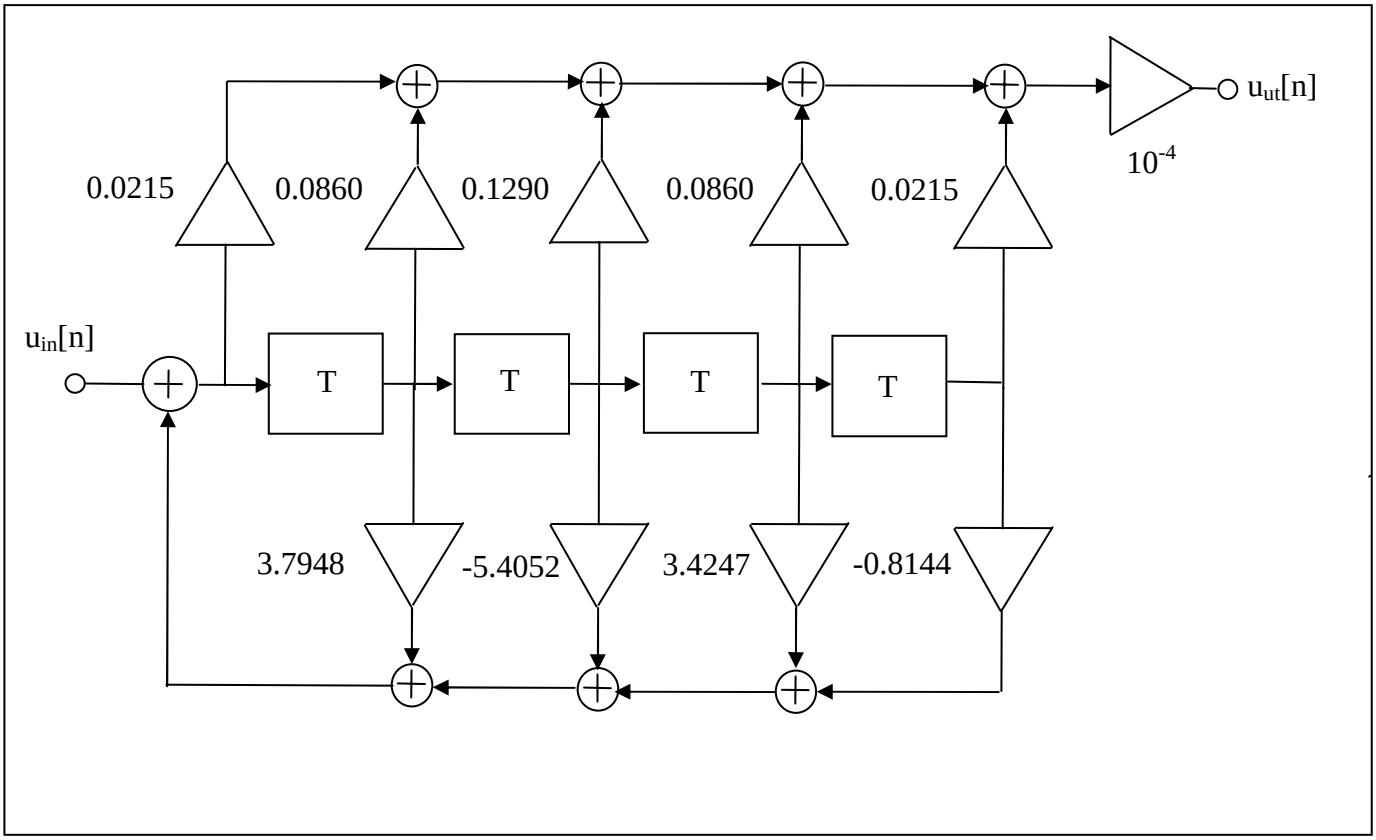


*Figure 4.11. Block diagram of the lowpass filter given by the transfer function in [4.23]*

The output signal from each filter is multiplied in block (4) resulting in the *instantaneous flicker power* $\Pi[n] = u_{\Pi}[n] \cdot i_{\Pi}[n]$. Finally, the *flicker power*, $\Pi$, is given by averaging of $\Pi[n]$, obtained in block (5). When studying [4.19] it is obvious that the modulating signals on the outputs from block (3A) and (3B) must be scaled with $\frac{1}{U_c}$ and $\frac{1}{I_c}$ respectively in order to recover the modulating signals correctly. Therefore, the output signal from the averaging filter is scaled in block (5) by a factor $\frac{1}{U_c \cdot I_c}$.

# 4.4 Block diagram of an instrument calculating flicker power

Figure 4.12 shows a block diagram of an instrument that can be used for calculation of flicker power. The instrument is based on digital signal processing and designed using a DSP (Digital Signal Processor). The DSP block (4) is calculating the flicker power according to the measurement methods described earlier. The DSP also administrates the A/D conversion and the presentation of the results. The signal flow in Figure 4.12 is described here:
The measurement signals (i.e. waveforms) of voltage and current are connected to the input of the instrument via voltage- and current transducers. The output signals of the transducers are scaled in block (1A) and (1B) to obtain the right signal level. The output signals from blocks (1A) and (1B) are connected to the anti-alias filter in block (2A) and (2B).

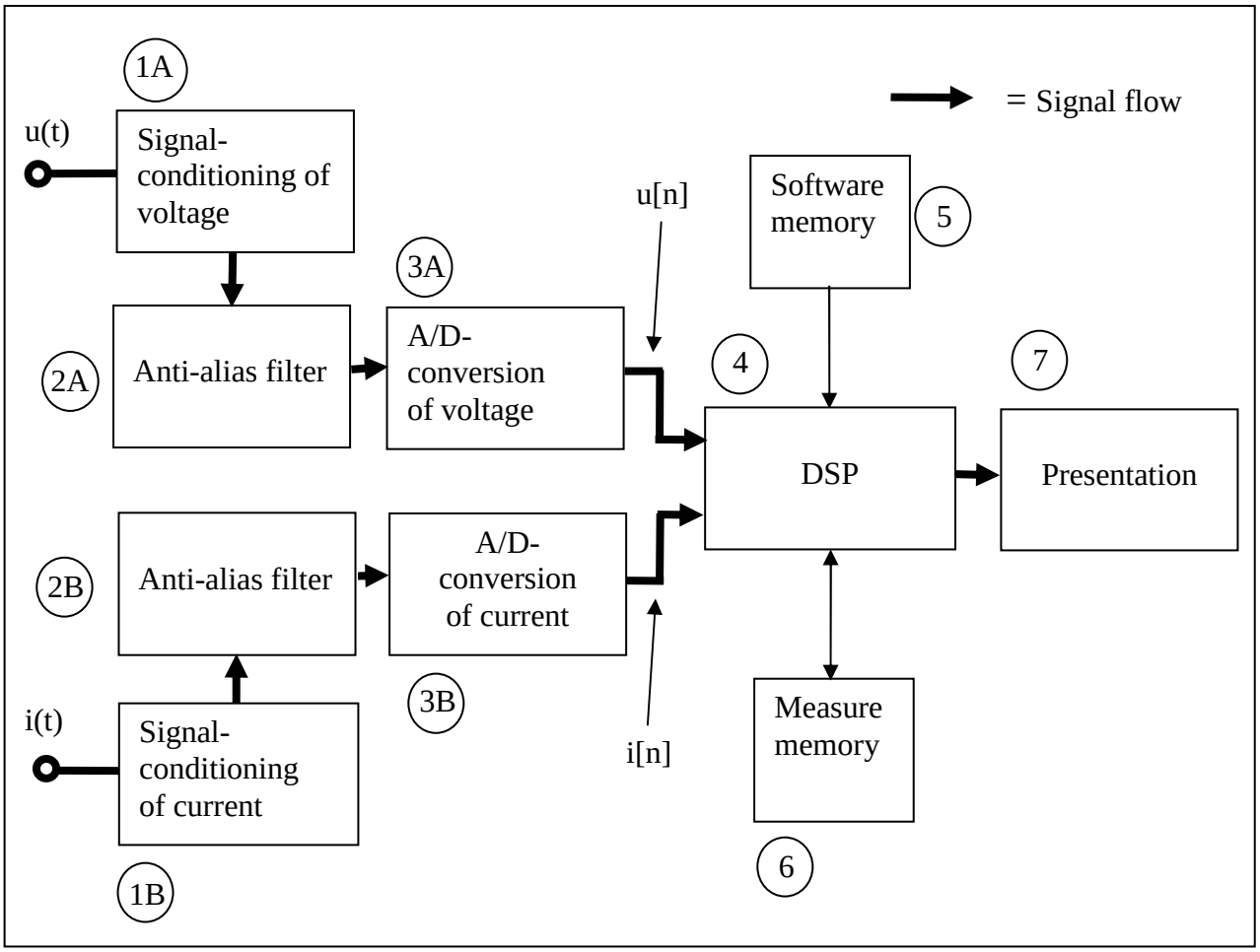


*Figure 4.12. Block diagram of a hardware calculating the flicker power.*

Since the amplitude spectrum of the input signals is centred on the power frequency, the cut-off frequency of the anti-alias filter is chosen to a frequency slightly above the power frequency. For example if using a cut-off frequency of 75 Hz the filter acts both as an anti-alias filter and filter attenuating frequency components lower than $f_s/2$ like harmonics and inter-harmonics. The analogue output signals from the anti-alias filter are converted into digital representation by the ADCs in block (3A) and (3B) giving the sampled data *u[n]* and *i[n]*. The sampled data are temporarily stored in the measurement memory (block (6)) and are the input signals for the measurement methods 1-3. The instrument software is stored in a non-volatile memory (block (5)) and the instant value of the flicker power is presented numerically or graphically in block (7).

# Chapter 5

# Simulations and field tests based on developed measurement methods

## 5.1. Introduction

In order to validate the measurement methods developed in Chapter 4, simulations in Matlab and field tests have been performed. The results of these activities will be discussed in this chapter.
It is interesting to note the high accuracy achieved when testing the methods by simulations in Matlab. Comparing the simulation results with the theoretical ones, the measurement methods are giving very precise results.
Regarding the field tests, measurement method 3 has been validated since it is the one which is most interesting to implement in an instrument.

# 5.2. Simulation of measurement method 1 and 2 in Matlab

The accuracy of measurement methods 1 and 2 was validated by using Simulink in Matlab. Six amplitude modulated input signals with different modulation index and different phase shifts were used for this verification. The modulating voltage signals were used as reference signals with a phase of 0°. For the modulating current signals, the phases 0°, 90° and 180° were chosen. The modulating signal was a sinusoidal with a frequency of 8.8 Hz corresponding to the peak response of the lamp-eye filter in the standard IEC 61000-4-15. The input data sequence to the model consisted of time discrete sampled data of voltage *u[n]* and current *i[n]* with a sampling frequency $f_s$ of 409.6 Hz. In order to achieve high accuracy when calculating the flicker power, a 4096-point DFT calculation was used. The large number of points *N* used in the DFT calculation highlights the major disadvantage using measurement method 1 and 2. Making a 4096-point DFT puts extreme demands on the computation speed of an instrument. It leads to a more complex and expensive hardware compared to an instrument designed for time domain calculations like in measurement method 3.

The theoretical value of the flicker power $\Pi$ is calculated from the formula:

$$\Pi = \frac{1}{2}\Delta U \cdot \Delta I \cdot \cos(\varphi) \qquad [\mathrm{W}]$$

The amplitudes of the modulating signals $\Delta U$ and $\Delta I$ are calculated from the formulas:

$$U = \sqrt{2} \cdot 230\,V \quad \rightarrow \quad \Delta U = 0.2 \cdot U = \sqrt{2} \cdot 46\,V \qquad \text{(20\% modulation)}$$

$$I = \sqrt{2} \cdot 10\,V \quad \rightarrow \quad \Delta I = 0.2 \cdot I = \sqrt{2} \cdot 2\,A \qquad \text{(20\% modulation)}$$

The phase shift $\varphi$ is 0°, 90° and 180°.

| Measurement method 1 | | |
|---|---|---|
| Sim-ulation No. | Voltage:<br>Carrier ampl. / mod. % / mod. freq / $\varphi_u$ /<br><br>Current:<br>Carrier ampl. / mod. % / mod. freq / $\varphi_i$ / | Flicker power Π [W]<br><br>Calculated results / simulated results / relative error |
| 1.1 | Voltage : √2·230V / 20% / 8.8 Hz / 0°<br>Current : √2·10A / 20% / 8.8 Hz / 0° | 92W / 92W / 0.0% |
| 1.2 | Voltage : √2·230V / 20% / 8.8 Hz / 0°<br>Current : √2·10A / 20% / 8.8 Hz / 90° | 0.0W / 0.0W / 0.0% |
| 1.3 | Voltage : √2·230V / 20% / 8.8 Hz / 0°<br>Current : √2·10A / 20% / 8.8 Hz / 180° | -92W / -92W / 0.0% |
| 1.4 | Voltage : √2·230V / 0.25% / 8.8 Hz / 0°<br>Current : √2·10A / 0.25% / 8.8 Hz / 0° | 14.4mW / 14.4mW / 0.0% |
| 1.5 | Voltage : √2·230V / 0.25% / 8.8 Hz / 0°<br>Current : √2·10A / 0.25% / 8.8 Hz / 90° | 0.0W / 0.0W / 0.0% |
| 1.6 | Voltage : √2·230V / 0.25% / 8.8 Hz / 0°<br>Current : √2·10A / 0.25% / 8.8 Hz / 180° | -14.4mW / -14.4mW / 0.0 % |

*Table 5.1. Simulation results of measurement method 1.*

Table 5.1 shows high accuracy in the simulation results of measurement method 1. This high accuracy is expected since no demodulation is performed. A sampling frequency of 409.6Hz and a 4096-point DFT gives a frequency resolution of 0.1Hz which reduces the leakage phenomenon significantly.

| Measurement method 2 | | |
|---|---|---|
| Sim-ulation No. | Voltage:<br>Carrier ampl. / mod. % / mod. freq / $\varphi_u$ /<br><br>Current:<br>Carrier ampl. / mod. % / mod. freq / $\varphi_i$ / | Flicker power Π [W]<br><br>Calculated results/ simulated results,/ relative error |
| 2.1 | Voltage : √2·230V / 20% / 8.8 Hz / 0°<br>Current : √2·10A / 20% / 8.8 Hz / 0° | 92W / 92.23W / 0.25% |
| 2.2 | Voltage : √2·230V / 20% / 8.8 Hz / 0°<br>Current : √2·10A / 20% / 8.8 Hz / 90° | 0.0W / 0.0W / 0.0% |
| 2.3 | Voltage : √2·230V / 20% / 8.8 Hz / 0°<br>Current : √2·10A / 20% / 8.8 Hz / 180° | -92W / -91.77W / -0.25% |
| 2.4 | Voltage : √2·230V / 0.25% / 8.8 Hz / 0°<br>Current : √2·10A / 0.25% / 8.8 Hz / 0° | 14.4mW / 14.2mW / -1.4% |
| 2.5 | Voltage : √2·230V / 0.25% / 8.8 Hz / 0°<br>Current : √2·10A / 0.25% / 8.8 Hz / 90° | 0.0W / 0.0W / 0.0% |
| 2.6 | Voltage : √2·230V / 0.25% / 8.8 Hz / 0°<br>Current : √2·10A / 0.25% / 8.8 Hz / 180° | -14.4mW / -14.2mW / 1.4% |

*Table 5.2. Simulation results of measure method 2.*

Table 5.2 shows a high accuracy also for measurement method 2. However a small error is introduced due to the demodulation process. In a practical implementation, the accuracy will probably be at the same level for both measurement methods 1 and 2 because of leakage occurring in the measurement method 1. However, field tests must be performed of both measurement methods before any conclusions regarding the overall accuracy can be stated.

# 5.3. Simulation of measurement method 3

Simulations according to measurement method 3 have been performed by using the Simulink model in Figure 5.1. In order to get comparable results between the three measurement methods the same input signals as in Section 5.2 have been used.

The amplitude-modulated signal is generated on the left-hand side in Figure 5.1. Next, the modulating signal is recovered by a square demodulation. The output signal from the demodulator is connected to the filter chain with transfer functions given in [4.22] and [4.23] (see Section 4.3.3). The output signal from each filter is multiplied (resulting in the instantaneous flicker power $\Pi[n]$) and averaged in order to get the flicker power $\Pi$. Before displaying the result, the output signal of the averaging filter is scaled to give the right level of the flicker power (see discussions in Section 4.3.3).

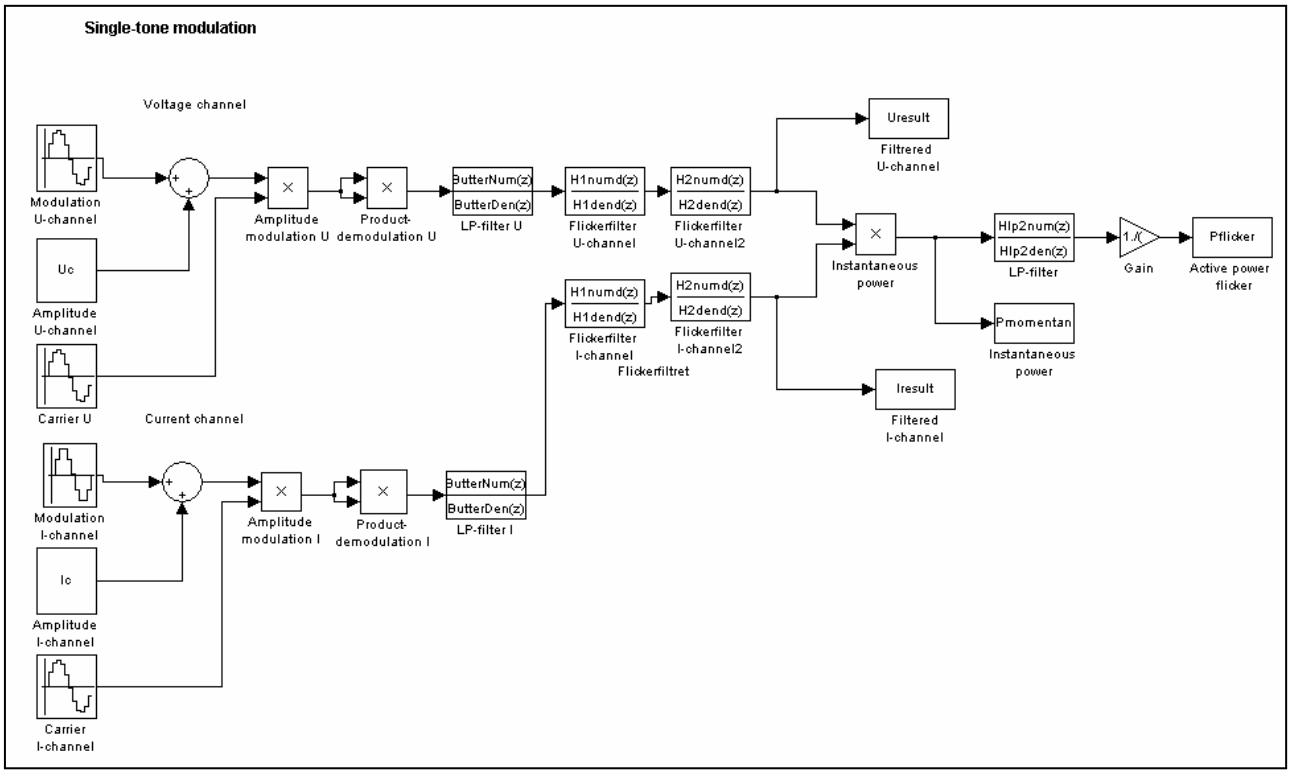


*Figure 5.1. Simulation model for measurement method 3.*

Six different simulations have been performed (see Table 5.3). Three of the simulations are used with a high level of modulation (20%) and the other three with a low level (0.25%). For each modulation level, three different phase shifts have been used (0°, 90° and 180°). The results of the simulations are presented in Table 5.3 and in Figure 5.2 – 5.7. As shown in Table 5.3, some errors are

introduced in the results. There are two sources contributing to the total error. The first one is from the demodulating process and the other one is from the amplitude spectrum of the filters being used. The error due to the demodulation process has been discussed in the previous section. The second error occurs because the amplitude response component of the filter at 8.8 Hz is not exactly 1.0. Examining the amplitude spectrum of the cascade filter chain with transfer function in [4.22] and in [4.23], the amplitude spectrum component is 0.984 at 8.8 Hz instead of 1.0. If making a compensation for this error, a result very close to the theoretical value is achieved. Figure 5.2 – 5.7 shows the calculated flicker power for each simulation. Since the averaging filter does not attenuate the *instantaneous flicker power* $\Pi[n]$ completely, a small signal component of the instantaneous flicker power is superimposed to the averaged value (i.e. the flicker power $\Pi$). This is shown as a sinusoidal oscillation superimposed on the average in Figure 5.2 – 5.7.

| Measurement method 3 | | | |
|---|---|---|---|
| Sim-ulation No. | Voltage:<br>Carrier ampl. / mod. % / mod. freq / $\varphi_u$ /<br><br>Current:<br>Carrier ampl. / mod. % / mod. freq / $\varphi_i$ / | Π [W]<br><br>Calculated results/<br>simulated results/<br>relative error | Figure No. |
| 3.1 | Voltage : √2·230V / 20% / 8.8 Hz / 0°<br>Current : √2·10A / 20% / 8.8 Hz / 0° | 92W / 91W / 1.1% | 5.2 |
| 3.2 | Voltage : √2·230V / 20% / 8.8 Hz / 0°<br>Current : √2·10A / 20% / 8.8 Hz / 90° | 0.0W / 0.0W / 0.0% | 5.3 |
| 3.3 | Voltage : √2·230V / 20% / 8.8 Hz / 0°<br>Current : √2·10A / 20% / 8.8 Hz / 180° | -92W / -91W / -1.1% | 5.4 |
| 3.4 | Voltage : √2·230V / 0.25% / 8.8 Hz / 0°<br>Current : √2·10A / 0.25% / 8.8 Hz / 0° | 14.4mW / 14.2mW / -1.4% | 5.5 |
| 3.5 | Voltage : √2·230V / 0.25% / 8.8 Hz / 0°<br>Current : √2·10A / 0.25% / 8.8 Hz / 90° | 0.0W / 0.0W / 0.0% | 5.6 |
| 3.6 | Voltage : √2·230V / 0.25% / 8.8 Hz / 0°<br>Current : √2·10A / 0.25% / 8.8 Hz / 180° | -14.4mW / -14.2mW / -1.4 % | 5.7 |

*Table 5.3. Simulation results of measurement method 3.*

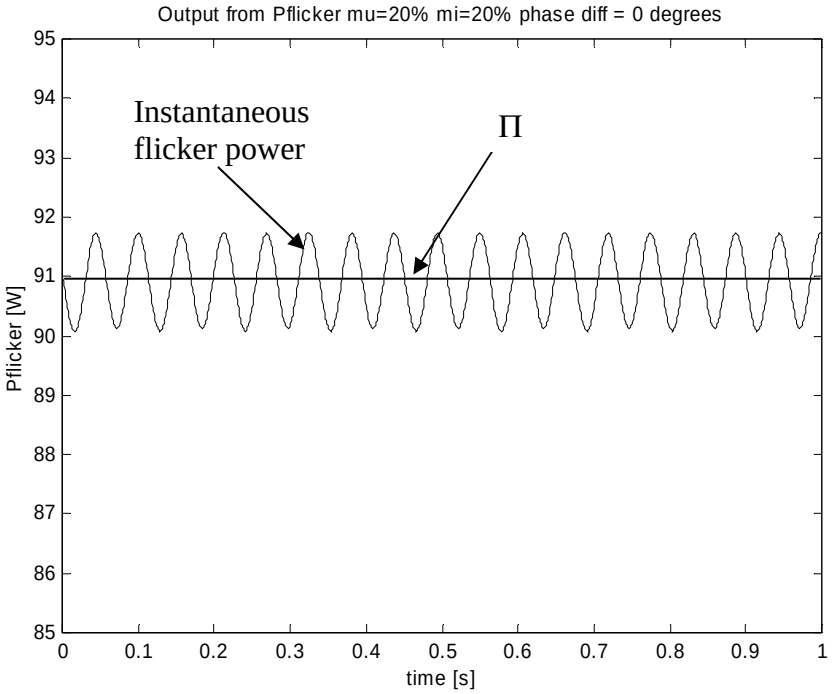


*Figure 5.2. Output signal of simulation No 3.1. Π =91W.*

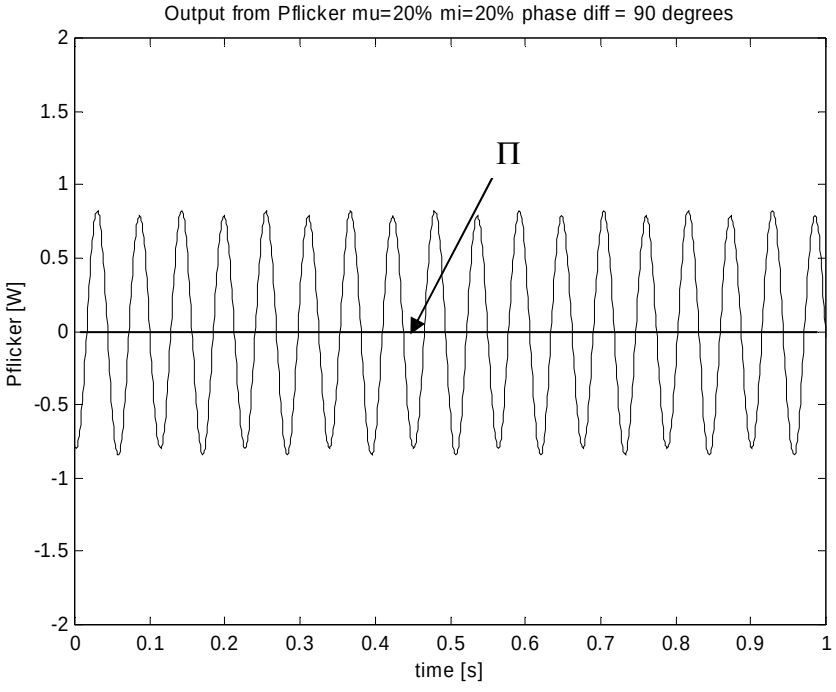


*Figure 5.3. Output signal of simulation No 3.2. Π =0W*

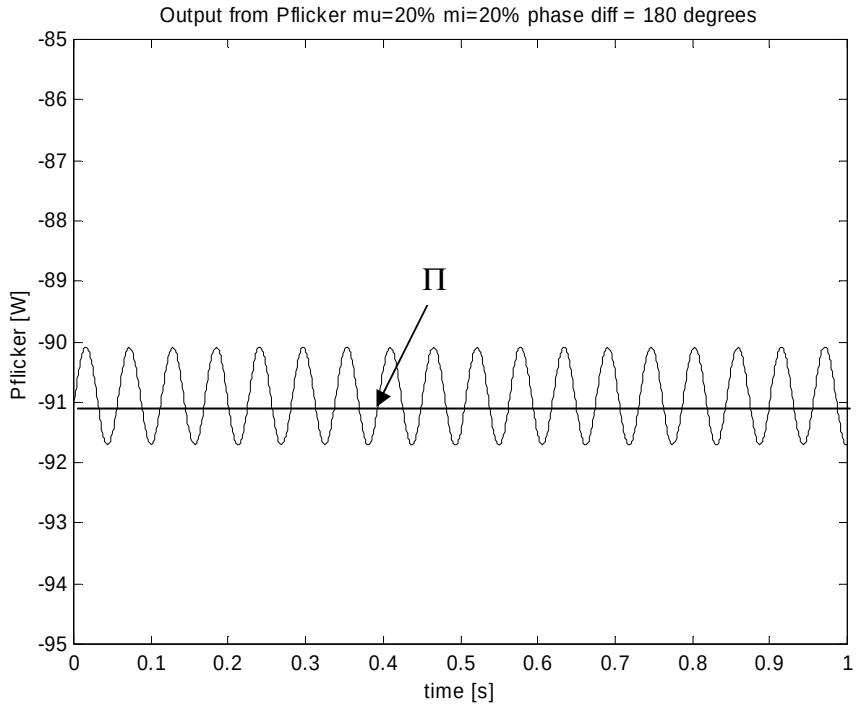


*Figure 5.4. Output signal of simulation No 3.3 Π=-91W.*

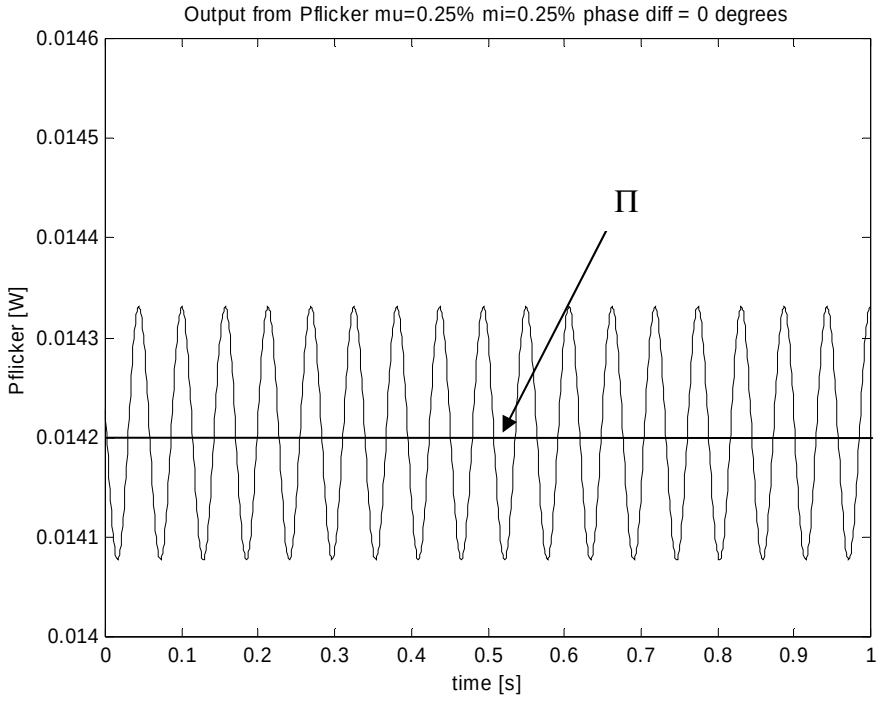


*Figure 5.5. Output signal of simulation No 3.4. Π=14.2mW.*

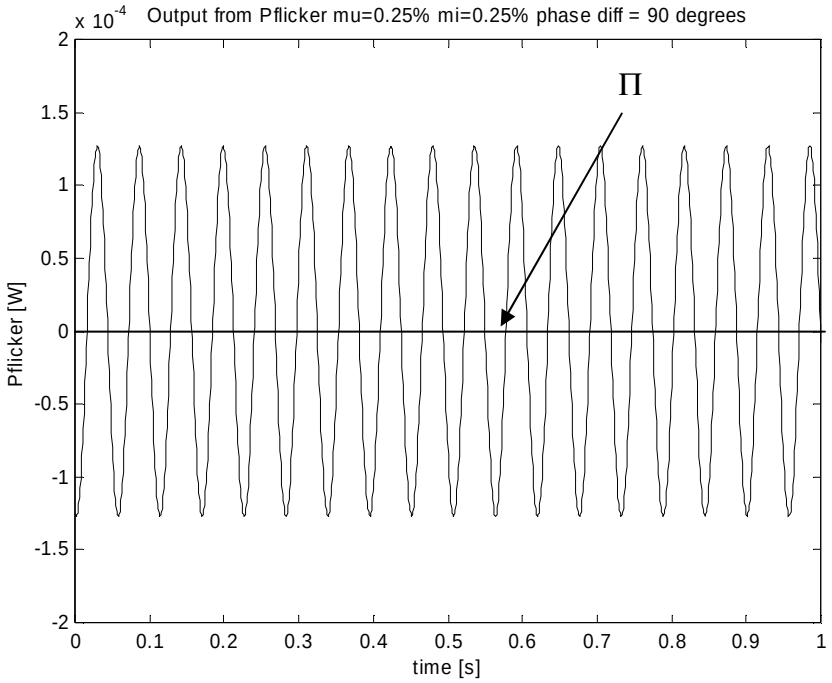


*Figure 5.6. Output signal of simulation No 3.5 Π=0W.*

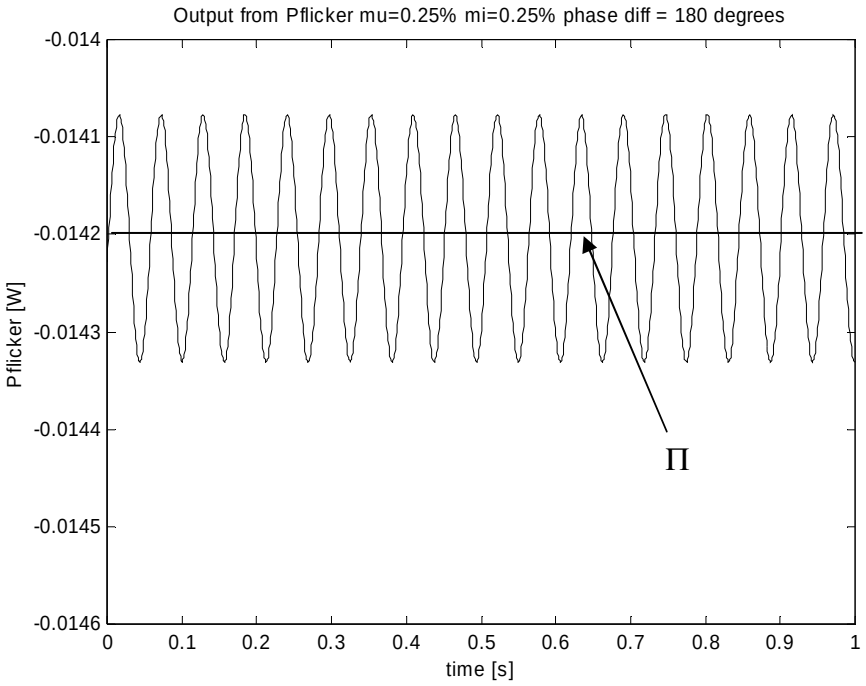


*Figure 5.7. Output signal of simulation No 3.6 Π= -14.2mW.*

# 5.4. Field test performed on an ON-OFF load.

The very first field test was performed on a small 2kW electric heater. The test set-up is shown in Figure 5.8. The load was connected via a manual switch manoeuvred periodically at a modulating frequency within the flicker spectrum. In order to calculate the flicker power $\Pi$ a model in Simulink for use with imported measurement data was developed (see Figure 5.9).
The waveforms of voltage *u(t)* and current *i(t)* were recorded at a sampling frequency of 1200 Hz using the instrument Unipower Recorder.

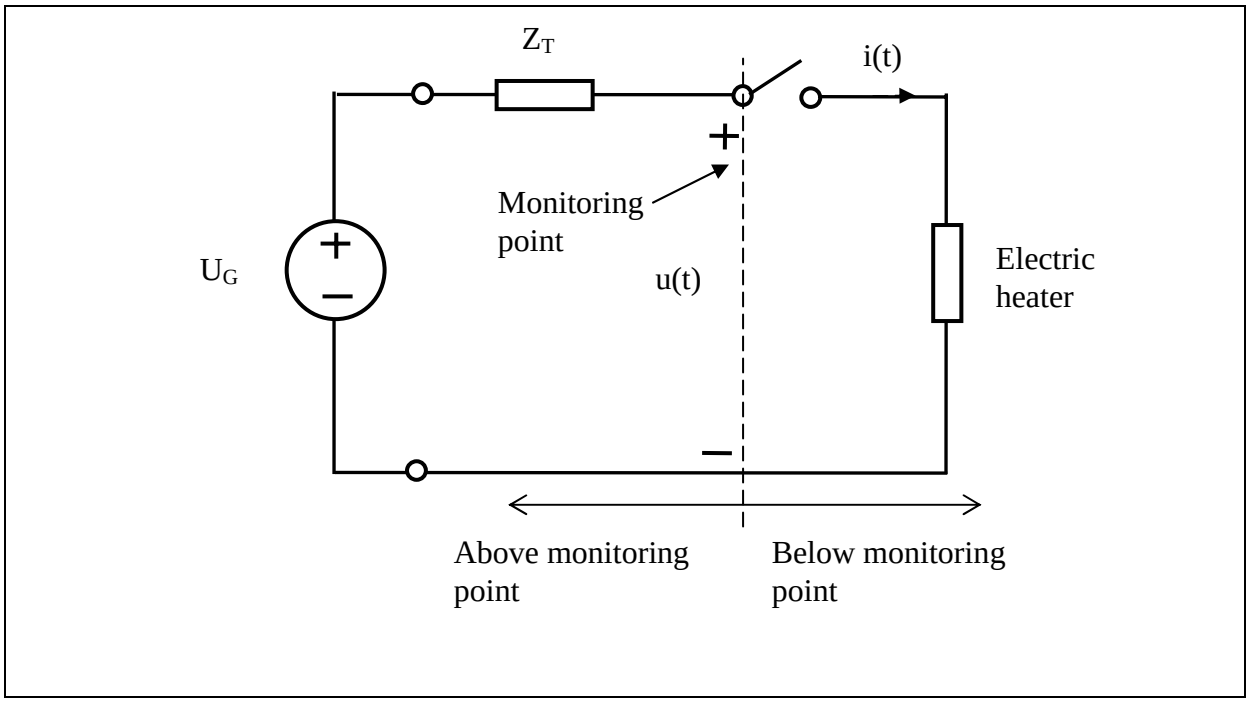


*Figure 5.8. Equivalent circuit for ON-OFF modulation of resistive load.*

The waveform data of *u[n]* and *i[n]* were demodulated (by squaring each element in *u[n]* and *i[n]*) before being input to the Simulink model of measurement method 3. The flicker source is placed below the monitoring point and thus, according to the conditions stated in Section 4.2, the flicker power $\Pi$ is expected to be negative. Looking at the result (Figure 5.10), the flicker power is negative (-90W). Thus, the source of flicker has been correctly identified by the measurement.

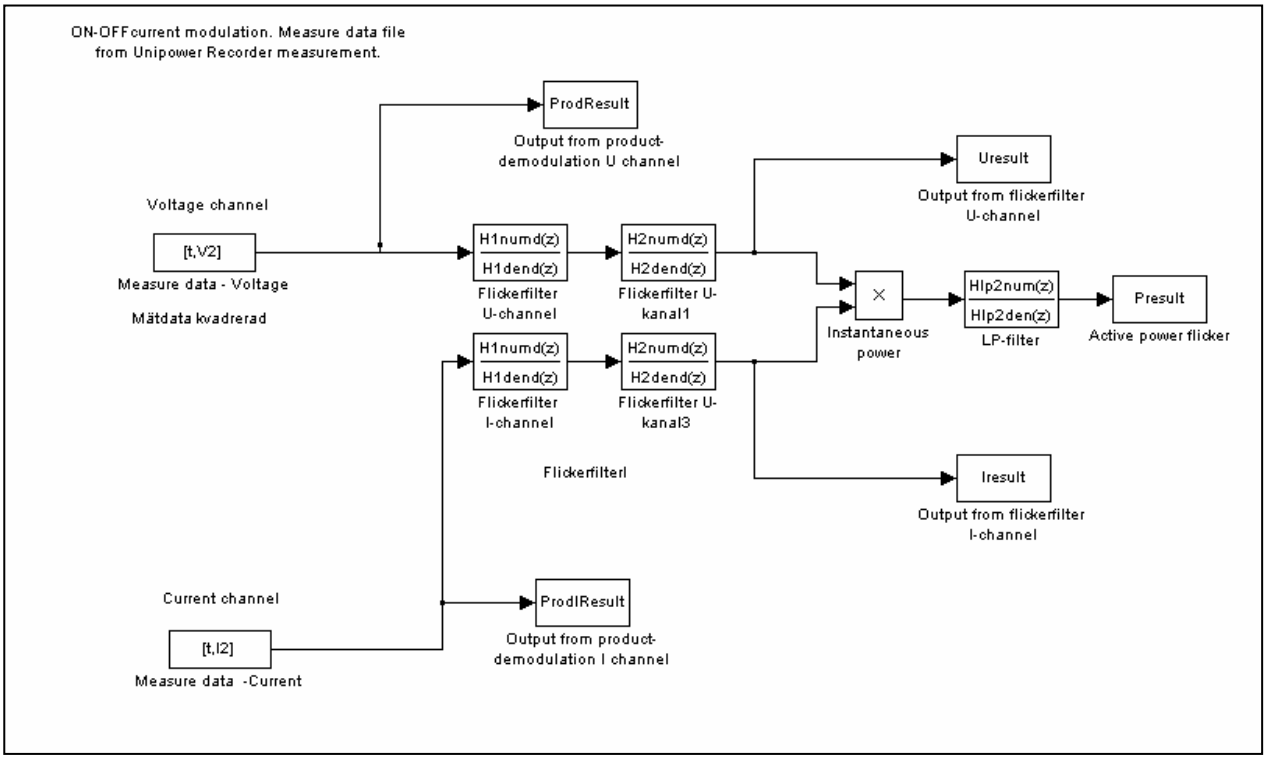


*Figure 5.9. Model in Simulink for calculation of single-phase flicker power according to measurement method 3. Used for the field test described in Section 5.3.*

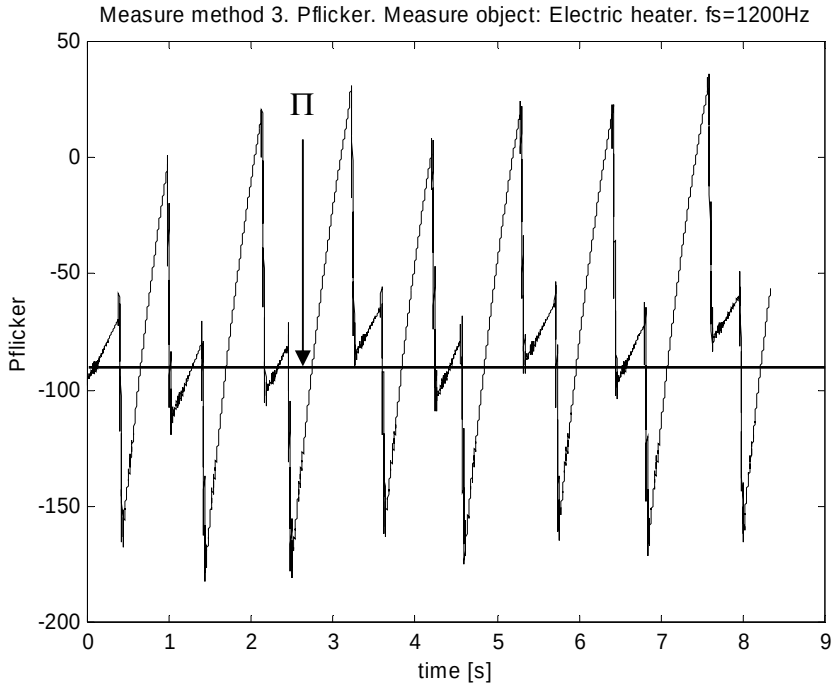


*Figure 5.10. Calculated flicker power from field test with ON-OFF load (Section 5.3). The average value of the flicker power is negative which means the flicker source is located below the monitoring point.*

Figure 5.11 shows a model in Simulink *simulating* the field test of the ON-OFF load. In the model a square wave generator (0V and 1V with 50% duty cycle) is simulating the ON-OFF sequence (see lower left in Figure 5.11). The square wave is multiplied with the current signal giving the same ON-OFF pattern as the current waveform in the field test. The same square wave generator is also used as the modulating signal to the voltage. The result of the simulations is shown in Figure 5.12 and 5.13. In Figure 5.12 the result is very much the same as the field test result in Figure 5.10. This is also the expected result since the simulated modulating signal of voltage was chosen negative and the frequency of the square wave generator was chosen close to the frequency of the ON-OFF modulation in the field test. In this first simulation, the envelopes of the voltage and the current signals were 180 degrees out of phase (i.e. producing negative flicker power). In a second simulation, the square wave signal which is modulating the voltage signal is multiplied by minus one (-1) which means the envelopes of voltage and current will be in phase and positive flicker power is produced. The result is shown in Figure 5.13. Conclusion: The field test as well as the simulation of the ON-OFF load clearly shows that the direction of propagation of the flicker power can be calculated and interpreted by using measurement method 3.

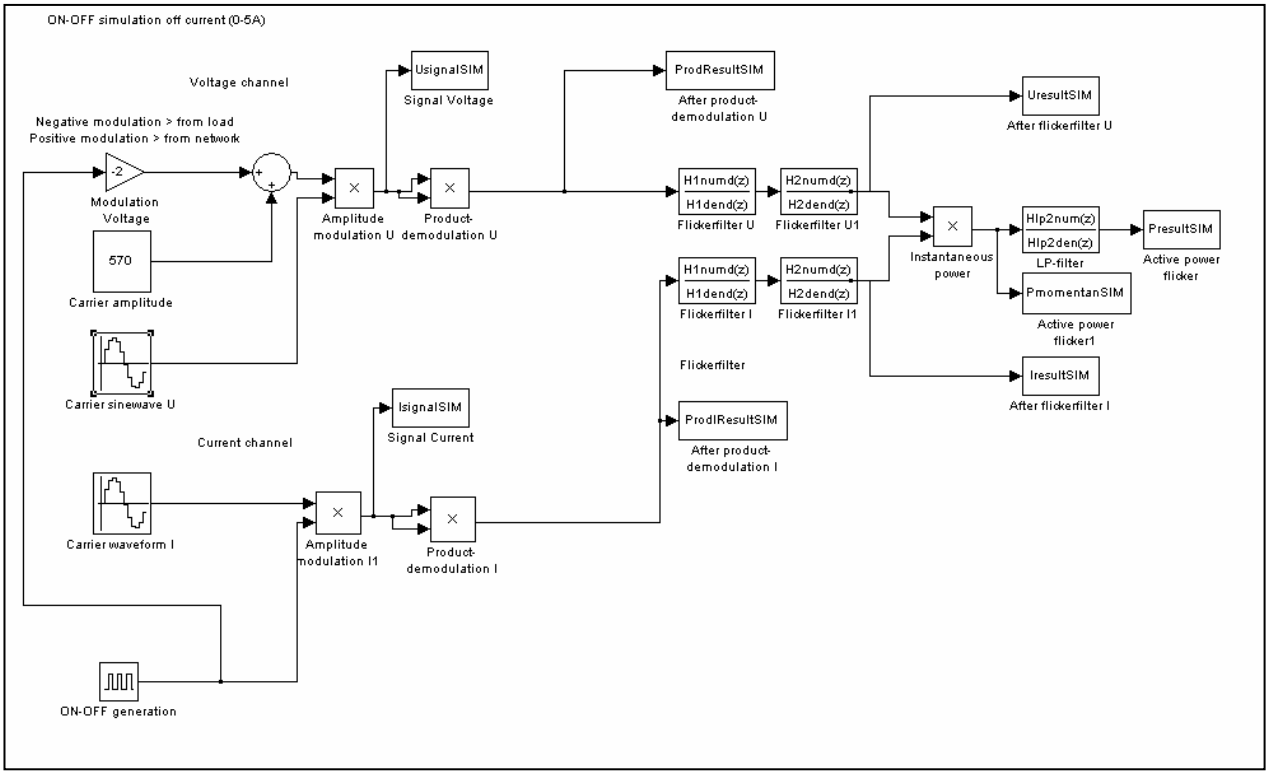


*Figure 5.11. Simulation model of the ON-OFF load.*

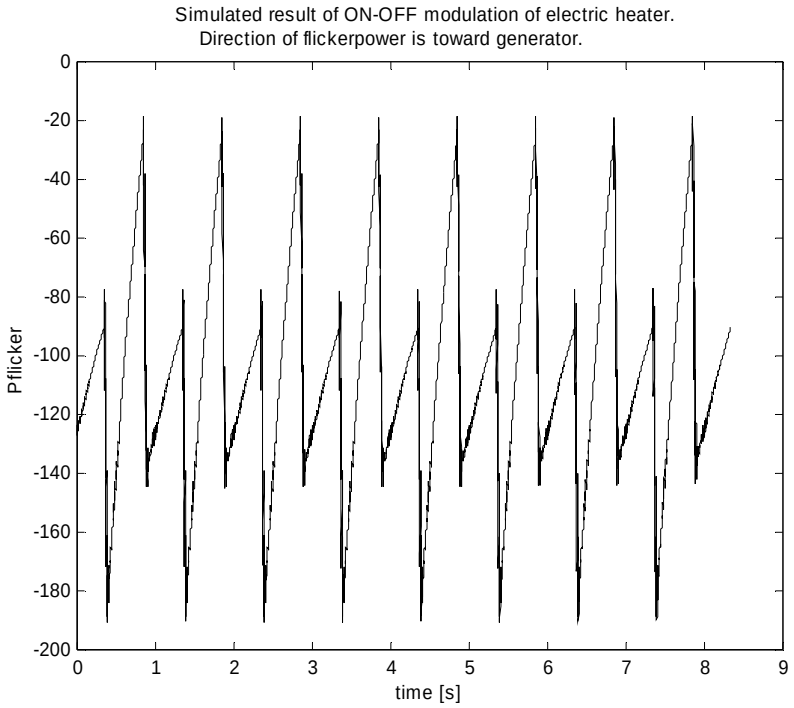


*Figure 5.12. Result of simulated flicker power of the ON-OFF load. The simulation result corresponds with high accuracy to the field test result in Figure 5.10.*

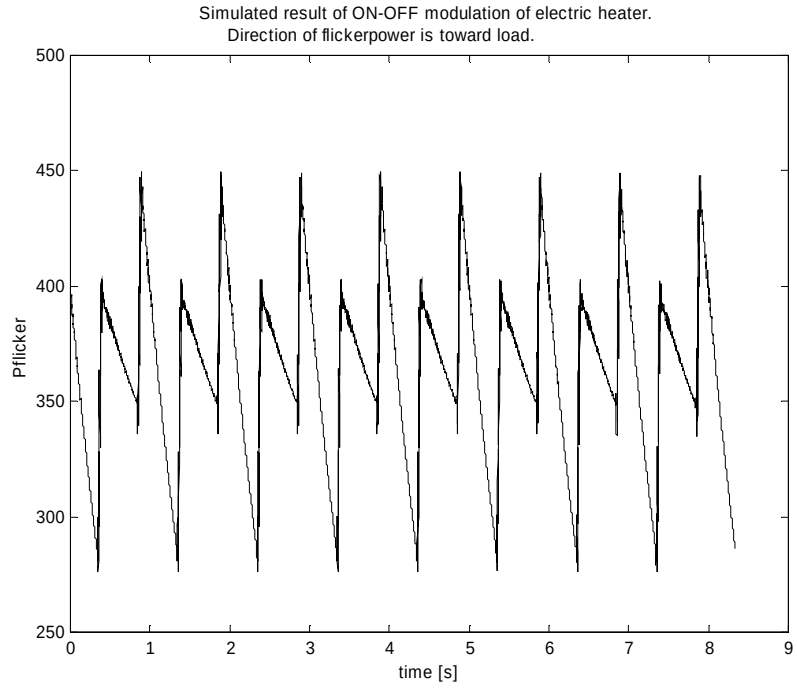


*Figure 5.13. The same simulation model used as in Figure 5.12. In this simulation the flicker power is positive which means the flicker source is located above the monitoring point.*

# 5.5. Field measurement on a Vestas V52 wind turbine

A field measurement according to measurement method 3 has been performed in the point of connection to a Vestas V52 wind turbine. The wind turbine generates up to 850 kW and is connected to a 10 kV distribution network (see Figure 5.14). The purpose of the measurement was to determine if flicker power could be measured in the connection point of the wind turbine. If so, it was interesting to know the direction of propagation in order to trace the flicker source. The location of the wind turbine is in a rural area and the loads connected close to the wind turbine are mainly agriculture, small size industries and households. Thus, the load is expected not to cause any voltage fluctuations leading to light flicker.

The measurement made use of three voltage and three current channels. The monitoring point was on the low voltage side of the step-up transformer, approximately 75 m from the generator of the wind turbine. The instrument being used was a Unipower Recorder using a sampling frequency of 1200 Hz. The measurement period was approximately 20 minutes and the wind turbine was generating all the time during the measurement.

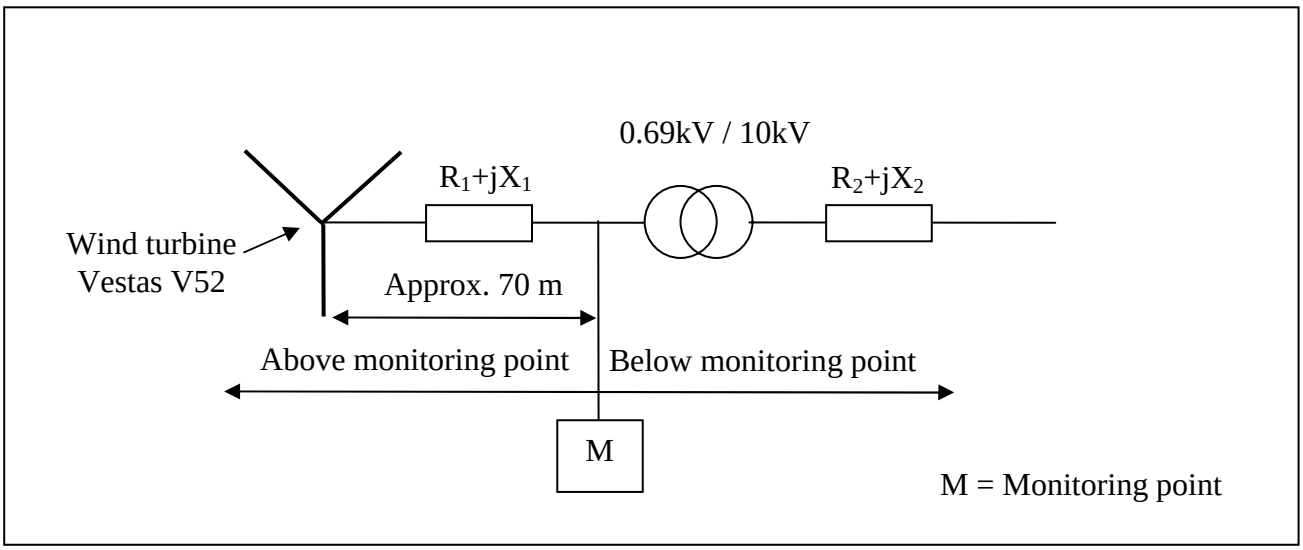


*Figure 5.14. One-line diagram at the monitoring point.*

The measurement data recorded were imported into Matlab for evaluation using the Simulink model in Figure 5.15. which is fully based on measurement method 3 and is implemented for three-phase measurements.

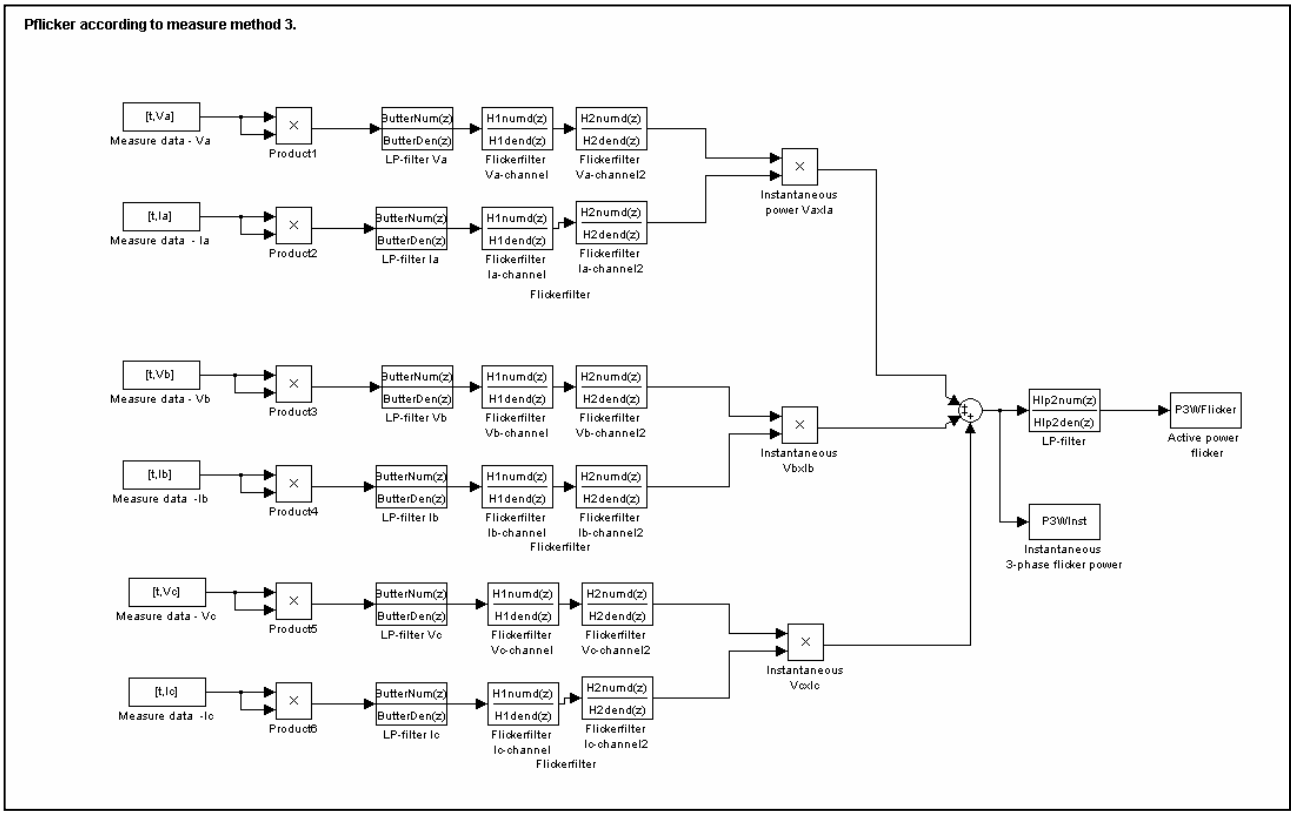


*Figure 5.15. Model in Simulink calculating the three phase flicker power according to measurement method 3.*

The result of the measurement shows mainly positive flicker power which means the direction of propagation of flicker power is from the wind turbine toward the network grid (see Figure 5.16). The conclusion is that the wind turbine is a flicker source producing flicker power propagating into the 10kV network.

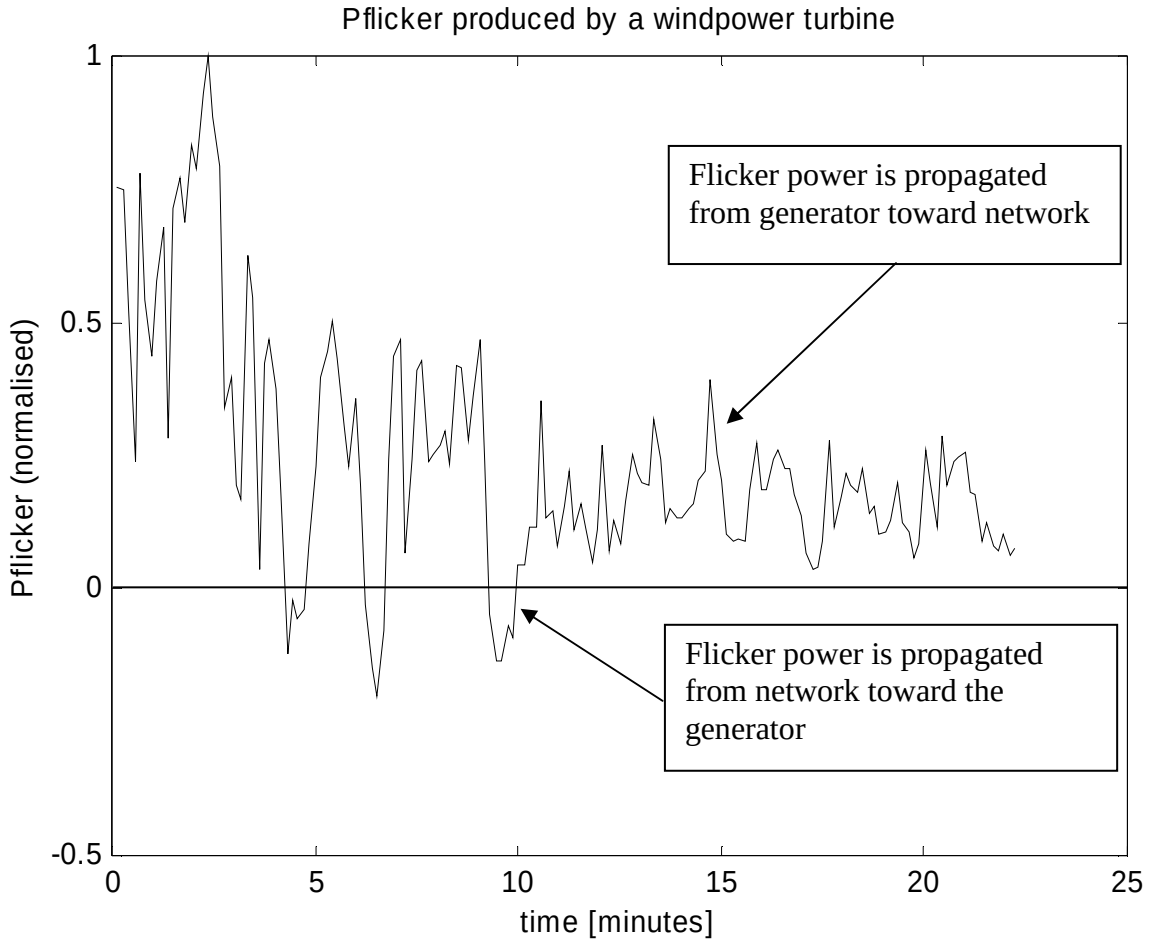


*Figure 5.16. Flicker power (normalised) according to measurement method 3 measured in the connection point of a Vestas V52 wind turbine. The direction of propagation of the flicker power is mainly positive i.e. from wind turbine toward the network grid.*

# 5.6. Flicker power measured in a 130 kV substation.

Two field measurements have been performed in a 130kV substation located in Sandviken, Sweden. The main purposes of the measurements were (1) to study the reliability of measurement method 3 and (2) to study the propagation of flicker power in the network close to the arc furnace in Sandviken.
Figure 5.17 shows the one-line diagram of the high voltage substation. The substation consists of incoming transmission lines from Forsbacka and from Stackbo; outgoing transmission lines feeding the village of Hofors and the arc furnace in the steelwork of Sandviken. Choosing the monitoring points was a quite straightforward task. Since an arc furnace is known for being a source of flicker it is quite obvious to monitor one of the transmission lines feeding the arc furnace (monitoring points M1a and M2a). The flicker source is located below the monitoring points M1a and M2a and thus, negative flicker power is expected. Point M1b monitors an incoming transmission line and the assumed flicker source is located below this monitoring point and therefore the flicker power is expected to be negative. In monitoring point M2b, the situation is assumed to be reversed since the transmission line is a feeding one. The flicker source is located above the monitoring point M2b. The sign of the flicker power is therefore expected to be positive. From the above discussion, validating measurements have been performed and the measurement results are compared with the expected results discussed above.
The situation is even somewhat more complicated. A second steelwork is located in Hofors. This steelwork is also a presumptive flicker source when operating. Thus, when both steelworks are operating, both will contribute to the flicker power measured in monitoring point M1b and M2b. However, since the steelwork in Sandviken is much closer to the 130 kV substation (just a few hundred meters) than the steelwork in Hofors (approximately 25km), the major part of the flicker power measured in monitoring point M2b (and M1b) is produced by the arc furnace in Sandviken.

The instruments being used for the measurements in Sandviken were two Unipower Recorders.

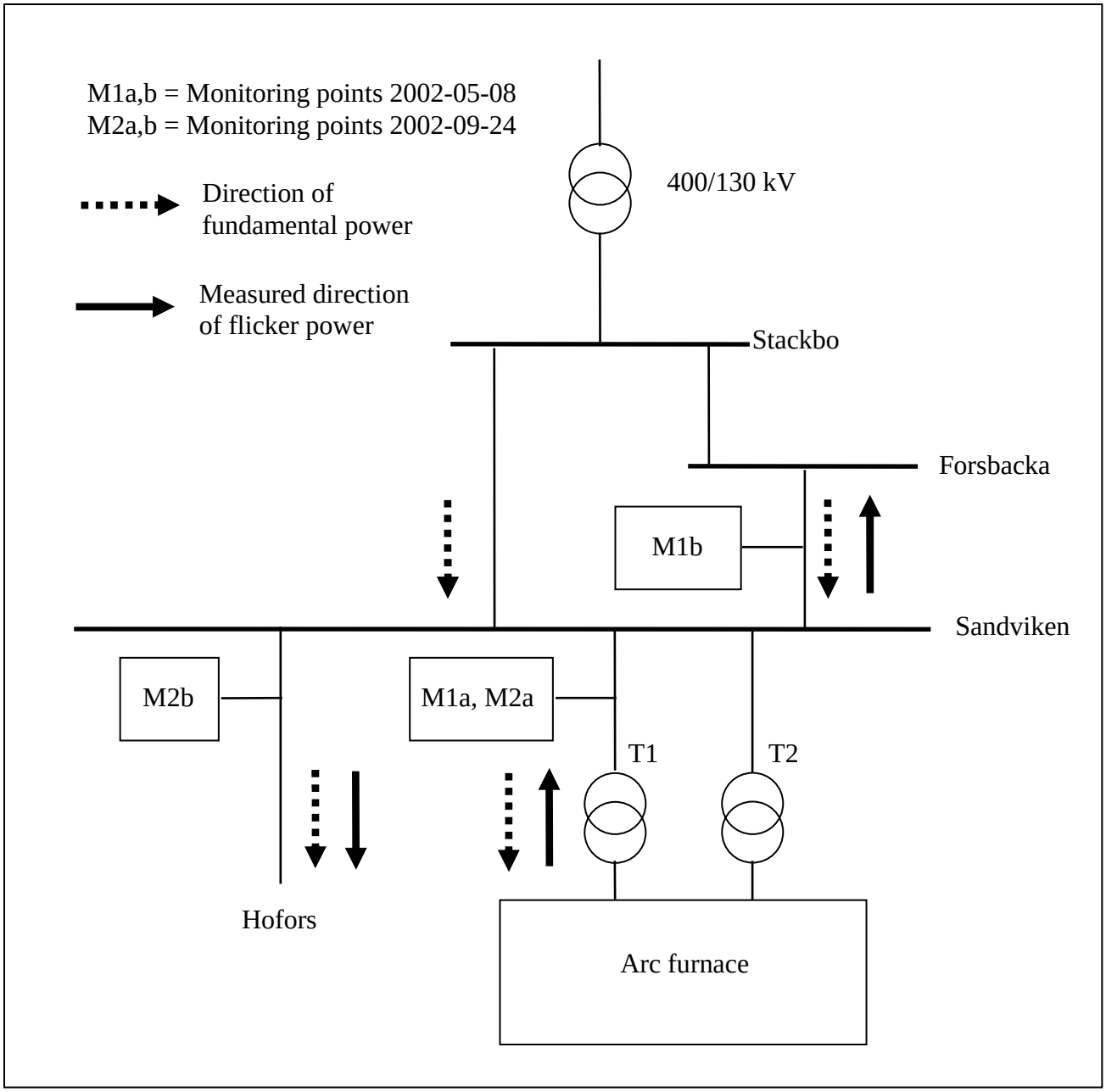


*Figure 5.17. One-line diagram for the 130kV substation in Sandviken. The arrows show the direction of the fundamental power (dotted arrows) and flicker power (solid arrows).*

## 5.6.1 Result of measurement M1 performed on May 8th 2002

The first field measurement was performed on May 8th 2002 in monitoring points M1a and M1b (see Figure 5.17). The three phase-to-neutral voltages and the three line currents were recorded in each monitoring point simultaneously. The results of the measurement are given in Figure 5.18-5.23. The flicker power flowing in the transmission line from Forsbacka is shown in Figure 5.18 and the flicker power flowing in the transmission line to the arc furnace is shown in Figure 5.19. The flicker power as shown in these two figures is exactly the expected result. In relation to the monitoring points, the source of flicker is located below the monitoring points and therefore, a flicker power of negative sign is expected in both transmission lines when the arc furnace is operating. Looking at the two figures, the flicker power is almost the same in the two transmission lines. Furthermore, when the arc furnace is not operating, the flicker power is close to zero. This is also the expected result.
The waveforms of voltage and current which are the input data to the measurement method 3 are given in Figure 5.20-5.23. During the non-operating period, the current and voltage amplitude is constant resulting in a flicker power of zero. During operation the voltage and current amplitude varies and flicker power is being produced, just as expected.

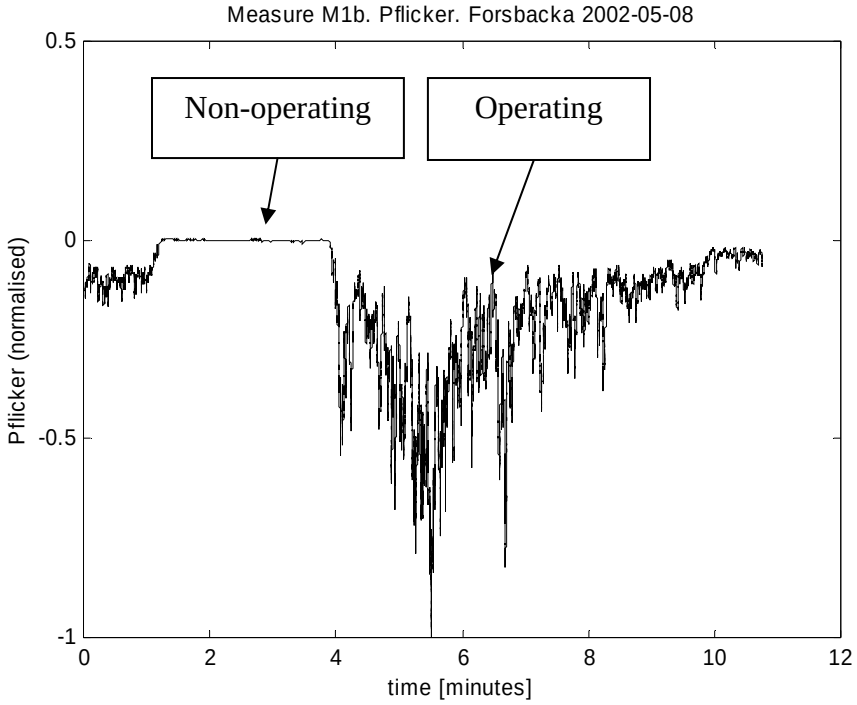


*Figure 5.18. Three phase flicker power measured in the transmission line from Forsbacka. The flicker source is located <u>below</u> the monitoring point and direction of propagation of flicker power is toward Forsbacka.*

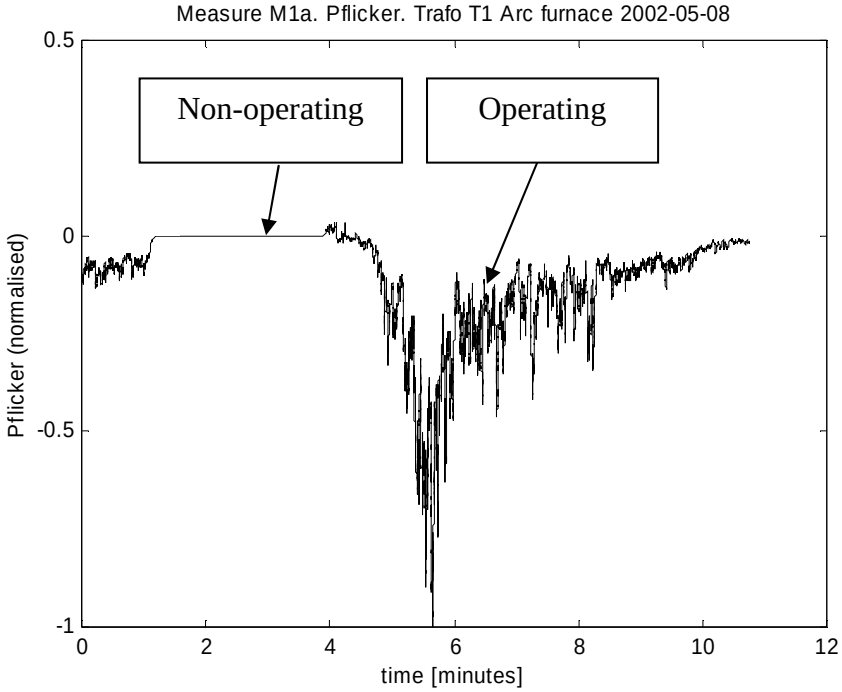


*Figure 5.19. Three phase flicker power measured in the transmission line feeding the arc furnace. As expected, the flicker source is located <u>below</u> the monitoring point.*

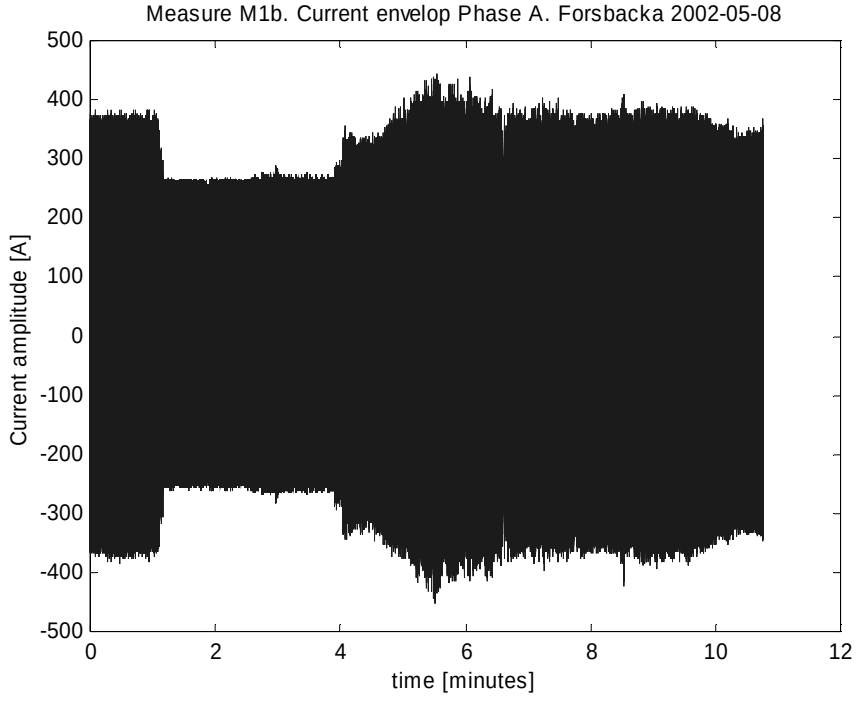


*Figure 5.20 . Current envelope (phase A) measured in monitoring point M1b. Note the correlation between the current envelope and flicker power in Figure 5.18.*

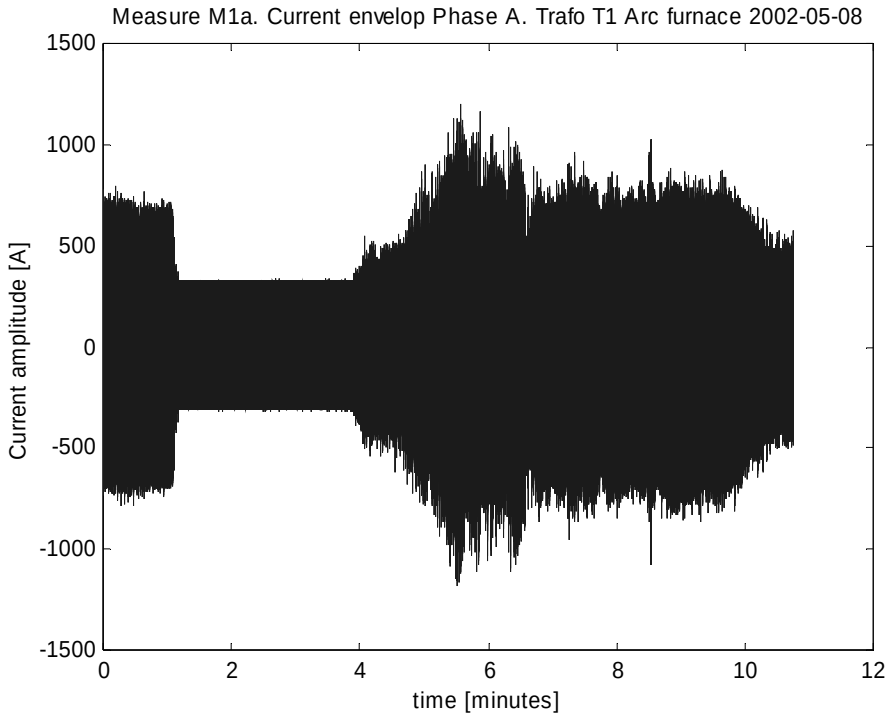


*Figure 5.21 . Current envelope (phase A) in transmission line feeding the arc furnace. Note the correlation to the flicker power in Figure 5.19.*

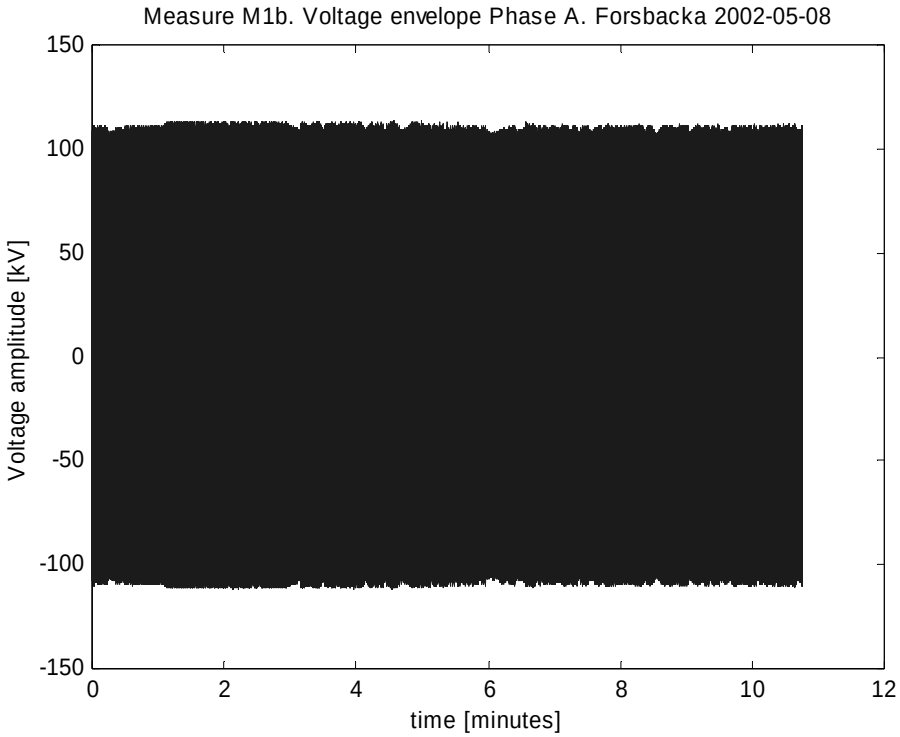


*Figure 5.22. Voltage envelope (phase A) measured in monitoring point M1b.*

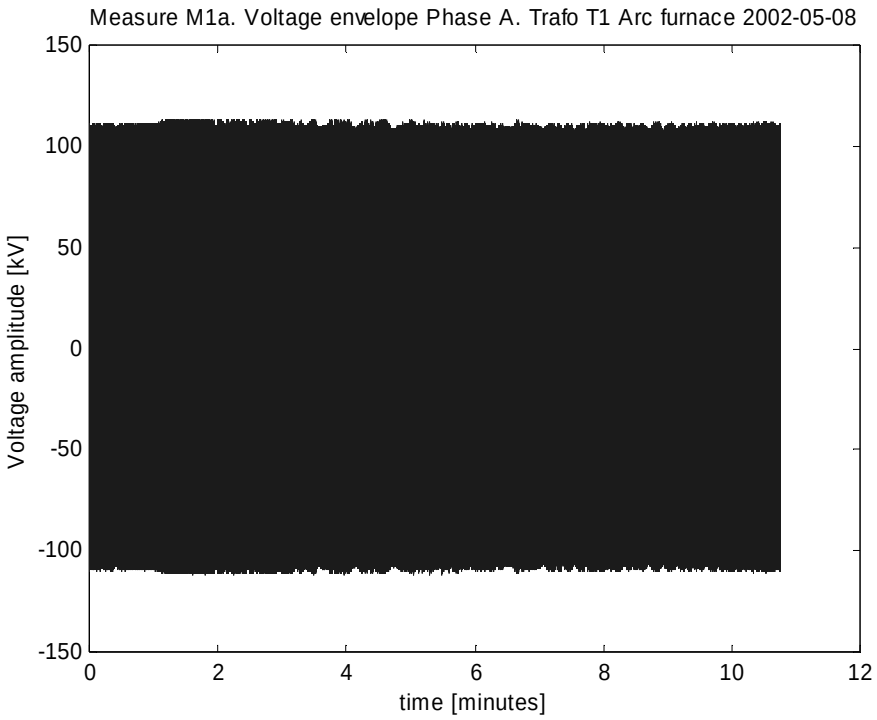


*Figure 5.23. Voltage envelope (phase A) measured in monitoring point M1a. Note the correlation to the voltage envelope in Figure 5.22.*

## 5.6.2 Result of measurement M2 performed on Sept 24th 2002

The second measurement in Sandviken was quite similar to the first one. Two monitoring points were chosen. M2a is the same monitoring point as M1a in the first measurement. Monitoring point M2b (i.e. the outgoing line to Hofors) was chosen at a location where flicker power is expected to be positive when the arc furnace in Sandviken is operating. The result of the measurement is given in Figure 5.24-5.29. Figure 5.24 and Figure 5.25 shows the flicker power in M2a and M2b plotted in the same graph. In Figure 5.25, the information is "smoothed" by a sliding-mean calculation using an averaging window of 2000 sampling points. It is interesting to see the correlation between the two curves in Figure 5.24/5.25. During operation of the arc furnace, negative flicker power is measured in monitoring point M2a. At the same time, positive flicker power is measured in monitoring point M2b. Referring to the conditions given in Chapter 4 the flicker source is located *above* the monitoring point M2b. The same conditions give that the flicker source is located *below* monitoring point M2a. Looking in Figure 5.17 the flicker power is propagated in direction from the arc furnace to the transmission line to Hofors. This is again the expected result. Furthermore, looking in Figure 5.25 both flicker powers are negative during a short period. Since the flicker power measured in M2b is a sum of flicker powers contributed from the arc furnace in Sandviken and the one in Hofors, the result in Figure 5.25 is possible. Especially since it is known that the arc furnace in Hofors was operating during the measurement. However, most of the time negative flicker power in M2a corresponds to positive flicker power in monitoring point M2b. Conclusion: the arc furnace in Sandviken is the dominating flicker source.
Like in previous measurement, the waveforms of voltage and current are also given (see Figure 5.26 - 5.29).

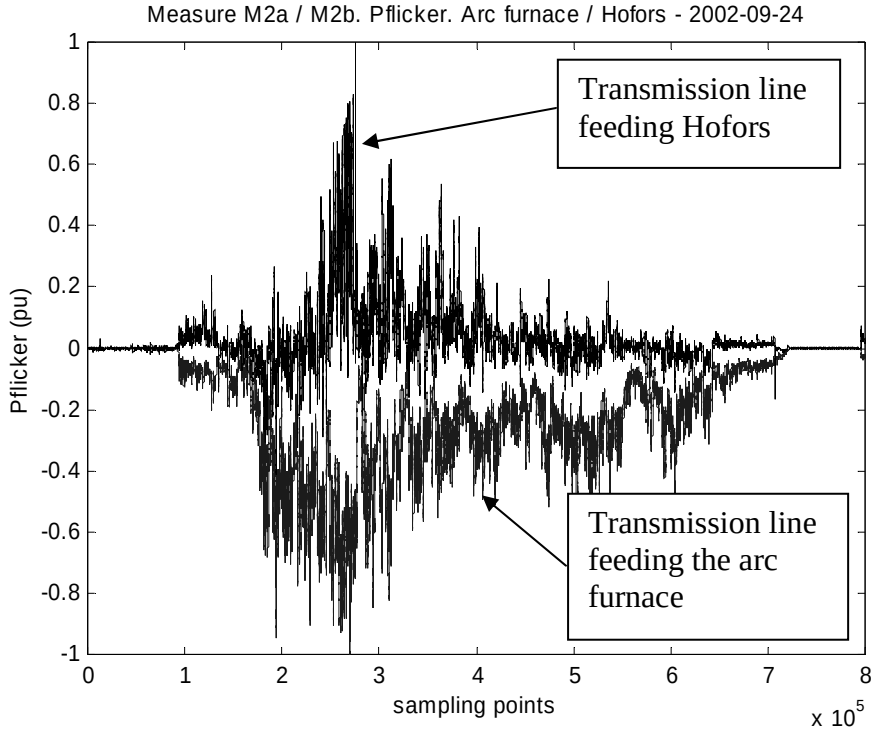


*Figure 5.24. Three phase flicker power in the monitoring points M2a and M2b measured at the same time. The strong correlation between the flicker power in M2a and M2b gives that the flicker power is created in the arc furnace in Sandviken and propagates to the outgoing transmission line to Hofors.*

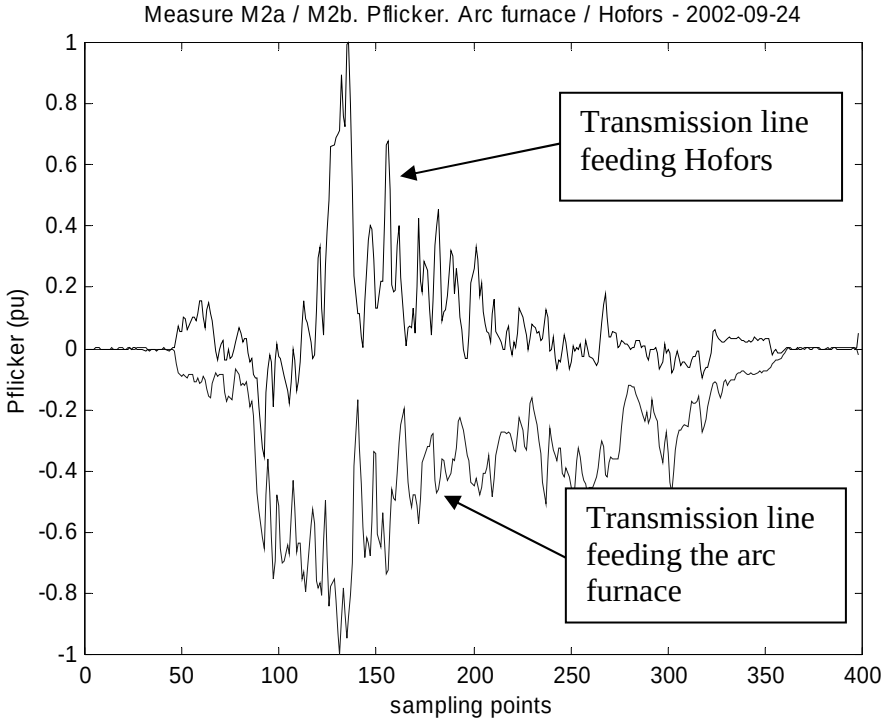


*Figure 5.25. Same information as in Figure 5.24 but the data is reduced by a sliding mean calculation.*

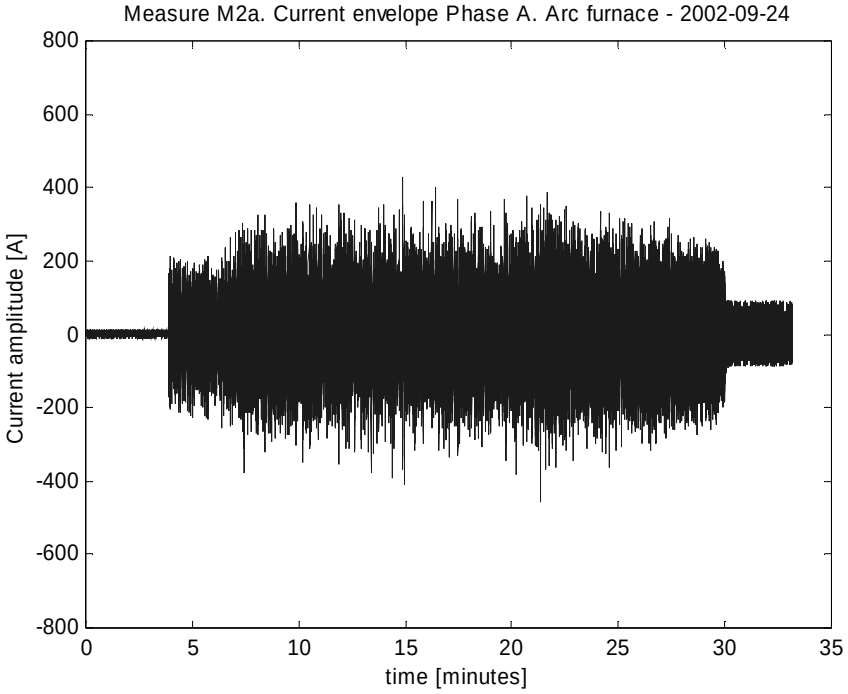


*Figure 5.26. Current waveform (phase A) measured in monitoring point M2a.*

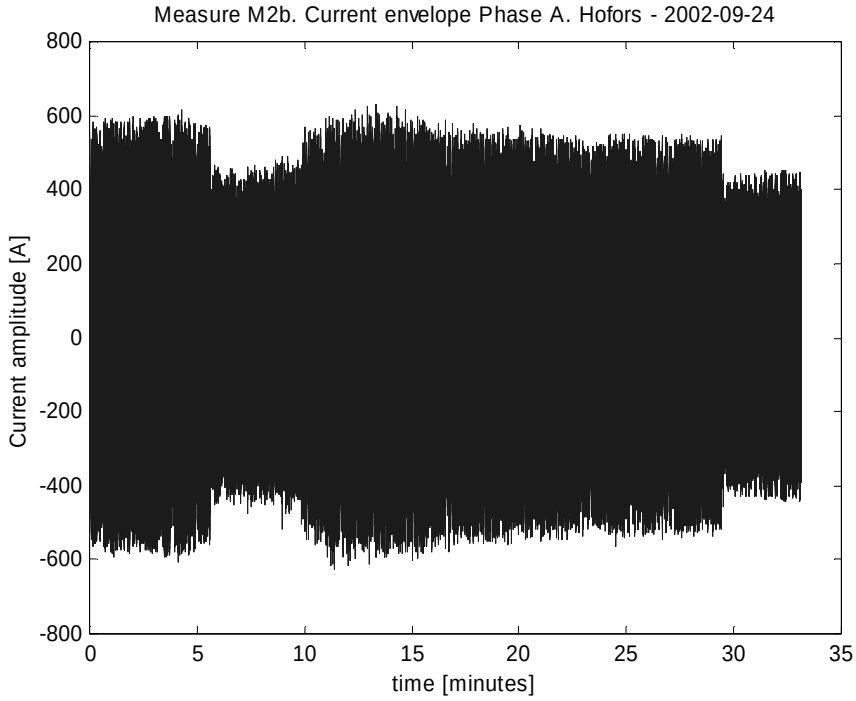


*Figure 5.27. Current waveform (phase A) measured in monitoring pointM2b. Note, no correlation to the current envelope in Figure 5.26.*

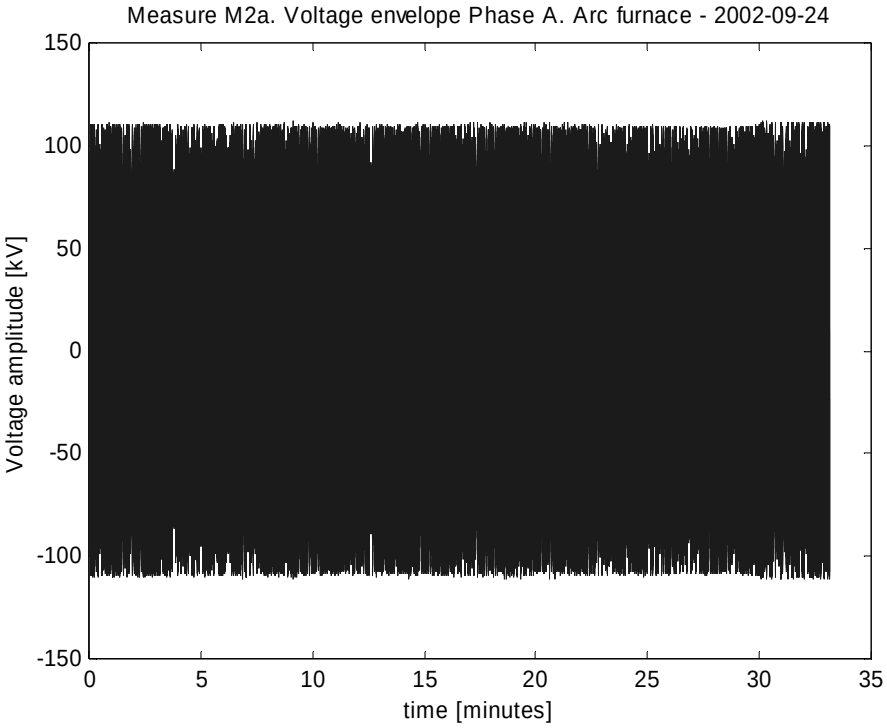


*Figure 5.28. Voltage envelope (phase A) measured in monitoring point M2a.*

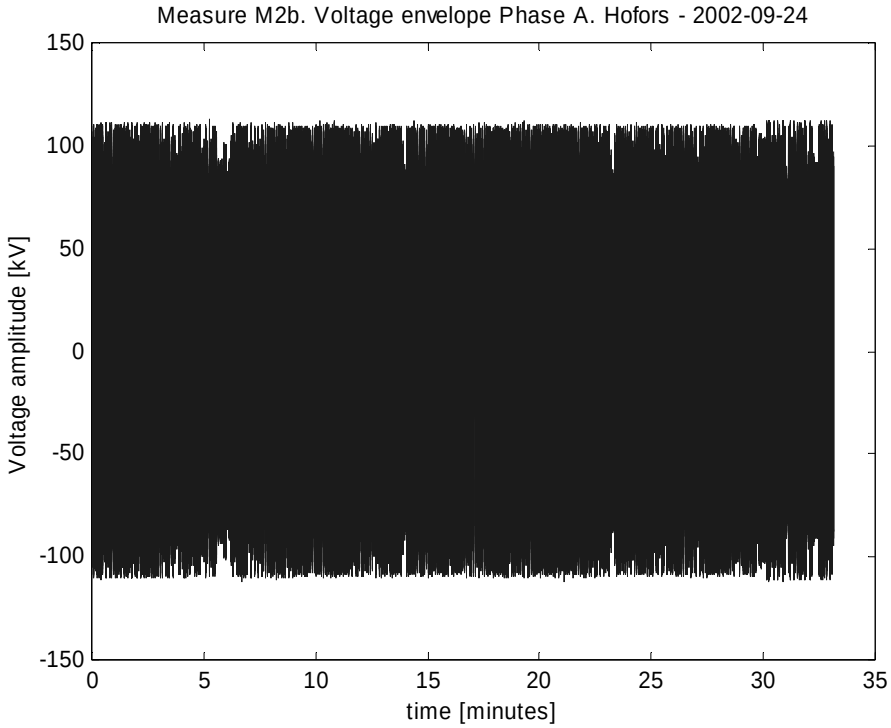


*Figure 5.29. Voltage envelope (phase A) measured in monitoring point M2b.*

## 5.7 General comments of the field measurements

The field measurements performed under the conditions given in Chapter 4, show high reliability of measurement method 3. In all the tests performed, the results were the expected ones.
It is interesting to study the waveforms of voltage and current in parallel with the study of flicker power. For example, in the first measurement M1 it is obvious that the flicker power will be quite equal in M1a and M1b since both voltage and current waveforms look the same. On the other hand, if looking at the corresponding waveforms in the second measurement M2, the waveforms of current in M2a and M2b look completely different. Thus, examining envelopes of voltage and current is of limited interest when studying how flicker propagates in the network. Calculating the flicker power is shown to be a far better method for extracting information. The developed measurement methods give a new dimension in understanding how a flicker source is “polluting” the network.

# Chapter 6

# Conclusions and future work

The work presented in this thesis concerns the development of methods for determining the direction to a flicker source with respect to a monitoring point. Surprisingly little academic research has been conducted on low frequency variations of voltage and current amplitudes in the power network. Therefore, this work had to define an appropriate working model from where the measurement methods could be derived. The defined model consists of a Thevenin equivalent circuit feeding a linear equivalent circuit consisting of a series impedance representing a transmission line and two shunt impedances placed on both sides of the series impedance. The values of the impedances can vary repeatedly with a frequency within the flicker frequency spectrum. In the model, a "monitoring point" is defined where the waveforms of voltage and current are obtained. By using this model and studying the voltage and current envelopes (i.e. modulating signals), the direction to the flicker source can be determined. By multiplying the modulating signals of voltage and current, a new quantity: "flicker power" is defined. The sign of the quantity gives the direction of propagation of the flicker power, which is essential when tracing a flicker source. The model, the conditions and the quantity flicker power form the platform from where three measurement methods have been developed. The measurement methods are based on sampled data and are using digital signal processing methods. In two of the methods, calculation of the flicker power is performed in the frequency domain. The third measurement method is based on calculations in the time domain.

The verification work has been concentrated on one of the method based on calculations in the time domain. This method is easiest to implement in hard-

and software and corresponds best to the methodology used in the flickermeter standards. In this method the weighting of voltage and current fluctuations is equal to the amount of disturbing light-intensity fluctuations they produce. By simulations in Matlab Simulink, the method was validated and showed high accuracy. These encouraging results were followed by field tests. The field tests were performed on a 2 kW electric heater, a 850 kW wind turbine and in a 130 kV substation feeding a 70 MW arc furnace. Analyses of the flicker power from the field tests confirmed the results obtained from theoretical analysis and simulations. For these particular field tests, the defined model and the measurement methods worked extremely well and the flicker sources were easily identified. The conclusion from these tests is that the developed measurement methods give reliable results.

More work is needed to develop the concept further. For example the two frequency-domain based methods have not yet been tested in field measurements. Also more field tests on different kind of loads are needed in order to further validate the methods.

The time length of the field measurements has been short. A next step is to perform long time studies of the flicker power, e.g. obtaining indices corresponding to the short-term and long-term flicker levels over a one-week period. Such a study will give valuable information regarding the overall applicability of the measurement methods.

In this work only the sign of the flicker power has been considered. It can be assumed that more interesting information can be found by studying the changes in flicker power over time. For example, does a flicker source produce a unique “fingerprint” in the flicker power? If it does, is it possible, by using pattern recognition techniques, to automatically detect the type of flicker source? To answer the above questions more research activities are needed.